E-ISSN 2146-3077

Cilt/Volume: 49
Sayı/Issue: 1
Mart/March 2025

Türkiye PARAZİTOLOJİ Dergisi

TURKISH JOURNAL OF PARASITOLOGY

Özgün Araştırmalar / Original Investigations

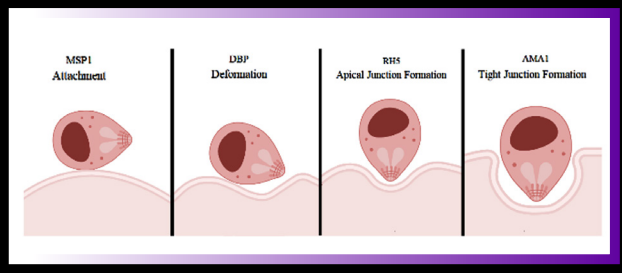

turkiyeparazitolderg.org

Türkiye Parazitoloji Derneği'nin Yayın Organıdır
Official Journal of The Turkish Society for Parasitology

galenos yayınevi

EDİTÖRDEN

2025 yılının ilk sayısını 6 özgün araştırma makalesi ve 1 video makale ile çıkarmaktayız. Özgün araştırmalar arasında; sıtma parazitlerinin eritrosit işgalini engellemeye yönelik bir ilaç çalışması, immünbaskın bireylerde Cryptosporidium prevalansını inceleyen bir çalışma, Blastocystis'in popülasyon yapısı ile ilgili bir çalışma, kist hidatik hastalarının tanısı ve takibinde kullanılabilecek bir markır ile ilgili bir araştırma yanı sıra uyuzlu hastalar ve Culicoides türlerinin vektörlük potansiyelleri ile ilgili birer çalışma yer almaktadır.

Video makale olarak; bilim alanlarında da yaygın olarak kullanılmaya başlayan akıllı telefonlar ve uygulamaları ile alınan görüntülerin Parazitoloji bilim alanında bir yansıması olan ve Sarcoptes scabiei ve Demodex folliculorum ektoparazitlerinin hareketlerini görüntüleyen bir çalışma yer almaktadır.

Dergimizin ESCI için de başvurusu yeniden yapılmış olup sonucu beklenmektedir. Bu sürece büyük katkısı olan ve gönderilen makalelere özveri ile hakemlik yapan, bu sayının sonunda da listesi yayınlanan akademisyenlerimize de teşekkür etmek ve minnetlerimi sunmak isterim.

SCI/SCI-Expanded kapsamında olan dergilerde yapacağınız yayınlarda dergimizde yer alan makalelere atıf yapılmasının, dergimizin bu endekse başvuru/kabul sürecinde büyük önem taşıdığını yeniden belirtmek isterim. Bilim alanımızın en önemli unsurlarından ve bizleri güçlendiren araçlarından biri olan "Türkiye Parazitoloji Dergisi"nin bu sayısının da bilimsel çalışmalarınıza ve birikimlerinize yararlı olmasını umuyorum.

Prof. Dr. Yusuf Özbel

Baş Editör

galenos yayınevi

Yayınevi İletişim/Publisher Contact

Address: Molla Gürani Mah. Kaçamak Sk. No: 21/1 34093 İstanbul, Türkiye

Telefon/Phone: +90 530 177 30 97

E-posta/E-mail: info@galenos.com.tr/ yayin@galenos.com.tr

Web: www.galenos.com.tr

Publisher Certificate Number: 14521

Online Publication Date: Mayıs / May 2025

E-ISSN: 2146-3077

Üç ayda bir yayımlanan süreli yayındır.
International scientific journal published quarterly.

Türkiye PARAZİTOLOJİ Dergisi

Please refer to the journal's webpage **(https://www.turkiyeparazitolderg.org/home)** for "Aims and Scope" and "Instructions to Authors" .

The editorial and publication process of the Journal of the **Turkish Academy of Dermatology** are shaped in accordance with the guidelines of the **ICMJE, WAME, CSE, COPE, EASE**, and **NISO**. Turkish Journal of Parasitology is indexed in **PubMed/ MEDLINE, BIOSIS-Zoological Record, EBSCO Host, Gale, ProQuest, SCOPUS, CINAHL, BIOSIS Previews Biological Abstracts, CABI, Embase, J-Gate, TÜBITAK ULAKBİM TR Dizin, DOAJ, ARDI, GOALI, Hinari, OARE, Turkish Medline, CNKI** and **Turkish Citation Index**.

Journal is published online.

Owner: Yusuf Özbel on Behalf of Turkish Society of Parasitology

Responsible Manager: Yusuf Özbel

Contact

Editorial Office

Editor in Chief: Yusuf Özbel, MD, Prof

Address: Ege Üniversitesi Tıp Fakültesi, Parazitoloji Anabilim Dalı, 35100 Bornova-İzmir, Türkiye

Phone: +90 232 390 47 24 / +90 232 373 00 08

Fax: +90 232 388 13 47

E-mail: yusuf.ozbel@ege.edu.tr / yusuf.ozbel@gmail.com

İÇİNDEKİLER/CONTENTS

ÖZGÜN ARAŞTIRMALAR / ORIGINAL INVESTIGATIONS

VİDEO MAKALE / VIDEO ARTICLE

Türkiye PARAZİTOLOJİ Dergisi

Original Investigation
Özgün Araştırma

Turkiye Parazitol Derg 2025;49(1):1-9
DOI: 10.4274/tpd.galenos.2025.37928

Identification of New Candidate Inhibitors Able to Prevent Erythrocyte Invasion in Malaria by Drug Screening

Sıtma Hastalığında Eritrosit İstilasını Engelleyebilen Yeni Aday İnhibitörlerin İlaç Taraması ile Belirlenmesi

Ahmet Burak Doğanoğlu[1], Vildan Enisoğlu Atalay[2]

[1]Üsküdar University Faculty of Medicine, Department of Bioinformatics, İstanbul, Türkiye
[2]İstanbul Technical University, Graduate School of Science/Bioinformaics, İstanbul, Türkiye

Cite this article as: Doğanoğlu AB, Enisoğlu Atalay V. Identification of new candidate inhibitors able to prevent erythrocyte invasion in malaria by drug screening. Turkiye Parazitol Derg. 2025;49(1):1-9.

ABSTRACT

Objective: In Nowadays malaria still remains the parasitic disease causing the highest number of deaths, accounting for 619,000 fatalities. The *Plasmodium* parasites that cause malaria have separate life cycles in both humans and female Anopheles mosquitoes, existing in various forms throughout this process. The main reason for observing the disease is that merozoites sustain their existence by invading erythrocytes. Existing drugs affect the parasite's ability to digest hemoglobin. Drug resistance is also involved in this process. In this study, have been focused to develop new drug candidate molecules for evade drug resistance. To evade drug resistance, the aim was to prevent merozoites from invading erythrocytes.

Methods: The invasion of merozoites into erythrocytes consists of several stages: Attachment, deformation, apical junction formation, and tight junction formation. For this purpose, the docking calculations have been done between the invasion proteins such as MSP1, pvDBP, phRH5, AMA1 and candidates. The candidates obtained from the malaria box set were subjected to conformational scanning and geometry optimization in the Spartan'14 program to determine their physicochemical properties. According to the obtained results from the AutoDock Vina and multiple regression analyses were conducted for each protein to examine the relationship between binding affinities and the calculated physicochemical parameters of the candidates.

Results: In the regression study of 200 molecules examined for 4 different proteins, 108 molecules were included for DBP, 96 for MSP1, 90 for AMA1 and 96 for RH5, and 21 common molecules were observed for all proteins.

Conclusion: Twenty-one molecules showed correlation with the proteins studied. Among these molecules, MMV019074, MMV019662 and MMV665881 were suggested as candidate drug leads in terms of their binding affinities, physicochemical properties and SwissADME values.

Keywords: Docking, erythrocytes, malaria, malaria box, merozoite

ÖZ

Amaç: Günümüzde sıtma, 619.000 ölümle en çok ölüme neden olan paraziter hastalık olmaya devam etmektedir. Sıtmaya neden olan *Plasmodium* parazitlerinin hem insanlarda hem de dişi Anopheles sivrisineklerinde ayrı yaşam döngüleri vardır ve bu süreç boyunca çeşitli biçimlerde var olurlar. Hastalığın gözlemlenmesinin temel nedeni, merozoitlerin eritrositleri istila ederek varlıklarını sürdürmeleridir. Mevcut ilaçlar parazitin hemoglobini sindirme yeteneğini etkiler. İlaç direnci de bu süreçte yer alır. Bu çalışmada, ilaç direncinden kaçınmak için yeni ilaç adayı molekülleri geliştirmeye odaklanılmıştır. İlaç direncinden kaçınmak için amaç, merozoitlerin eritrositleri istila etmesini önlemekti.

Yöntemler: Merozoitlerin eritrositlere invazyonu birkaç aşamadan oluşur: Tutunma, deformasyon, apikal bağlantı oluşumu ve sıkı bağlantı oluşumu. Bu amaçla, MSP1, pvDBP, phRH5, AMA1 gibi istilacı proteinler ile adaylar arasında kenetleme hesaplamaları yapılmıştır. Malaria box setinden elde edilen adaylar, fizikokimyasal özelliklerini belirlemek için Spartan'14 programında konformasyonel tarama ve geometri optimizasyonuna tabi tutulmuştur. AutoDock Vina'dan elde edilen sonuçlara göre, her protein için bağlanma afiniteleri ile adayların hesaplanan fizikokimyasal parametreleri arasındaki ilişkiyi incelemek için çoklu regresyon analizleri yapıldı.

Bulgular: Dört farklı protein için incelenen 200 molekülün regresyon çalışmasında DBP için 108, MSP1 için 96, AMA1 için 90 ve RH5 için 96 molekül dahil edilmiş olup tüm proteinler için 21 tane ortak molekül olduğu gözlenmiştir.

Received/Geliş Tarihi: 11.10.2023 **Accepted/Kabul Tarihi:** 24.03.2025 **Epub:** 29.04.2025 **Publication Date/Yayınlanma Tarihi:** 09.05.2025

Address for Correspondence/Yazar Adresi: Vildan Enisoğlu Atalay, İstanbul Technical University, Department of Computational Science and Engineering, İstanbul, Türkiye
E-mail/E-Posta: enisogluatalayv@itu.edu.tr **ORCID ID:** orcid.org/0000-0002-9830-9158

Türkiye PARAZİTOLOJİ Dergisi

Sonuç: Yirmi bir molekül çalışılan proteinlerle korelasyon gösterdi. Bu moleküller arasında, bağlanma afiniteleri, fizikokimyasal özellikleri ve SwissADME değerleri açısından MMV019074, MMV019662 ve MMV665881 aday ilaç öncüleri olarak önerildi.
Anahtar Kelimeler: Kenetleme, eritrosit, sıtma, malaria box, merozoit

INTRODUCTION

Malaria is an acute febrile disease caused by *Plasmodium* parasites transmitted by female Anopheles mosquitoes. The life cycle of the parasites starts when sporozoites are injected into the skin by female Anopheles mosquitoes. Due to environmental changes and immune factors, sporozoites need to quickly reach the liver (1). During this process, sporozoites utilize surface proteins like circumsporozoite protein and thrombospondin-related anonymous protein to pass through Kupffer macrophage cells, which are the first obstacle they encounter, and invade hepatocytes (2,3). After sporozoites transform into schizonts within hepatocytes, the schizonts release merozoites into the bloodstream by rupturing the hepatocyte.

After merozoites invade erythrocytes, it leads to the appearance of the disease's symptoms. The invasion process begins with the merozoite surface protein 1 (MSP1) attachment to the erythrocyte surface. Moreover, the MSP1 proteins abundantly present on the surface are highly polymorphic due to being exposed to a large number of antibodies (4). In the next stage, erythrocyte binding antigen (EBA) proteins and reticulocyte binding protein homologs (RH) move the merozoite towards erythrocytes. Thus, facilitating contact between the merozoite apex and the erythrocyte. The apex of the merozoite then attaches to the erythrocyte by the pfRH5 protein and becoming ready for invasion. Rhoptry neck protein 2 (RON2) is released from the rhoptry secretory organelles and binds to the erythrocyte surface. This allows Apical Membrane Antigen 1 (AMA1) protein to attach to the erythrocyte. The merozoite establishes a mobile tight junction with the AMA1-RON2 complex, to infect the erythrocyte (5). The stages of erythrocyte invasion are shown in Figure 1.

Merozoites differentiate into male and female gametocytes by invading erythrocytes. During erythrocyte invasion, not all merozoites differentiate into gametocytes; some of them revert back to merozoites after erythrocyte invasion. Once gametocytes are formed, the human life cycle comes to an end. When an infected individual is bitten by a mosquito again, the gametocytes are transferred to the mosquito (6). After erythrocyte invasion, the parasites sustain their lives by utilizing hemoglobin digestion within the erythrocyte. Trophozoites take up hemoglobin into the cytoplasm through endocytosis, creating a digestive vacuole with a pH of 5.2. Heme molecules produced from hemoglobin breakdown are detoxified inside this vacuole because of their toxic nature (7). All drugs that affect the current blood stage are used to prevent the detoxification of heme molecules, and all resistance mechanisms develop along this pathway. Merozoites can compensate for any issues that may arise during erythrocyte invasion by establishing alternative pathways (8).

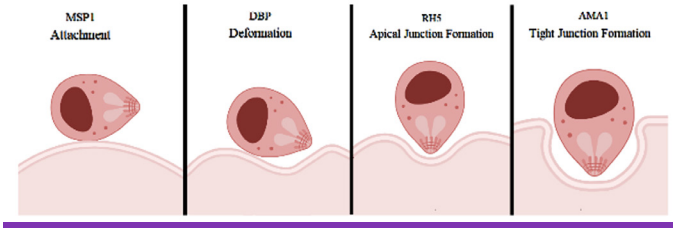

Figure 1. Erythrocyte invasion stages of merozoite (created with BioRender.com)

Therefore, this study, to target merozoite erythrocyte invasion by inhibiting pvDBP, MSP1, AMA1, and phRH5 proteins to evade resistance mechanisms. It has been demonstrated that the C-terminal region of the MSP1 protein (MSP1 19) binds to and inhibits the protein by targeting amino acids 29-36 and 51-56 through a ligand called NIC (9,10). In this context, the same region has been selected as the target binding sequence. The EBL protein family, which only has one member called the DBP protein in *P. vivax*, utilizes Duffy binding-like domains to attach to erythrocyte receptors (11). To determine the compatibility of the binding region of pvDBP with other proteins, sequence alignments were performed between erythrocyte membrane protein 1 (EMP1), EBA175 (12), EBA140 (13), and pvDBP. The DBP-Duffy Antigen Receptor (DARC) complex was found to be the preferred option (the aligned proteins are 4NUU_A, 1ZRO_A, AUF72533, 4GF2_A, and SBT76215). According to Batchelor et al. (11), the binding site of the PhRH5 protein involved in the RH5-basigin interaction, which is responsible for binding, has been identified as the active region. The protein has a pdb code of 4WAT (14). The active region amino acids for the AMA1 protein have been selected as the ones that interact with the AMA1-R1 inhibitor (15) and the AMA1-pfRON2 (16) complex in the 3SRI structure (17). Docking was done with these proteins and molecules in the "Malaria box" molecule set published by the Medicines for Malaria Venture Foundation. Thus, the correlation between the physicochemical properties of molecules and their binding affinities was studied.This novel approach provides a new drug and treatment pathway.

Additionally, the MMV020291 molecule from the study of Dans et al. (18) was preferred to compare binding affinities with experimental data. MMV020291, a molecule from the "Pathogen box" set published by the Medicines for Malaria Venture Foundation. It was observed that MMV020291 was in the deformation and tight junction stages specified in Figure 1. For this reason, the binding affinities of MMV020291 were accepted as the threshold value for the molecules to be recommended.

METHODS

As a target proteins pvDBP, MSP1, AMA1, and phRH5 were selected, which play a crucial role in the erythrocyte invasion mechanism mentioned above, have been identified for the binding procedures. The crystal structures of the these proteins were selected from the RCSB Protein Data Bank (19) as follows: pdb id: 4NUU, 1B9W, 3SRI and 4WAT. The central coordinates of the active region of the selected protein structures for the binding procedures are specified in Table 1, and the grid box has been scaled to 35x35x35Å^3. The binding studies were performed using the AutoDock Vina program (20), and the interaction maps and visualization processes were carried out using the BIOVIA Discovery Studio Visualizer program (21).

Table 1. The grid box coordinates

PDB ID	X	Y	Z
4NUU	47.655875	-44.833875	98.381875
1B9W	-3.335750	20.720000	53.636500
3SRI	9.933917	-1.080167	3.548250
4WAT	46.476750	38.165625	51.009750

The determine the binding and inhibition constants of new candidate drug molecules for treating malaria are crucial. To achieve this, 200 molecules were selected from the "Malaria box" molecules that target the blood stage (22). The chosen molecules went through a process of conformational searching using the molecular mechanics force field (MMFF) method, with single bonds being rotated in 60° increments in the Spartan'14 program (23) to obtain their most stable conformer structures. The molecules with stable conformers then underwent geometry optimizations using the semi-empirical PM6 method. Additionally, the drug-likeness potential of the candidate molecules was investigated using the SwissADME program (24). Their compliance with Lipinski's rules (25) was also assessed in the study.

Statistical Analysis

Linear correlations between binding affinities against physicochemical parameter values such as lipophilicity (LogP), dipole moment, molecular weight (M_W), volume (V), number of rotatable bonds (NRB) and topological polar surface area (TPSA) calculated as a result of geometry optimizations were determined using the Excel program (26).

RESULT

In this context, new candidate drug molecules targeting the 4WAT, 4NUU, 3SRI, and 1B9W pdb coded structures responsible for erythrocyte invasion in malaria treatment's blood stage were identified using computational methods. Table 2 displays the molecular weight (M_W), TPSA, NRB, LogP, dipole moment (μ), and hardness [$\eta=(E_{HOMO}-E_{LUMO})/2$] values, and SwissADME maps for 21 molecules that displayed correlation with all the proteins among the chosen 200 molecules (calculated parameters and binding affinity values for 200 molecules are shown in Supplementary Tables 1-3). The table also includes values for the MMV020291 structure. In the SwissADME maps that provide the initial criteria for drug-likeness in a collective manner, it was observed that only the compound with the number MMV665881 exceeded the limit value at the unsaturation point. However, all the other suggested candidate molecules meet Lipinski's drug-likeness criteria.

In this study, different affinity values were observed based on the QSAR parameters of the examined molecules. The binding affinity values for the reference structure MMV020291 were obtained as -7.1 and -7.7 kcal.mol^{-1} for the protein structures with pdb codes 4NUU and 3SRI, respectively. On the other hand, experimental data such as toxicity and inhibition were examined for the 200 molecules. In the binding calculations between the 4NUU pdb coded protein structure and the molecules, the binding affinities of MMV665881, MMV019074, and MMV019662 were calculated as -7.8, -8.2, and -8.4 kcal.mol^{-1}, respectively. For the 3SRI protein structure, the binding affinities of these molecules were calculated as -9.0, -8.2, and -8.9 kcal.mol^{-1}, respectively. Based on the obtained binding energies, it can be observed that the increase in affinity compared to the reference molecule MMV020291 is approximately 3 to 20 times for the 3SRI protein structure and between 5 to 20 times for the 4NUU structure.

In the conducted experimental studies, inhibition could not be achieved with the 1B9W and 4WAT pdb-coded structures, which are defined as the first and third stages of erythrocyte invasion stages, respectively (attachment and apical junction formation). However, in the binding studies, affinity values of -6.4 and -7.0 kcal.mol^{-1} were obtained for these structures with the MMV020291 reference molecule. On the other hand, it was determined that the increase in binding affinity for the prominent candidate structures MMV665881, MMV019074, and MMV019662 from the examined molecule set ranged from 2 to 8 times.

In the literature, experimental inhibition tests were conducted by Voorhis et al. (22). When Table 3 is examined, it can be observed that the structures MMV019662 and MMV019074 provided inhibition in both early and late ring stages for the HB3 strain. On the other hand, the structure MMV665881 inhibited subsequent steps instead of the targeted inhibition steps. The selected molecules exhibited nearly complete inhibition in the *Plasmodium* 3D7 strain, where no drug resistance was observed. However, achieving our main goal, these molecules particularly MMV019662, MMV665881, and MMV019074, demonstrated over 70% inhibition in the *Plasmodium* DD2 strain, which is known for chloroquine resistance, indicating their potential to evade resistance mechanisms.

When the physicochemical parameters of the candidate molecules listed in Table 2 were examined, a clear trend between calculated logP, hardness, and TPSA values and binding affinities could not be observed. However, a more distinct trend was obtained with the dipole moment (μ) and molecular weight (MW) properties. It is observed that the logP value, which has an effect on binding affinity, varies between 0.88 for the reference MMV020291 structure and in the range of (-1.41) - (+1.86) for the other prominent molecules. According to this, a very sharp change between logP values and binding affinity has not been observed. On the other hand, decreased dipole moment (μ) has been shown to impact binding affinity. The structure MMV019662, which h showed the highest affinity, has a dipole moment of μ=3.92, while the reference molecule MMV020291 has a dipole moment of μ=6.17. The decrease in the dipole moment (μ) of the other molecules given in Table 2 has resulted in higher binding affinities. It's important to mention that there is a clear correlation between higher molecular weight (M_W) values and a stronger binding affinity.

In the significant regression analyses obtained from the correlation curves performed for 6 different parameters with the calculated values given in Table 2 (using Microsoft Excel), a total of 107, 96, 90, and 96 candidate molecules have been included in the regression curves for the 4NUU, 1B9W, 3SRI, and 4WAT pdb-coded structures, respectively (molecules included in the regressions are shown in Supplementary Tables 4-7). The results are provided in Table 4 below. Furthermore, when the reference structure MMV020291 was included in the multiple regression analysis, no correlation was observed. In order to explain the binding affinities and identify important amino acids, interaction maps with the active site amino acids were generated for the candidate molecules MMV019662, MMV665881, MMV019074, and the reference structure MMV020291. The Table 5 provides

Table 2. 2D plots, SwissAdme maps, calculated logP, μ, η, MW, NRB, TPSA values and binding affinities (kcal.mol-1) of examined structures for 4WAT, 4NUU, 3SRI and 1B9W protein structures

MMV019662	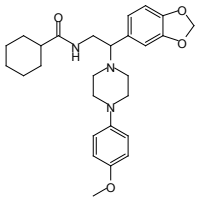	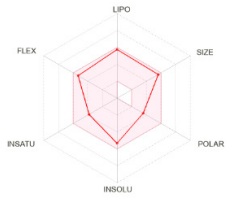	logP	μ	η	MW	NRB
			-0.49	3.92	-3.87	465.58	8
			TPSA	**4NUU**	**1B9W**	**3SRI**	**4WAT**
			63.27	-8.4	-7.3	-8.9	-7.1
MMV019110	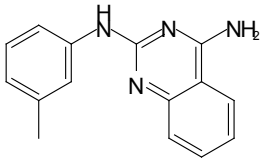	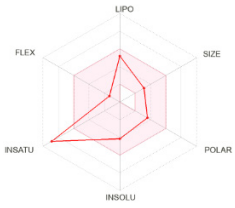	logP	μ	η	MW	NRB
			0.59	1.85	-3.77	286.76	2
			TPSA	**4NUU**	**1B9W**	**3SRI**	**4WAT**
			63.83	-6.8	-7.1	-6.9	-6.0
MMV666691	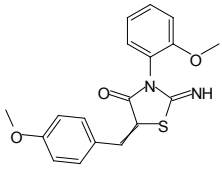	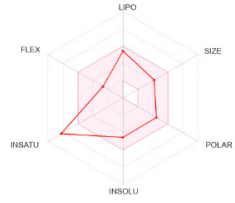	logP	μ	η	MW	NRB
			-0.32	4.22	-3.98	340.4	4
			TPSA	**4NUU**	**1B9W**	**3SRI**	**4WAT**
			87.92	-6.8	-6.3	-7.8	-6.6
MMV000653	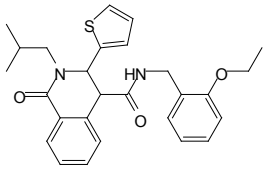	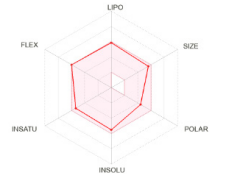	logP	μ	η	MW	NRB
			1.09	1.49	-4.21	462.6	9
			TPSA	**4NUU**	**1B9W**	**3SRI**	**4WAT**
			86.88	-7.1	-7.1	-8.6	-7.0
MMV666688	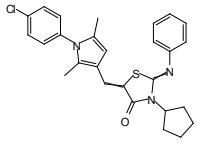	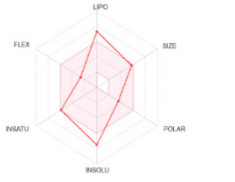	logP	μ	η	MW	NRB
			1.86	5.09	-3.81	476.03	4
			TPSA	**4NUU**	**1B9W**	**3SRI**	**4WAT**
			62.9	-8.2	-7.4	-8.6	-7.3
MMV020651	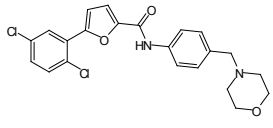	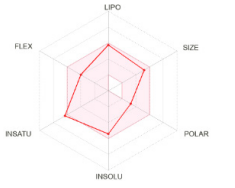	logP	μ	η	MW	NRB
			-1.19	4.92	-3.53	431.31	6
			TPSA	**4NUU**	**1B9W**	**3SRI**	**4WAT**
			54.71	-7.6	-7.5	-7.8	-6.4
MMV020788	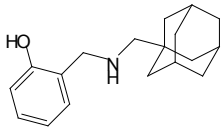	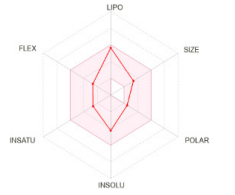	logP	μ	η	MW	NRB
			2.23	3.36	-4.49	307.86	4
			TPSA	**4NUU**	**1B9W**	**3SRI**	**4WAT**
			32.26	-6.7	-6.5	-7.8	-5.8
MMV665800	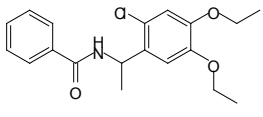	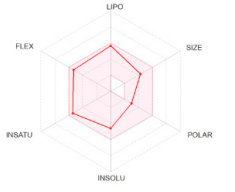	logP	μ	η	MW	NRB
			0.22	0.96	-4.19	347.84	8
			TPSA	**4NUU**	**1B9W**	**3SRI**	**4WAT**
			47.56	-6.8	-6.7	-7.0	-6.6

Table 2. Continued

MMV020505	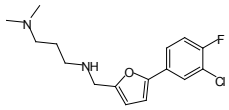	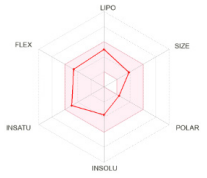	logP	μ	η	MW	NRB
			-0.6	1.17	-3.83	347.26	7
			TPSA	**4NUU**	**1B9W**	**3SRI**	**4WAT**
			28.41	-6.6	-7.0	-6.9	-6.1
MMV665881	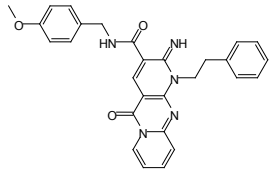	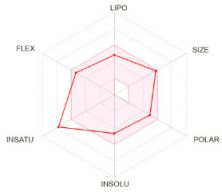	logP	μ	η	MW	NRB
			1.2	5.82	-3.66	479.53	8
			TPSA	**4NUU**	**1B9W**	**3SRI**	**4WAT**
			101.48	-7.8	-7.9	-9.0	-7.3
MMV019074	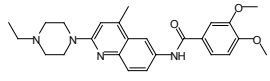	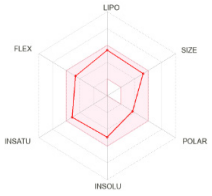	logP	μ	η	MW	NRB
			-1.41	3.06	-3.61	434.53	7
			TPSA	**4NUU**	**1B9W**	**3SRI**	**4WAT**
			66.93	-8.2	-7.3	-8.2	-6.8
MMV665875	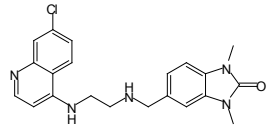	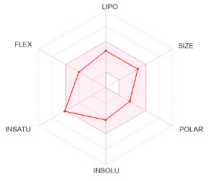	logP	μ	η	MW	NRB
			-1.16	7.52	-3.99	432.35	6
			TPSA	**4NUU**	**1B9W**	**3SRI**	**4WAT**
			63.88	-7.1	-7.3	-7.8	-6.6
MMV665994	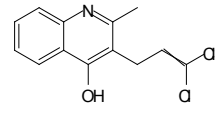	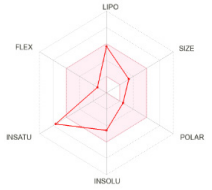	logP	μ	η	MW	NRB
			1.47	6.37	-4.18	268.14	2
			TPSA	**4NUU**	**1B9W**	**3SRI**	**4WAT**
			33.12	-6.4	-6.7	-6.4	-5.7
MMV665939	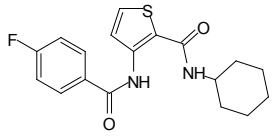	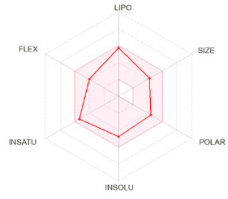	logP	μ	η	MW	NRB
			0.19	3.24	-3.87	346.42	6
			TPSA	**4NUU**	**1B9W**	**3SRI**	**4WAT**
			86.44	-7	-6.6	-7.7	-6.8
MMV006913	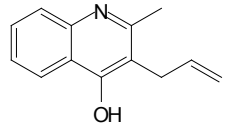	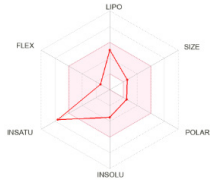	logP	μ	η	MW	NRB
			0.8	6.05	-4.16	199.25	2
			TPSA	**4NUU**	**1B9W**	**3SRI**	**4WAT**
			33.12	-5.2	-6.4	-6.2	-5.6
MMV007041	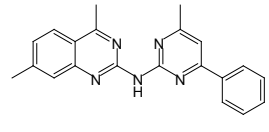	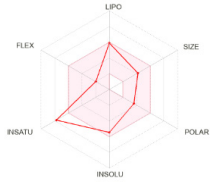	logP	μ	η	MW	NRB
			3.97	1.99	-3.98	341.41	3
			TPSA	**4NUU**	**1B9W**	**3SRI**	**4WAT**
			63.59	-7.6	-7.3	-7.9	-6.5

Table 2. Continued

MMV665836	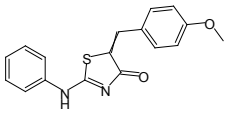	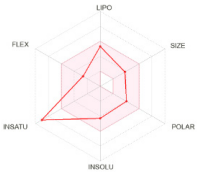	logP	μ	η	MW	NRB
			0.66	3	-3.85	310.37	3
			TPSA	**4NUU**	**1B9W**	**3SRI**	**4WAT**
			75.99	-6.6	-6.6	-8.3	-6.1
MMV000478	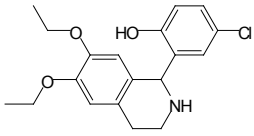	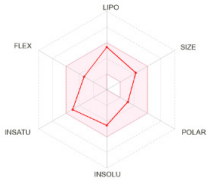	logP	μ	η	MW	NRB
			-1.11	3.26	-4.2	347.84	5
			TPSA	**4NUU**	**1B9W**	**3SRI**	**4WAT**
			50.72	-6.2	-6.6	-6.4	-6.0
MMV085203	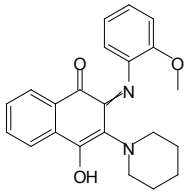	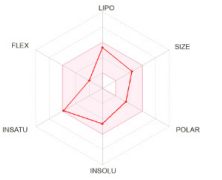	logP	μ	η	MW	NRB
			-0.12	4.81	-3.57	362.42	4
			TPSA	**4NUU**	**1B9W**	**3SRI**	**4WAT**
			58.64	-6.9	-7.7	-7.6	-6.6
MMV008212	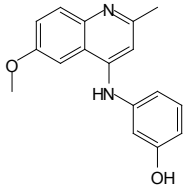	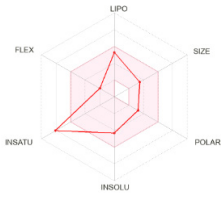	logP	μ	η	MW	NRB
			-1.06	2.42	-3.82	317.78	3
			TPSA	**4NUU**	**1B9W**	**3SRI**	**4WAT**
			54.38	-6.5	-7.1	-7.2	-6.2
MMV000662	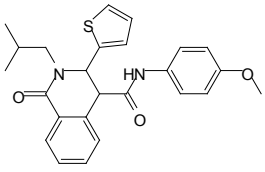	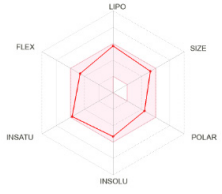	logP	μ	η	MW	NRB
			0.3	1.58	-3.86	434.55	7
			TPSA	**4NUU**	**1B9W**	**3SRI**	**4WAT**
			86.88	-7.2	-6.8	-8.6	-6.8
MMV020291	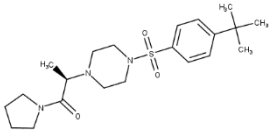	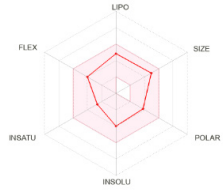	logP	μ	η	MW	NRB
			0.88	6.17	-4.085	407.57	6
			TPSA	**4NUU**	**1B9W**	**3SRI**	**4WAT**
			69.31	-7.1	-7	-7.7	-6.4

NRB: Number of rotatable bonds, TPSA: Topological polar surface area

information on which amino acids are involved in the closest and strongest interactions. When the interactions between the molecules and the 4NUU protein were examined, a relationship was observed between the binding energies, the number of amino acids involved in the interaction, and the distances of the interactions. Particularly, the hydrogen bond distance with amino acid R368 was obtained at a very good level with a distance of 2.49 Å. In addition, for the 4NUU protein, it has been observed that the active site amino acids A360 and Y363 have π-alkyl, alkyl, and hydrophobic interactions with all the molecules studied at distances ranging from 4.79 to 5.36 Å and 4.30 to 5.36 Å, respectively. Upon examination of the interactions obtained for the 1B9W structure, it was found that only amino acid R29 was repeated with all the selected molecules. Conversely, it has been reported in the literature that the reference structure MMV020291 molecule does not experimentally interact with 1B9W. In this regard, the lengths of the interactions and the affinity value of -7.0 kcal.mol^{-1} support the experimental data. It has been observed that the MMV665881 candidate structure has the best binding affinity with 1B9W with a value of -7.9 kcal.mol^{-1}, the closest hydrogen bond distance of 3.09 Å, and the highest number of amino acid interactions. Upon analyzing the outcomes, for the 3SRI protein, it was determined as the structure with the highest number of amino acid interactions and consequently the best binding affinities. Despite the lower number of amino acids involved in the interaction for the MMV665881 structure, the obtained binding affinity value of -9.0 kcal.mol^{-1}, which is the lowest, was interpreted as having two hydrogen bonds at distances of 2.95 and 3.04 Å. However, despite MMV019074 structure having three hydrogen bonds, its binding affinity is approximately reduced by 6 times compared to the MMV665881 structure due to the fact that

Table 3. Staged inhibition assay

	Molecules		
	MMV019662	**MMV665881**	**MMV019074**
DD2 strain, asexual blood stage inhibition (10 μM)	71%	70%	80%
3D7 strain, asexual blood stage inhibition (5 μM)	97%	91%	99%
HB3 strain, early ring (EH) stage	+	GH	+
HB3 strain, late ring (GH) stage	+	T	+
HB3 strain, trophozoite (T) stage	+	S	-
HB3 strain, schizont (S) stage	-	-	-
HB3 strain, merozoite (M) stage	-	-	-
HB3 strain, viability <50% (10 μM)	+	+	+

Table 4. Multiple regression analysis results

PDB ID	Multiple R	R^2	Adjustable R^2	Observation
4NUU	0.936118	0.87632	0.86890	107
1B9W	0.904718	0.81851	0.80628	96
3SRI	0.917513	0.84183	0.83039	90
4WAT	0.905308	0.81958	0.80742	96

Table 5. Molecule-amino acid interaction map (blue, pink, purple, green, brown and yellow colors indicate Hydrophobic, Alkyl, π-Alkyl, H-Bond, π-Cation and π-Anion interactions respectively)

Molecule	**4NUU**							**1B9W**				
	R274	**I277**	**Y278**	**A281**	**A360**	**Y363**	**R368**	**R29**	**C30**	**E36**	**K52**	**G55**
MMV019662	5.10	4.24	5.21	4.08	4.94	4.30	2.49	5.00		4.74	4.72	
MMV665881		4.25		3.51	5.36	4.76	3.00	3.09	4.60	4.32	4.93	
MMV019074		5.15	5.43	4.93	4.79	4.76	2.86	4.46				3.40
MMV020291	2.75		3.74		5.16	5.36		4.69	5.10			3.60
Molecule	3SRI											
	L131	**V137**	**Y142**	**P226**	**Y234**	**Y236**	**Y251**	**A254**	**P350**			
MMV019662		4.95		4.91	5.41		2.79	4.02	4.03			
MMV665881		4.36	4.42		2.95			3.04				
MMV019074	4.28	3.75	3.61	3.04	3.73	3.41	3.21	3.68				
MMV020291	5.43						5.18		5.45			
Molecule	4WAT											
	S197	**Y200**	**F350**	**N352**	**N354**	**R357**	**W447**	**T449**				
MMV019662					3.23		4.81					
MMV665881			5.42				4.19	3.4				
MMV019074	3.65	3.8			3.34	4.57						
MMV020291				2,81								

these hydrogen bonds are at more distant distances. On the other hand, the fact that amino acid Y251 forms 2 hydrogen bonds indicates its effectiveness in the active site. When examining the interaction types and bond distances identified for 4WAT, it is observed that the MMV665881 molecule forms a hydrogen bond with amino acid T449 at a distance of 3.4 Å, and π-alkyl interactions with amino acids W447 and F350, resulting in the most stable binding affinity for the respective protein with a value of -7.3 $kcal.mol^{-1}$. The MMV019662 molecule, on the other hand, forms one hydrogen bond and one π-alkyl interaction, resulting in a binding affinity of -7.1 $kcal.mol^{-1}$. For the 4WAT structure, the experimentally inactive MMV020291 molecule, which was selected as the reference structure, forms only one hydrogen bond with amino acid N352, resulting in the weakest binding energy with a value of -6.4 $kcal.mol^{-1}$.

DISCUSSION

In this study, the values of physicochemical parameters, radar plots, and binding affinities obtained from the docking processes with the 4WAT, 4NUU, 3SRI, and 1B9W PDB coded structures, which are responsible for erythrocyte invasion in malaria disease, are given in Table 2 above. In the regression analysis conducted for the 200 molecules on the 4 different proteins, 107 molecules were included for DBP (PDB id: 4NUU), 96 molecules for MSP1 (PDB id: 1B9W), 90 molecules for AMA1 (PDB id: 3SRI), and 96 molecules for RH5 (PDB id: 4WAT). It was observed that there are 21 common molecules (from Table 2) for all proteins. The results obtained from multiple regression analyses for each protein are provided in Table 6 below. The findings in Table 6 can serve as guiding factors for ligand design. These results have the potential to offer valuable insights for the design of molecules in future studies.

In the study conducted by Dans et al. (18), it was observed that the molecule with the code MMV020291 found in the "Pathogen box" inhibits the deformation and tight junction stages of erythrocyte invasion. Therefore, the binding affinities of MMV020291 with the 4NUU and 3SRI proteins involved in these stages were considered as the ideal binding affinities. At the same time, since it did not bind experimentally in the stages where 1B9W and 4WAT were included, the binding affinities obtained here were determined as the values that needed to be exceeded. MMV019074, MMV019662, and MMV665881 exceeded these threshold values and were recommended based on their physicochemical parameters and SwissADME values. On the other hand, Voorhis et al. (22) experimentally observed that the structures MMV019662 and MMV019074 provide early and late ring stage inhibitions for the HB3 strain, while the structure MMV665881 inhibits the next steps. After merozoites invade the erythrocytes, ring, trophozoite, schizont and merozoite formation occurs, respectively. Since the aim of this study is to prevent erythrocyte invasion, it is very important to observe inhibition especially in the ring stages in the tests mentioned here. Therefore, MMV019662 and MMV019074 stand out slightly over MMV665881 according to inhibition tests.

CONCLUSION

In conclusion, 200 molecules were screened for their potential to inhibit erythrocyte invasion. It was found that 21 of them could be effective in 4 different stages of erythrocyte invasion. When the threshold values determined for the reference molecule known to work in the experiment and the inhibition tests of the screened molecules are examined, MMV019074, MMV019662 and MMV665881 stand out. After analyzing the docking study results of the pertinent molecules, it is apparent that the modeled proteins, 4NUU and 3SRI, exhibit excellent binding affinities that align with the experimental data. These results have provided reliability to the obtained theoretical data, and the molecules MMV019074, MMV019662, and MMV665881 are suggested as potential drug candidates for future experimental stages in malaria treatment research.

Table 6. Affinity coefficient formulas

PDB ID	Affinity
4NUU	$-7{,}416+(-0.010*M_W)+(0.103*NRB)+(0.041*\mu)+(0.008*TPSA)+(-0.066*logP)+(-0.752*\eta)$
1B9W	$-9.685+(-0.004*M_W)+(-0.035*NRB)+(-0.025*\mu)+(0.009*TPSA)+(-0.086*logP)+(-1.029*\eta)$
3SRI	$-5.797+(-0.010*M_W)+(0.081*NRB)+(0.039*\mu)+(-0.004*TPSA)+(-0.154*logP)+(-0.438*\eta)$
4WAT	$-6.170+(-0.005*M_W)+(0.034*NRB)+(0.051*\mu)+(-0.004*TPSA)+(0.042*logP)+(-0.323*\eta)$

*Ethics

Ethics Committee Approval: This study did not involve human participants or animal subjects, and was entirely conducted using publicly available data and computer-based analysis; therefore, ethical approval was not required.

Informed Consent: Not applicable.

Acknowledgments

Thank you to the Medicines for Malaria Venture foundation, which has made open source sets of molecules to find new drugs against malaria.

Footnotes

*Authorship Contributions

Concept: A.B.D., V.E.A., Design: A.B.D., V.E.A., Data Collection or Processing: A.B.D., V.E.A., Analysis or Interpretation: A.B.D., V.E.A., Literature Search: A.B.D., V.E.A., Writing: A.B.D., V.E.A.

Conflict of Interest: No conflict of interest was declared by the authors.

Financial Disclosure: The authors declared that this study received no financial support.

REFERENCES

1. Somer PDA. Sıtma (Malarya) ve tedavisi. Pediatri. 2018; 10: 35-40.
2. Wilder BK, Vigdorovich V, Carbonetti S, Minkah N, Hertoghs N, Raappana A, et al. Anti-TRAP/SSP2 monoclonal antibodies can inhibit sporozoite infection and may enhance protection of anti-CSP monoclonal antibodies. NPJ Vaccines. 2022; 7: 58.
3. Lu C, Song G, Beale K, Yan J, Garst E, Feng J, et al. Design and assessment of TRAP-CSP fusion antigens as effective malaria vaccines. PLoS One. 2020; 15: e0216260.
4. Putaporntip C, Kuamsab N, Rojrung R, Seethamchai S, Jongwutiwes S. Structural organization and sequence diversity of the complete nucleotide sequence encoding the *Plasmodium malariae* merozoite surface protein-1. Sci Rep. 2022; 12: 15591.
5. Wright GJ, Rayner JC. *Plasmodium falciparum* erythrocyte invasion: combining function with immune evasion. PLoS Pathog. 2014; 10: e1003943.
6. Garrido-Cardenas JA, González-Cerón L, Manzano-Agugliaro F, Mesa-Valle C. *Plasmodium* genomics: an approach for learning about and ending human malaria. Parasitol Res. 2019; 118: 1-27.
7. Wicht KJ, Mok S, Fidock DA. Molecular mechanisms of drug resistance in *Plasmodium falciparum* malaria. Annu Rev Microbiol. 2020; 74: 431-54.
8. Yahata K, Hart MN, Davies H, Asada M, Wassmer SC, Templeton TJ, et al. Gliding motility of *Plasmodium* merozoites. Proc Natl Acad Sci U S A. 2021; 118: e2114442118.
9. Chandramohanadas R, Basappa, Russell B, Liew K, Yau YH, Chong A, et al. Small molecule targeting Malaria merozoite surface protein-1 (MSP-1) prevents host invasion of divergent plasmodial species. The J Infect Dis. 2014; 210: 1616-26.
10. Chitarra V, Holm I, Bentley GA, Pêtres S, Longacre S. The crystal structure of C-terminal merozoite surface protein 1 at 1.8 Å resolution, a highly protective malaria vaccine candidate. Molecular Cell. 1999; 3: 457-64.
11. Batchelor JD, Malpede BM, Omattage NS, DeKoster GT, Henzler-Wildman KA, Tolia NH. Red blood cell invasion by *Plasmodium vivax*: structural basis for DBP engagement of DARC. PLoS Pathog. 2014; 10: e1003869.
12. Tolia NH, Enemark EJ, Sim BKL, Joshua-Tor L. Structural basis for the EBA-175 erythrocyte invasion pathway of the Malaria parasite *Plasmodium falciparum*. Cell. 2005; 122: 183-93.
13. Malpede BM, Lin DH, Tolia NH. Molecular basis for sialic acid-dependent receptor recognition by the *Plasmodium falciparum* invasion protein erythrocyte-binding antigen-140/BAEBL. J Biol Chem. 2013; 288: 12406-15.
14. Chen L, Xu Y, Healer J, Thompson JK, Smith BJ, Lawrence MC, et al. Crystal structure of PfRh5, an essential *P. falciparum* ligand for invasion of human erythrocytes. Elife. 2014; 3: e04187.
15. Wang G, MacRaild CA, Mohanty B, Mobli M, Cowieson NP, Anders RF, et al. Molecular insights into the Interaction between *Plasmodium falciparum* apical membrane antigen 1 and an invasion-inhibitory peptide. PLoS One. 2014; 9: e109674.
16. Richard D, MacRaild CA, Riglar DT, Chan JA, Foley M, Baum J, et al. Interaction between *Plasmodium falciparum* apical membrane antigen 1 and the rhoptry neck protein complex defines a key step in the erythrocyte invasion process of malaria parasites. J Biol Chem. 2010; 285: 14815-22.
17. Normand BVL, Tonkin ML, Lamarque MH, Langer S, Hoos S, Roques M, et al. Structural and functional insights into the Malaria parasite moving junction complex. PLoS Pathog. 2012; 8: e1002755.
18. Dans MG, Weiss GE, Wilson DW, Sleebs BE, Crabb BS, de Koning-Ward TF, et al. screening the medicines for Malaria venture pathogen box for invasion and egress inhibitors of the blood stage of *Plasmodium falciparum* reveals several inhibitory compounds. Int J Parasitol. 2020; 50: 235-52.
19. Berman HM, Westbrook J, Feng Z, Gilliland G, Bhat TN, Weissig H, et al. The protein data bank. Nucleic Acids Res. 2000; 28: 235-42.
20. Trott O, Olson AJ. AutoDock vina: improving the speed and accuracy of docking with a new scoring function, efficient optimization, and multithreading. J Comput Chem. 2010; 31: 455-61.
21. Discovery studio modeling environment. San Diego: Dassault Systèmes: Dassault Syst`emes BIOVIA; 2016.
22. Voorhis WCV, Adams JH, Adelfio R, Ahyong V, Akabas MH, Alano P, et al. Open source drug discovery with the malaria box compound collection for neglected diseases and beyond. PLoS Pathogens. 2016; 12: e1005763.
23. Spartan'14, Wavefunction, Inc., Irvine, CA. Available from: https://www.wavefun.com/
24. Daina A, Michielin O, Zoete V. SwissADME: a free web tool to evaluate pharmacokinetics, drug-likeness and medicinal chemistry friendliness of small molecules. Sci Rep. 2017; 7: 42717.
25. Lipinski CA, Lombardo F, Dominy BW, Feeney PJ. Experimental and computational approaches to estimate solubility and permeability in drug discovery and development settings. Adv Drug Deliv Rev. 2001; 46: 3-26.
26. Microsoft Corporation. (2018). Microsoft Excel. Available from: https://office.microsoft.com/excel

Supplementary Tables 1-7: https://l24.im/Q2h1V

Turkiye Parazitol Derg 2025;49(1):10-6
DOI: 10.4274/tpd.galenos.2025.88700

Investigation of the Frequency of *Cryptosporidium* spp. in Immunosuppressed Patients with Diarrhea

İmmünosüpresif İshalli Hastalarda Cryptosporidium spp. Sıklığının Araştırılması

Duygu Beder[1], Fatma Esenkaya Taşbent[2]
[1]Meram State Hospital, Clinic of Medical Microbiology, Konya, Türkiye
[2]Necmettin Erbakan University Meram Faculty of Medicine, Department of Medical Microbiology, Konya, Türkiye

Cite this article as: Beder D, Esenkaya Taşbent F. Investigation of the frequency of *Cryptosporidium* spp. in immunosuppressed patients with diarrhea. Turkiye Parazitol Derg. 2025;49(1):10-6.

ABSTRACT

Objective: We aimed to investigate the frequency of *Cryptosporidium* spp. in immunosuppressed patients who were admitted with diarrhea by microscopic, serological, and molecular methods and to evaluate the results in comparison with the direct fluorescent antibody (DFA) method.

Methods: We analyzed 90 stool samples from immunosuppressed patients with diarrhea. All stool samples were examined using modified acid-fast staining, polymerase chain reaction (PCR) and enzyme-linked immunosorbent assay (ELISA) tests for the detection of *Cryptosporidium* spp. samples examined with the DFA method were selected randomly, including samples found positive in other diagnostic tests. Stool samples that were positive in any of these diagnostic tests were evaluated by immunochromatographic card test.

Results: Our study included 90 samples, of which 44 (48.8%) and 46 (51.2%) were from male and female patients, respectively. The mean age of the patients was 37.8±27.5. Thirty-one (34.4%) of the samples were from pediatric patients and their mean age was 5.3±4.34. The methods used did not show a statistically significant difference between the positivity status and patient age and gender ($p>0.05$). *Cryptosporidium* spp. positivity was detected in five samples (5.6%), two samples (2.2%), and one sample (1.1%) by using the modified acid-fast staining, PCR, and ELISA methods, respectively. Six of 51 samples to which the DFA method was applied were detected positive. In 4 of the 7 stool samples that were found positive by any of these methods, *Cryptosporidium* spp. was detected positive by the immunochromatographic card test.

Conclusion: When the DFA method is accepted as the gold standard method in the diagnosis of *Cryptosporidium* spp., the modified acid-fast method can be used in routine diagnosis with high sensitivity and specificity. Besides, it immunochromatographic diagnostic tests thought to be useful in laboratories with intensive workflow due to their practical use and rapid results.

Keywords: *Cryptosporidium*, diarrhea, direct fluorescent antibody, immunosuppressive

ÖZ

Amaç: Bu çalışmada ishal şikayeti ile başvuran immünosüpresif hastalarda *Cryptosporidium* spp. sıklığını mikroskobik, serolojik ve moleküler yöntemlerle araştırmayı ve sonuçları direkt floresan antikor (DFA) yöntemi ile karşılaştırarak değerlendirmeyi amaçladık.

Yöntemler: İmmünosüpresif ishalli hastalardan alınan 90 dışkı örneği çalışmaya alınmıştır. *Cryptosporidium* spp. tespiti amacıyla tüm dışkı örneklerine modifiye asit fast boyama, polimeraz zincir reaksiyonu (PZR) ve enzyme-linked immunosorbent assay (ELISA) testi uygulanmıştır. DFA yöntemi ile incelenen örnekler, diğer tanı testlerinde pozitif bulunan örneklere ek olarak diğer örneklerden rastgele seçilmiştir. Bu tanı yöntemlerinden herhangi biriyle pozitif saptanan dışkı örnekleri immünokromatografik kart test ile değerlendirilmiştir.

Bulgular: Çalışmaya alınan 90 örneğin 44'ü (%48,8) erkek, 46'sı (%51,2) kadın hastalara aittir. Hastaların yaş ortalaması 37,8±27,5 olarak bulunmuştur. Çalışmada çocuk hastalara ait 31 (%34,4) örnek bulunmaktadır ve bu hastaların yaş ortalamaları 5,3±4,34 olarak tespit edilmiştir. Kullanılan yöntemlerin hiçbirinde hastaların pozitiflik durumu ile yaşı ve cinsiyeti arasında istatistiksel olarak anlamlı bir farklılık bulunmamıştır ($p>0,05$). Çalışılan dışkı örneklerinde modifiye asit fast yöntemiyle 5 (%5,6), PZR ile 2 (%2,2), ELISA yöntemiyle 1 (%1,1) örnekte *Cryptosporidium* spp. pozitif tespit edilmiştir. DFA yöntemi uygulanan 51 örneğin 6'sı pozitif saptanmıştır. Bu yöntemlerden herhangi biri ile pozitif bulunan 7 dışkı örneğinin 4'ünde immünokromatografik kart test ile *Cryptosporidium* spp. pozitif tespit edilmiştir.

Received/Geliş Tarihi: 09.01.2025 **Accepted/Kabul Tarihi:** 14.04.2025 **Epub:** 17.04.2025 **Publication Date/Yayınlanma Tarihi:** 09.05.2025

Address for Correspondence/Yazar Adresi: Duygu Beder, Meram State Hospital, Clinic of Medical Microbiology, Konya, Türkiye
E-mail/E-Posta: duyguzel29@gmail.com **ORCID ID:** orcid.org/0000-0001-5647-8458

***The study was prested as an oral presentation at the 1st International MİKPEDKON Congress (15-18 May 2024, Bolu, Türkiye).**

Türkiye PARAZİTOLOJİ Dergisi

Sonuç: *Cryptosporidium* spp. tanısında DFA yöntemi altın standart yöntem kabul edildiğinde modifiye asit fast yöntemi yüksek duyarlılık ve özgüllükle rutin tanıda kullanılabilir. Ayrıca yoğun iş akışı olan laboratuvarlarda immünokromatografik tanı testlerinin pratik kullanımı ve hızlı sonuç sağlaması nedeniyle faydalı olacağı düşünülmektedir.
Anahtar Kelimeler: *Cryptosporidium*, ishal, direkt floresan antikor, immünosüpresif

INTRODUCTION

The severity and duration of infections caused by *Cryptosporidium* spp. vary depending on the type, immunity, and host age (1). Cryptosporidiosis involves the jejunum and ileum in patients, making diarrhea the most typical clinical finding of the infection (2). Other less frequently detected clinical findings are abdominal pain, nausea, and vomiting (3). Extraintestinal system involvement, such as cholecystitis, pancreatitis, and cholangitis can also be observed in immunosuppressive patient groups, such as acquired immunodeficiency syndrome (AIDS) (1).

Respiratory cryptosporidiosis commonly occurs in children, and although the presentation is generally asymptomatic, pulmonary infiltration and respiratory distress can be detected (4). Cough is the main symptom when the lungs or trachea is involved (1). In addition, cryptosporidiosis persisting for a long time in childhood may lead to growth and developmental retardation (5).

Additionally, asymptomatic infections have also been reported (3). Anorexia, depression, myalgia, headache, and fatigue have been reported in asymptomatic cases. Asymptomatic patients are more common than diagnosed patients in developed or developing countries (6-8).

Although clinical symptoms vary individually, the excreted amount of oocyst is closely related to the immune status and host age. The infection, which generally has an asymptomatic course in healthy people or heals spontaneously within 2-3 weeks causes more severe clinical symptoms, particularly in children, those with insufficient oral intake, and immunosuppressed and elderly people (9). Persistent diarrhea lasting for a long time can become chronic and lead to resulting in death (10).

Infections caused by intestinal parasites are commonly seen in immunosuppressed patients. Parasitic agents can cause diarrhea varying in severity and may result in mortality (11). In developing countries, the frequency of diarrhea due to parasitic agents was >90% in the immunosuppressed patient population. *Cryptosporidium* is one of the most frequently detected pathogens in these patients (12).

Cases of this agent may not be adequately detected due to symptoms of cryptosporidiosis being similar to other gastroenteritis symptoms, stool samples of patients complaining of diarrhea not being routinely evaluated for *Cryptosporidium*, and not using advanced diagnostic techniques in many cases (13).

Cryptosporidiosis can be diagnosed using histological and molecular methods, microscopic examination, and serological techniques, such as direct fluorescent antibody (DFA) and enzyme-linked immunosorbent assay (ELISA) (14,15). The development of microscopical techniques revolutionized the morphological sciences, progressively providing new levels of magnification and resolution for exploring biological and non-biological samples. Furthermore, the high resolution of microscopic techniques also allowed the detection and visualization of different types of microorganisms, by exploring in a deep way the causative agent of different pathologies (16).

Microscopic examination is the most commonly preferred method. However, evaluating *Cryptosporidium* oocysts using direct microscopic examination is challenging due to their small size which is very similar to yeasts. The chance of diagnosing *Cryptosporidium* spp. can be increased with concentration methods (17,18). Microscopic examination after acid-fast staining is preferable because it is cheap, allows the internal structure of oocysts to be evaluated, and preparations can be stored for a long time thanks to permanent staining. However, due to disadvantages such as the need for a long time and experience for evaluation and low reproducibility, different diagnostic methods are also needed (17).

Molecular techniques are diagnostic methods that provide rapid results with high specificity and sensitivity based on the amplification of the appropriate gene region. Nowadays, it has started to replace conventional diagnostic techniques based on the identification of phenotypic characteristics and even became the gold standard for the detection of some microorganisms. It can distinguish between closely species or subtypes. It is also of great importance in the diagnosis of microorganisms that have lost their viability during the transport phase (19).

The DFA method, which detects surface antigens, technique offers the highest combination of sensitivity and specificity and is considered the gold standard by many laboratories (20).

We aimed to investigate the frequency of *Cryptosporidium* spp. in immunosuppressed patients who were admitted with diarrhea by microscopic, serological, and molecular methods and to evaluate the results in comparison with the DFA method.

METHODS

This prepared study was evaluated and approved by Necmettin Erbakan University Faculty of Medicine Hospital Non-Drug and Non-Medical Device Research Ethics Committee on 15.04.2022 with decision number 2022/3755. Since our study was conducted on stool samples routinely sent to the microbiology laboratory, patient consent was not obtained. This study, with project number 221518022, was supported by Necmettin Erbakan University Scientific Research Project Coordination Office.

Gender, age, clinical and diagnostic information of the patients were obtained from our hospital's laboratory information system. The study included patients receiving immunosuppressive therapy after transplantation, patients receiving chemotherapy due to malignant solid tumors or hematological malignancies, patients immunosuppressed due to hematological malignancies, patients receiving corticosteroid therapy for more than two months, and patients diagnosed with primary immunodeficiency.

A simple sedimentation technique was applied to the samples for fecal concentration. Subsequently, direct microscopic examination was performed with physiological saline (0.9% NaCl) on the slides. For stained microscopic examination, a smear was prepared from the stool samples, and modified acid-resistant Ehrlich-Ziehl-Neelsen (EZN) was performed. We also recorded other parasitic agents detected during direct microscopic examination or stained

(modified acid-resistant staining) microscopic examination was recorded.

The remaining samples were divided into three for ELISA, DFA, and polymerase chain reaction (PCR) analyses without adding any preservative solution, divided into 1.5 mL eppendorf tubes, and kept at -80 °C to be stored until analyses.

In the ELISA method, the *Cryptosporidium* RIDASCREENR, C 1201 r-Biopharm commercial kit was used to detect *Cryptosporidium parvum* and *Cryptosporidium hominis* antigens.

Before the molecular study, the QIAamp DNA Stool Mini Kit (QIAGEN GmbH, Hilden, Germany) was used for DNA extraction of stool samples. Subsequently, probe-based real-time PCR analysis of the extracted samples was performed using the Roche real-time PCR device (Roche, Switzerland 2004). The probe and primer sequences defined in the PCR study in the literature were used for *Cryptosporidium* (22). These sequences are shown in Table 1.

PCR primers and probes (Table 1) were designed using the BioEdit software program, version 7.0.9.0 (http://www.mbio.ncsu.edu/BioEdit/bioedit.html) to create Clustal W (23) alignments of representative *Cryptosporidium* sequences from GenBank [National Center for Biotechnology Information (NCBI)]; http://www.ncbi.nlm.nih.gov/GenBank/). The Primer Express software program (Applied Biosystems, Warrington, United Kingdom) was used to calculate melting temperatures and check for undesirable inter and intramolecular binding. Primer and probe sequences were then checked for cross-reactions with non-target sequences on the GenBank database using the basic local alignment search tool (http://www.ncbi.nlm.nih.gov/blast/Blast.cgi).

Cryptosporidium and *Giardia* antigens were investigated using the DFA method with the Merifluor *Cryptosporidium/Giardia* Direct Immunofluorescence Assay (DFA; Meridian Diagnostics, Inc., Cincinnati, Ohio, USA) commercial kit. Samples examined with the DFA method were selected randomly by including samples found positive in other diagnostic tests. The samples detected as positive by any of the diagnostic methods were evaluated with an immunochromatographic card test as a using the commercial *Entamoeba/Giardia/Crypto* Combo Rapid Cassette test (Microcult, Biotech, China). ELISA, DFA, PCR and card tests were used following the manufacturer's recommendations.

Using the DFA method as the reference method, the positive and negative predictive values, specificity, sensitivity and accuracy rates of serological, molecular and microscopic methods were determined. The accuracy value was found by dividing the sum of the true positive and true negative values by the total data.

Statistical Analysis

Statistical analysis of the data was analyzed with SPSS (Statistical Package for Social Sciences) ver.23 statistical package program. Continuous variables are expressed as mean ± standard deviation, minimum and maximum values, and categorical variables are expressed as numbers and percentages. Differences between categorical variables were examined with Pearson chi-square and Fisher-Freeman-Halton Exact tests. The significance level was determined as $p<0.05$.

RESULTS

The frequency of *Cryptosporidium* spp. was investigated in 90 immunosuppressed patients with diarrhea, of whom 31 were children, between May 2022-December 2022.

The ages of the patients ranged between 0 and 81 years, and the mean age was 37.8±27.5 years. Moreover, 31 (34.4%) samples were from pediatric patients, of which 18 (58%) and 13 (42%) were from men and women, respectively, and their mean age was 5.3±4.34 years. Of the 59 adult patients, 26 (44%) and 33 (56%) were men and women, respectively. Of the 90 included samples, 44 (48.8%) and 46 (51.2%) were from men and women patients, respectively. The methods used did not show a statistically significant difference between the positivity status and patient age (p=0.688) or between the positivity status and sex (p=0.261).

The study patients frequently consist of patients in pediatrics, oncology and hematology clinics. The positivity rates of patients coming from these departments are 11.1%, 11.7% and 8.3% respectively. In this study, there were 4 patients from the immunology and allergic diseases clinics, and the positivity rate in this patient group was 25%. Table 2 shows the distribution and rates of patients included in the study according to clinics.

Among the study participants, 54.4%, 14.4%, 11.1%, 8.8%, and 7.7% were diagnosed with a malignant solid tumor, lymphoma, primary immunodeficiency, multiple myeloma, and leukemia, respectively.

In the microscopic examination using acid-fast modified EZN staining, *Cryptosporidium* spp. oocysts were detected in five samples (Figure 1). *Cyclospora* spp. oocyst was seen in one sample. In microscopic examination, *Giardia* spp. and *Blastocystis* spp. were detected in 2 and 26 samples, respectively.

Cryptosporidium positivity was detected in one and two samples using ELISA and PCR methods, respectively. In this study, in which *Cryptosporidium* and *Giardia* antigens were investigated by DFA in 51 stool samples, including those positive in any of the microscopic, ELISA or PCR evaluations, *Cryptosporidium* spp. was found positive in six samples and *Giardia* spp. was found positive in three samples (Figure 2).

Because the DFA is considered the gold standard method, the DFA results were considered as the main results in the comparative evaluation of the methods in statistical analysis. Based on the DFA method, the modified acid-fast staining method had a sensitivity, specificity, positive predictive value, negative predictive value, and accuracy rate of 83.33%, 100%, 100%, 97.82%, and 98.03%,

Table 1. Real-time PCR primers and probes used in this study

Target locus	Primer/probe	Position (nt)[a]	Sequence (5'-3')[b]
Cryptosporidium species SSU *rRNA* gene	CRU18SF[c]	440-468	GAGGTAGTGACAAGAAATAACAATACAGG
	CRU18SR[c]	710-738	CTGCTTTAAGCACTCTAATTTTCTCAAAG
	CRU18STM	587-609	FAM-TACGAGCTTTTTAACTGCAACAA MGB-NFQ

[a]: Positions on *Cryptosporidium* species SSU *rRNA* gene (GenBank accession numbers AF164102). nt: Nucleotide(s), [b]: MGB: Minor groove binder, NFQ: Non-fluorescent quencher, [c]: Modified from reference (21), PCR: Polymerase chain reaction

Table 2. Distribution and rates of patients included in the study according to clinics

Clinics	Number of samples (n)	Rate in the sample group (%)
Pediatrics	27	30
Medical oncology	17	18.9
Hematology	12	13.3
Gastroenterology	11	12.2
Pediatric hematology-oncology	7	7.7
Internal medicine	4	4.4
Immunology and allergic diseases	4	4.4
Radiation oncology	3	3.3
Bone marrow transplantation unit	2	2.2
Nephrology	1	1.1
Organ and tissue transplantation center	1	1.1
Chest diseases	1	1.1
Total	90	100

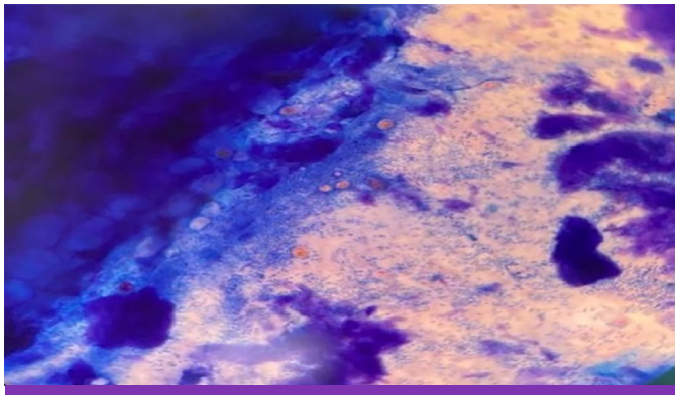

Figure 1. *Cryptosporidium* spp. oocysts in EZN staining (x100)
EZN: Ehrlich-Ziehl-Neelsen

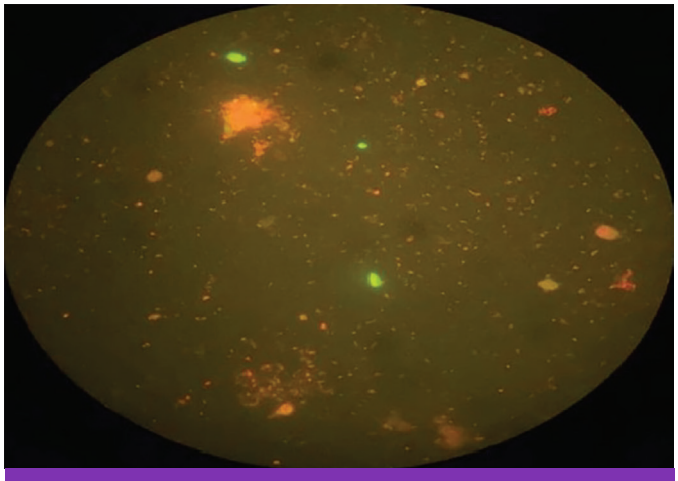

Figure 2. In the examination performed by the DFA method, *Cryptosporidium* spp. oocysts and *Giardia* spp. cysts (x100)
DFA: Direct fluorescent antibody

respectively. Based on the DFA method, PCR had a sensitivity, specificity, positive predictive value, negative predictive value, and accuracy rate of 33.3%, 100%, 100%, 91.83%, and 92.15%, respectively. Based on the DFA method, ELISA had a sensitivity, specificity, positive predictive value, negative predictive value, and accuracy rate of 0%, 97.77%, 0%, 88%, and 86.27%, respectively. The specificity and sensitivity, positive and negative predictive values and accuracy rates of serological, molecular and microscopic methods compared to the gold standard method the DFA method, are shown in Table 3. The stool samples of seven patients found to be positive with any of the other diagnostic tests were re-examined with the immunochromatographic card test, resulting in four samples being positive. The characteristics of patients with *Cryptosporidium* positivity are shown in Table 4.

DISCUSSION

Cryptosporidium spp., one of the factors causing infectious diarrhea, is an opportunistic agent that inhabits most commonly in the jejunum and less frequently in organs, such as the lungs, gallbladder, and liver. This parasite can cause mortality in older people and children, in the immunosuppressive patient group, and malnourished individuals (20). Initially, it causes watery diarrhea in immunosuppressive patients. Furthermore, it also causes gastroenteritis with a more benign course in immunocompetent individuals (24).

After evaluating the literature, sex was not associated with the incidence of *Cryptosporidium* (25). In our study, sex did not affect the positivity of *Cryptosporidium*. *Cryptosporidium* is an important cause of diarrhea in childhood, and the parasite is more symptomatic in children (4). In this study, the positivity rate was higher in children than in the adult age group, but the difference was not statistically significant.

This parasite is found worldwide and may be the underlying cause of diseases with diarrhea as the main symptom (26). *Cryptosporidium,* which is associated with premature deaths and growth and development retardation in childhood, caused a waterborne epidemic affecting 400,000 people in Milwaukee, USA, in the 1990s. Currently, it can be found almost everywhere, except in Antarctica. Although *Cryptosporidium* is detected in 1% of immunocompetent people in developed countries, it is 5-10% in countries with low socioeconomic levels. This rate varies between 10% and 25% in children who consult with complaints of diarrhea (4).

Because this pathogen is more commonly detected in immunocompromised patients, epidemiological studies were mostly conducted on immunosuppressed patients with diarrhea (27). Therefore, the data were highly inconsistent, which may be due to the stage of the infection, characteristics and number of the evaluated patient population, sensitivity of the diagnostic methods, and the climatic conditions (28).

Cryptosporidium spp. positivity was found in 6.3% of 427 immunocompromised patients with diarrhea in a study conducted in Egypt, 12.6% of 87 patients with colorectal malignancy and diarrhea in a study conducted in Poland (29,30), 12% of 137 HIV patients with diarrhea, and 12.4% of 84 immunocompromised patients with diarrhea (31,32).

In the studies evaluating *Cryptosporidium* spp. incidence in the immunocompromised patient population in Türkiye, *Cryptosporidium* spp. positivity was found in 6.4% of 47

Table 3. Specificity and sensitivity, positive and negative predictive values and accuracy rates of serological, molecular and microscopic methods compared to the gold standard method DFA method

	Microscopy (%)	PCR (%)	ELISA (%)
Sensitivity	83.33	33.3	
Specificity	100	100	97.77
Positive predictive value	100	100	0
Negative predictive value	97.82	91.83	88
Accuracy rate	98.03	92.15	86.27

PCR: Polymerase chain reaction, ELISA: Enzyme-linked immunosorbent assay, DFA: Direct fluorescent antibody

Table 4. Characteristics of patients with *Cryptosporidium* positivity

Age	Sex	Department	Diagnosis	Microscopy	PCR	DFA	ELISA	Card test
0	Men	Pediatrics	Lymphoma	Positive	Negative	Positive	Negative	Positive
0	Women	Pediatrics	ALL	Positive	Negative	Positive	Negative	Positive
7	Men	Pediatrics	Solid tumor	Positive	Negative	Positive	Negative	Negative
54	Men	Medical oncology	Solid tumor	Negative	Negative	Negative	Positive	Negative
61	Men	Hematology	Lymphoma	Positive	Positive	Positive	Negative	Negative
67	Women	Medical oncology	Solid tumor	Positive	Negative	Positive	Negative	Positive
77	Men	Immunology and allergic diseases	Primary immune deficiency	Negative	Positive	Positive	Negative	Positive

PCR: Polymerase chain reaction, DFA: Direct fluorescent antibody, ELISA: Enzyme-linked immunosorbent assay

patients diagnosed with chronic renal failure (33), 5.3% of 94 immunosuppressive patients with malignant solid tumors receiving chemotherapy and complaining of diarrhea for >5 days, and 8.3% in 72 stool samples of immunosuppressive patients with diarrhea (34,35).

In our study, *Cryptosporidium* spp. was detected in 7 (7.8%) of 90 patients with complaints of immunosuppressive diarrhea, by at least one of the methods used.

The DFA method is used as the gold standard in reference laboratories in the USA and Europe (4). Therefore, in our study, based on DFA, in the modified acid-fast EZN staining method, the sensitivity and specificity were 83.33% and 100%, respectively. The high cost of DFA tests is the most important problem that limits their use in routine laboratories. Modified EZN staining, which has high sensitivity and specificity, can be used to detect *Cryptosporidium* spp. as a more cost-effective method in experienced laboratories, particularly in sensitive groups, such as immunosuppressed and pediatric patients.

Depending on the commercial kit used, the efficacy of the ELISA method varies. In our study, ELISA was unsuccessful in detecting *Cryptosporidium* spp. In another study, PCR was considered 10^3-10^4 times more sensitive than the ELISA method (36). Moreover, false-positive results can be due to cross-reactions against common antigens in many pathogens, particularly apicomplexan parasites (27). The high cost of this method is another disadvantage, as well as sample collection before the examination (34).

A previous study evaluated 80 stool samples of patients presenting with gastrointestinal system complaints, and *Cryptosporidium* spp. positivity was found in three (3.75%) and five samples (6.25%) by using acid-fast staining and ELISA, respectively. Three positive samples detected using acid-fast staining were also positive with the ELISA technique (37). In another study, the ELISA method detected *Cryptosporidium* spp. in 2.8% of 723 stool samples in the patient group presenting with the same complaints (27). In our study, the ELISA method detected positivity in only one patient, which could not be confirmed by other diagnostic methods. The low sensitivity of the ELISA method may be related to the kit used or the *Cryptosporidium* spp. oocysts may not have been distributed homogeneously in the stool of the positive samples.

Recently, molecular methods have been preferred because they can perform genotyping based on nucleic acid analysis, and the opportunity to easily evaluate many samples, and guide the treatment process (38). In order to apply molecular biology techniques in studies with genetic material, DNA and RNA molecules must be obtained in pure form before PCR, taking into account that they will also contain inhibitors. Otherwise, results may be masked by taq polymerase enzyme inhibitors in the sample. The basic components used in PCR are target DNA or RNA (template), taq DNA polymerase enzyme, primers, deoxynucleotides, buffer liquid, pH, Mg+2 ions. Temperature parameters (especially annealing temperature) and Mg+2 concentration that are not in the appropriate range, and the use of poor quality polymerase enzyme may lead to erroneous PCR results. Additionally, the design of oligonucleotide primers is only possible with known strains of microorganisms and known sequences of these strains. False negatives may occur in inappropriate primer selections. Another factor that may cause problems in the functions of PCR is unexpected mutations that occur in microbial genomes (19). In conditions where parasite oocysts are not homogeneously distributed throughout the stool, molecular techniques detect fewer positive samples than microscopic examination (39). Furthermore, polysaccharides, bile salts, or bilirubin in the stool can inhibit the PCR study (34). If oocyst damage occurs before DNA isolation PCR can not detect *Cryptosporidium* spp., resulting in discrepant data

between microscopic evaluation data and PCR results (39,40). The inclusion of molecular techniques in routine diagnosis will only be possible when these problems are solved and ensure a certain standardization (40).

In our study, only two patients were positive using PCR, and based on the DFA test, the sensitivity and specificity were 33.3% and 100%, respectively. False negative results in PCR studies are thought to be caused by inhibitors in the stool sample, problems in the DNA extraction stage, or primer probe optimization. Some studies in the literature also showed that PCR had lower sensitivity than microscopic evaluation (38,41).

In a study conducted in our country on 36 immunosuppressed patients with diarrhea, the *Cryptosporidium* was investigated using microscopic examination with modified acid-fast staining, molecular techniques, and DFA testing. Based on the data, one sample and three samples were positive with acid-fast staining and DFA method, respectively; however, no positive sample could be detected with the molecular technique used (41). Another study evaluating 80 immunosuppressed patients with diarrhea, three, five, and four positive samples were found by microscopic examination, ELISA, and DFA, respectively, whereas PCR did not detect positivity (38).

In the stool samples of 90 immunosuppressive patients in our study, positivity was detected in five, one, and two samples by microscopic examination, ELISA, and PCR, respectively. All the positive samples were positive with DFA, except for the positive sample detected by ELISA, and DFA positivity was detected in 6 of the 51 samples studied. An immunochromatographic rapid diagnostic test was used in seven positive samples by any of the methods, and four samples were positive with the rapid diagnostic test. Rapid diagnostic tests will be useful in rapid diagnosis in laboratories with intensive sample studies, particularly in sensitive groups with chronic diarrhea. In the study, *Cyclospora* spp., another opportunistic pathogen, were detected in one patient, and *Giardia* spp., an important causative agent of diarrhea, were detected in three patients.

The inadequate effectiveness of the commercial kit used in the ELISA test and the problems experienced in the DNA extraction phase and/or primer probe optimization in PCR caused limitations in our study. In addition, DFA and immunochromatographic rapid diagnostic tests could not be applied to all samples. The small number of positive samples does not allow for a fully accurate assessment of the usefulness of these methods. Studies in which all diagnostic techniques are applied on more samples are needed.

CONCLUSION

Our study especially showed that the probability of detection of *Cryptosporidium* spp. in stool samples from immunosuppressed patients with diarrhea should not be underestimated. Considering that the number of immunosuppressive patients increases daily, rapid and reliable detection of this agent is extremely important in the routine work of laboratories, particularly for the immunosuppressive patient group. Therefore, diagnostic algorithms should be created for the diagnosis of *Cryptosporidium* spp. in secondary and tertiary care hospitals with more immunosuppressive patient follow-up.

Although diagnostic methods used to detect *Cryptosporidium* oocysts have advantages, each has its disadvantages. Based on the gold standard method DFA, modified acid-fast staining has high sensitivity and specificity, but it requires labor and technical experience. Performing modified acid-fast staining and evaluating all stool samples received in laboratories with intensive sample flow may not be possible. However, in high-risk patient groups, evaluation of samples using modified acid-fast staining as a minimum diagnostic method will be useful for the diagnosis of *Cryptosporidium*. Besides, it immunochromatographic diagnostic tests will be useful in laboratories with intensive workflow due to their practical use and rapid results.

*Ethics

Ethics Committee Approval: Non-Drug and Non-Medical Device Research Ethics Committee on 15.04.2022 with decision number 2022/3755.

Informed Consent: Since our study was conducted on stool samples routinely sent to the microbiology laboratory, patient consent was not obtained.

Footnotes

*Authorship Contributions

Surgical and Medical Practices: D.B., Concept: F.E.T., Design: F.E.T., Data Collection or Processing: D.B., Analysis or Interpretation: F.E.T., Literature Search: D.B., Writing: D.B.

Conflict of Interest: No conflict of interest was declared by the authors.

Financial Disclosure: This study, with project number 221518022, was supported by Necmettin Erbakan University Scientific Research Project Coordination Office.

REFERENCES

1. Sen ZS, Tasar MA, Kaya FD, Gunes A, Vezir E, Gulsen HH. A rare complication of acute diarrhae caused by *Cryptosporidium*: possible hepatobiliary system involvement in a child without immunodeficiency. Mikrobiyol Bul. 2019; 53: 464-71.
2. Yalçın S, Doğan NY, Mor N. Determination of *Cryptosporidium* spp. by molecular methods in different water resources of Erzincan province. Erzincan University Journal of Science and Technology. 2019; 12: 1-13.
3. Ekici A, Unlu A, Aydemir S, Barlik F, Yilmaz H. Subtyping of *Cryptosporidium parvum* obtained from humans and calves in Van, Turkey. Iran J Parasitol. 2022; 17: 366-74.
4. Miman O, Saygi G. Temel Tibbi Parazitoloji. Istanbul: Istanbul Yayınevi; 2018: 241-248.
5. Hossain MJ, Powell H, Sow SO, Omore R, Roose A, Jones JCM, et al. Clinical and epidemiologic features of *Cryptosporidium*-associated diarrheal disease among young children living in sub-Saharan Africa: the vaccine impact on diarrhea in Africa (VIDA) study. Clin Infect Dis. 2023; 76: S97-S105.
6. Robinson P, Okhuysen PC, Chappell CL, Lewis DE, Shahab I, Janecki A, et al. Expression of tumor necrosis factor alpha and interleukin 1 beta in jejuna of volunteers after experimental challenge with *Cryptosporidium parvum* correlates with exposure but not with symptoms. Infect Immun. 2001; 69: 1172-4.
7. Dann SM, Wang HC, Gambarin KJ, Actor JK, Robinson P, Lewis DE, et al. Interleukin-15 activates human natural killer cells to clear the intestinal protozoan cryptosporidium. J Infect Dis. 2005; 192: 1294-302.
8. Huang DB, White AC. An updated review on *Cryptosporidium* and *Giardia*. Gastroenterol Clin North Am. 2006; 35: 291-314.
9. Zhao W, Ren G, Jiang W, Wang L, Wang J, Yuan Z, et al. Genetic characterizations of *Cryptosporidium* spp. from children with or without diarrhea in Wenzhou, China: high probability of zoonotic transmission. BMC Microbiol. 2024: 24: 113.

10. Aydemir S, Durmaz H, Aydemir ME, Kılıc S, Demir A, Halidi AG, et al. Investigation of the effect of pasteurization on the viability of *Cryptosporidium parvum* in cow's milk by propidium monoazide qPCR. Mikrobiyol Bul. 2023; 57: 660-6.
11. Atasever M, Mazlum H, Cevik B, Uzum H. Investigating the quality of public fountain water in Gümüşhane province and the presence of *Cryptosporidium* spp. using the PCR method. Turkish Journal of Agriculture Food Science and Technology. 2024; 12: 1530-8.
12. Zorbozan O, Quliyeva G, Tunalı V, Özbilgin A, Turgay N, Gökengin AD. Intestinal protozoa in HIV-infected patients: A retrospective analysis. Turk J Parazitol. 2018; 42: 187-90.
13. Khalil SB, Mirdha BR, Paul J, Panda A, Makharia G, Chaudhry R, et al. Development and evaluation of molecular methods for detection of *Cryptosporidium* spp. in human clinical samples. Exp Parasitol. 2016; 170: 207-13.
14. Sears CL, Kirkpatrick BD. Cryptosporidiosis and isosporiosis. In: Principles and Practice of Clinical Parasitology; 2001; 139-164.
15. Çuhadar V, Sengül M, Mete E. Investigation of *Cryptosporidium parvum* in water resources in Mardin province. Turk Mikrobiyol Cemiy Derg. 2023; 53: 156-62.
16. Torge D, Bernardi S, Ciciarelli G, Macchiarelli G, Bianchi S. Dedicated protocol for ultrastructural analysis of farmed rainbow trout (Oncorhynchus mykiss) tissues with red Mark syndrome: The Skin-Part One. Methods and Protocols. 2024; 7: 37.
17. Usluca S, Babur C, Kilic S. Current status in intestinal parasitic infections: a reference laboratory results. Klimik J. 2020; 33: 307-14.
18. Centers for Disease Control and Prevention (CDC). Laboratory Identification of Parasites of Public Health Concern. Cryptosporidiosis. June 3, 2024. Available from: https://www.cdc.gov/dpdx/cryptosporidiosis/index.html (accessed: March 7, 2025).
19. Kahya S, Büyükcangaz E, Carlı KT. Polimeraz zincir reaksiyonu (PCR) optimizasyonu. Uludag Univ J Fac Vet Med. 2013; 32: 31-8.
20. Centers for Disease Control and Prevention (CDC). Diagnostic Procedures. September 24, 2024. Available from: https://www.cdc.gov/dpdx/diagnosticprocedures/index.html (accessed: March 7, 2025).
21. Hadfield SJ, Robinson G, Elwin K, Chalmers RM. Detection and differentiation of *Cryptosporidium* spp. in human clinical samples by use of real-time PCR. J Clin Microbiol. 2011; 49: 918-24.
22. Morgan UM, Constantine CC, Forbes DA, Thompson RC. Differentiation between human and animal isolates of *Cryptosporidium parvum* using rDNA sequencing and direct PCR analysis. J Parasitol. 1997; 83: 825-30.
23. Thompson JD, Higgins DG, Gibson TJ. Clustal W: Improving the sensitivity of progressive multiple sequence alignment through sequence weighting, position-specific gap penalties and weight matrix choice. Nucleic Acids Res. 1994; 22: 4673-80.
24. Şahin S, Ağaoğlu S, Alemdar S. *Cryptosporidium* ve Cryptosporidiosis. Doğruer Y, editör. Gıda kaynaklı paraziter hastalıklar. Ankara: Türkiye Klinikleri; 2018; 35-41. (Turkish)
25. Ekici A, Gunay C, Sahin M, Aydemir S, Yılmaz H. Spread of intestinal parasites in patients presenting with gastrointestinal complaints. Turk J Parazitol. 2023; 47: 224-8.
26. Leder K, Weller PF. Epidemiology, clinical manifestations, and diagnosis of cryptosporidiosis.2017. Available from: https://www.uptodate.com/contents/epidemiology-clinical-manifestations-and-diagnosis-of-cryptosporidiosis.
27. Beyhan YE, Yılmaz H. Investigation of *Cryptosporidium* spp. Antigen by ELISA in stool specimens: nine year evaluation. Turk J Parazitol. 2020; 44: 68-71.
28. Brooks G, Carroll KC, Butel JS, Morse SA, Mietzner TA. Jawetz, Melnick, Adelberg Tıbbi Mikrobiyoloji. Yenen Ş, editör. Ankara: 2014.
29. Abaza SM, Makhlouf LM, El-Shewy KA, El-Moamly AA. Intestinal opportunistic parasites among different groups of immunocompromised hosts. J Egypt Soc Parasitol. 1995; 25: 713-27.
30. Sulżyc-Bielicka V, Kołodziejczyk L, Jaczewska S, Bielicki D, Kładny J, Safranow K. Prevalence of *Cryptosporidium* spp. in patients with colorectal cancer. Pol Przegl Chir. 2012; 84: 348-51.
31. Sane SS, Thakar MR, Mehendale SM. Opportunistic parasitic infections in HIV/AIDS patients presenting with diarrhoea by the level of immunesuppression. Indian J Med Res. 2009; 130: 63-6.
32. Jayalakshmi JB, Appalaraju B, Mahadevan K. Evaluation of an enzyme-linked immunoassay for the detection of *Cryptosporidium* antigen in fecal specimens of HIV/AIDS patients. Indian J Pathol Microbiol. 2008; 51: 137-8.
33. Sari C, Sari K, Ertug S. Investigation of the frequency of *Cryptosporidium* spp. and *Blastocystis hominis* in patients with chronic renal failure. Turk J Parazitol. 2003; 27: 187-90.
34. Karabey M, Can H, Öner TÖ, Döşkaya M, Alak SE, Döşkaya AD, et al. *Cryptosporidium* spp. during chemotherapy: a cross-sectional study of 94 patients with malignant solid tumor. Ann Saudi Med. 2021; 41: 293-8.
35. Yıldız M, Çöplü N, Kılıç S, Babür C, Öncül Ö, Esen B. Investigation of *Cryptosporidium* spp. in solid tumor cases with diarrhea. Turk J Parazitol. 2001; 25: 1-8.
36. Leng X, Mosier DA, Oberst RD. Simplified method for recovery and PCR detection of *Cryptosporidium* DNA from bovine feces. Appl Environ Microbiol. 1996; 62: 643-47.
37. Tamer GS, Gülenç S. Investigation of *Cryptosporidium* spp. antigens in stool by ELISA. Turk J Parazitol. 2008; 32: 198-201.
38. Yılmaz, A. The investigation of *Cryptosporidium* spp. in patients with diarrhea by microscopic and ELISA methods. Selcuk Med J. 2016; 32: 61-4.
39. Magi B, Canocchi V, Tordini G, Cellesi C, Barberi A. *Cryptosporidium* infection: diagnostic techniques. Parasitol Res. 2006; 98: 150-2.
40. Amar CFL, Dear PH, McLauchlin J. Detection and identification by real time PCR/RFLP analyses of *Cryptosporidium* species from human faeces. Lett Appl Microbiol. 2004; 38: 217-22.
41. Ulçay A, Görenek L, Coşkun O, Araz E, Acar A, Eyigün CP. Diagnosis of intestinal-protozoa in patients with immune deficiency. Turk J Parazitol. 2008; 32: 328-33.

Turkiye Parazitol Derg 2025;49(1):17-22
DOI: 10.4274/tpd.galenos.2025.56933

The First Microsatellite-based Characterisation of *Blastocystis* sp. ST3 Isolates and Population Structure Analysis

Blastocystis sp. ST3 İzolatlarının Mikrosatelit Temelli İlk Karakterizasyonu ve Popülasyon Yapısının Analizi

Sema Ertuğ[1], Erdoğan Malatyalı[1], Hatice Ertabaklar[1], Bülent Bozdoğan[2], Mahmut Sinecen[3], Özgür Güçlü[4]

[1]Aydın Adnan Menderes University Faculty of Medicine, Department of Parasitology, Aydın, Türkiye
[2]Aydın Adnan Menderes University Faculty of Medicine, Department of Microbiology, Aydın, Türkiye
[3]Aydın Adnan Menderes University Faculty of Engineering, Department of Computer Engineering, Aydın, Türkiye
[4]Aydın Adnan Menderes University, Sultanhisar Vocational School, Department of Plant and Animal Production, Aydın, Türkiye

Cite this article as: Ertuğ S, Malatyalı E, Ertabaklar H, Bozdoğan B, Sinecen M, Güçlü Ö. The first microsatellite-based characterisation of *Blastocystis* sp. ST3 isolates and population structure analysis. Turkiye Parazitol Derg. 2025;49(1):17-22.

ABSTRACT

Objective: *Blastocystis* sp. is an intestinal Stramenopile that can infect both humans and animals. Genetic variability of *Blastocystis* has been investigated with a variety of molecular methods and different subtypes (ST) have been identified. The present study aimed to characterize microsatellite loci and population structure for *Blastocystis* sp. ST3, the most common ST in human faecal samples.

Methods: The genome of *Blastocystis* sp. ST3 in GenBank was analyzed for the presence of microsatellites containing at least eight repeat units. Specific primers were designed for each locus and polymorphisms were identified using bioinformatics tools. The population structure was determined, and microsatellite typing was conducted on 18 *Blastocystis* sp. ST3 genomic DNA samples from the routine laboratory at Aydın Adnan Menderes University Hospital.

Results: The whole-genome scan of *Blastocystis* sp. ST3 revealed 12 microsatellite loci with at least eight repeats. All loci were successfully amplified with the designed primers and eight of them were selected for genotyping. Microsatellite polymorphism analysis showed that each isolate had a unique profile (18 isolates, 18 different microsatellite types). Furthermore, the isolates were grouped into two distinct population clusters.

Conclusion: *Blastocystis* sp. ST3 isolates exhibited significant variability in their microsatellite repeats. The polymorphic microsatellite loci offer a novel approach to study the detailed genetic diversity and population structure of *Blastocystis* sp. ST 3.

Keywords: *Blastocystis* sp., genetic diversity, microsatellite, polymorphism

ÖZ

Amaç: *Blastocystis* sp. hem insanları hem de hayvanları enfekte edebilen intestinal yerleşimli bir Stramenopil türü olarak sınıflandırılmaktadır. Genetik çeşitliliği farklı moleküler yöntemlerle araştırılmış ve çok sayıda alt tipi (ST) tanımlanmıştır. Bu çalışmada insan dışkısı örneklerinde en yaygın saptanan *Blastocystis* sp. ST olan ST3'e özgü mikrosatelit lokusların karakterizasyonu ve popülasyon yapısının belirlenmesi amaçlanmıştır.

Yöntemler: *Blastocystis* sp. ST3'ün tüm genom dizisi taranarak en az sekiz tekrarlı mikrosatelit lokusları belirlenmiştir. Her bir lokusa spesifik primerler dizayn edilmiş ve polimorfizmler biyoinformatik araçlar ile analiz edilmiştir. Aydın Adnan Menderes Üniversitesi Hastanesi rutin laboratuvarından elde edilen 18 *Blastocystis* sp. ST3 genomik DNA örneği kullanılarak popülasyon yapısı belirlenmiş ve mikrosatelit tiplendirme gerçekleştirilmiştir.

Bulgular: *Blastocystis* sp. ST3 tüm genom taraması sonucu en az sekiz tekrarlı 12 mikrosatelit lokusu tespit edilmiştir. Dizayn edilen primerler ile lokusların tümü başarıyla amplifiye edilmiş ve bunlardan sekizi genotiplendirmede kullanılmak üzere seçilmiştir. *Blastocystis* sp. ST3 izolatları mikrosatelit polimorfizmlerine göre tiplendirildiğinde her bir izolat farklı bir profil (18 izolat, 18 farklı mikrosatelit tipi) göstermiştir. Ayrıca izolatların iki ayrı popülasyon grubunda toplandığı saptanmıştır.

Received/Geliş Tarihi: 24.11.2024 **Accepted/Kabul Tarihi:** 15.04.2025 **Epub:** 18.04.2025 **Publication Date/Yayınlanma Tarihi:** 09.05.2025

Address for Correspondence/Yazar Adresi: Erdoğan Malatyalı, Aydın Adnan Menderes University Faculty of Medicine, Department of Parasitology, Aydın, Türkiye
E-mail/E-Posta: erdogan.malatyali@adu.edu.tr **ORCID ID:** orcid.org/0000-0002-3943-467X

Türkiye PARAZİTOLOJİ Dergisi

Sonuç: *Blastocystis* sp. ST3 izolatlarının mikrosatelit tekrarları açısından birbirlerinden oldukça farklı bir yapıya sahip oldukları belirlenmiştir. Polimorfik mikrosatelit lokusları, *Blastocystis* sp. ST3 izolatlarının detaylı genotiplendirilmesine ve popülasyon yapılarının araştırılmasına olanak sağlayan yeni bir yaklaşım olarak görülmektedir.
Anahtar Kelimeler: *Blastocystis* sp., genetik çeşitlilik, mikrosatelit, polimorfizm

INTRODUCTION

Blastocystis is one of the most common protozoa in the human gastrointestinal system. Most researchers have agreed that *Blastocystis* transmission occurs via the faecal-oral route, primarily through the ingestion of cyst forms in water or food (1). Zoonotic transmission between a variety of animals and humans may also be possible (2). Many subtypes (STs) have been identified to date mostly relying on 18S rRNA coding gene polymorphisms, ST1-4 accounts for the great majority of human samples in many studies (3-5). The genetic diversity of *Blastocystis* is among the most interesting topics in recent years because it has a great contribution to host specificity, pathogenicity, experimental studies and also microbiota (5,6). Amplification of specific parts of *rRNA* genes and sequencing is the most common method for detecting genotypes. Moreover, Matrix-assisted laser desorption/ionisation mass spectrometry (MALDI MS) has been used for genotype determination (7).

Microsatellites are 2-9 bp length genetic markers that can be found abundantly in the genomes of eukaryotic organisms. They allow the identification of the causative agents precisely in populations of different genotypes because they contain high amounts of genetic diversity (8). Microsatellite markers are generally regarded as neutral alleles, which makes them ideal markers for determining the history of populations. In addition, up to today, MS markers have been used in several parasitic protozoa including *Leishmania tropica*, *Trypanosoma* sp., *Plasmodium* sp., and *Toxoplasma gondii* (9-12).

The development and application of alternative genotyping methods may contribute to the understanding of controversial issues in *Blastocystis* sp. pathogenicity such as pathogenicity. In the present study, we aimed to characterize the microsatellite loci for *Blastocystis sp.* ST3 for the first time in the literature and analyse the genetic structure of *Blastocystis* sp. ST3 isolates.

METHODS

Determination of Microsatellite Markers and Primer Design

The complete genomic sequence of a human *Blastocystis* sp. ST3 isolate, an assemblage of 917 partial sequences, was acquired from the National Center for Biotechnology Information database (Genbank, Acc. no: JZRK00000000). Microsatellites mining was carried out using the software Msatcommander 0.8.1 and http://insilico.ehu.es/mini_tools/microsatellites/website with the motif criteria, di-, tri-, tetra-, penta-, and hexanucleotide repeats of microsatellites at least 8 within the complete genome of *Blastocystis* sp. ST3 (13). Primers for microsatellite loci (n=2) were designed with Primer3, the online version, with default settings (14,15). For potential repetitive elements other than perfect repeats, the flanking regions were also analysed. In order to identify robust loci with an annealing temperature of at least 55 ºC, approximately 150-200 bp flanking each side of the repeat were included.

Blastocystis sp. ST3 Isolates

The ethical approval from a Local Ethical Committee in Aydın Adnan Menderes University Faculty of Medicine (no: 2015/10) was obtained. A total of 18 *Blastocystis sp.* ST3 isolates were used in the study. The isolates were previously acquired by culturing direct microscopy-positive faecal samples in the routine diagnostic laboratory at Aydın Adnan Menderes University Hospital. The cultures in 3 mL of Jones medium were subjected to genomic DNA isolation with DNAzol kit (Invitrogen, Life Technologies). *Blastocystis* sp. *SSU-rDNA* gene was partially amplified with the primers RD5 and BhRDr in a single round of polymerase chain reaction (PCR) (16). The amplicons were sequenced, and ST were detected using the *Blastocystis* sp. sequence typing database (pubmlst.org/*Blastocystis*) (17).

PCR Amplification and Genotyping

The optimal annealing temperature for the PCR amplification for each microsatellite locus was determined with gradient PCR. The fluorophores FAM and HEX were used to label the 5′ ends of the forward primer. The amplifications were performed in 30 µL of volume: 0.5 mM each of the primers, 1.5 mM $MgCl_2$, 2.5 mM dNTP, 1.0 U Taq polymerase, and 1-2 µL of template DNA. The reaction for each locus was set as follows: 95 °C for 5 min, 35 cycles (at 95 °C for 30 s, 55-60 °C for 30 s and 72 °C for 45 s), and a final extension at 72 °C for 7 min. The length of alleles was detected with an automatic sequencer.

Statistical Analysis

The allele sizes of microsatellites were exactly determined with Genemarker 2.6.3 (Soft Genetics LLC, USA). The calculation of genetic variation in microsatellite loci was performed with GenAlEx 6.5 (18). GENEPOP 3.3 software was used to detect genotypic linkage disequilibrium between pairwise loci (19). GenAlEx 6.5 program was used to detect the allele numbers (N_A), effective allele numbers (N_E), the frequencies of alleles, intra-population diversity of alleles, and pairwise comparisons of the isolates (18). The expected heterozygosity (H_E) of loci was calculated using the Arlequin 3.11 (20). In multiple loci, haplotype overlaps were determined with GenAlEx 6.5 (18).

Population Structure and Microsatellite Typing

Population structure was analysed with a Bayesian clustering method in STRUCTURE ver. 2.3 program (21). The admixture model with correlated allele frequency parameters was used to to detect the estimated number of genetic clusters (K). Ten runs were performed for each K value (ranging from 1 to 10) with 100.000 MCMC repetitions and a burn-in periods of 10,000. The ad hoc estimated likelihood of K (ΔK) was included in the determination of the most likely number of populations (K) based on the rate of change in the log probability of the data [Ln Pr (X/K)] (22). Structure Harvester version 0.6.94 was used to infer the most likely number of genetic clusters (K) with both the Evanno and Delta K methods (23). The first isolate was defined as MT1 and

the remaining different isolates (at least one different allele type) were annotated with a new MT number.

RESULTS

Microsatellite Variability and Population Structure

We detected 12 microsatellite loci with at least 8 repeats in *Blastocystis* sp. ST3 genome and of these 11 loci were polymorphic. All loci have three repeats, and most were characterized with $(GAT)_n$ and $(ATC)_n$ (Table 1).

There was no significant linkage disequilibrium when the loci were compared dually (p>0.05). The total number of alleles (N_A) for each locus changed from three to 11, the average was 6.55 alleles per locus (Table 1). The mean effective number of alleles (N_E) was 4.06 (range from 1.841 to 8.526). BHST3-142 loci (h=0.457) provided the minimum intra-population diversity, while BHST3-838 locus (h=0.883) provided the highest. The average expected heterozygosity value was determined as 0.740±0.146 (min: 0.399 and max: 0.935). Two distinct genetic groups were suggested with the analyses of microsatellite data by a structure clustering algorithm (K=2.297) (Figure 1).

Microsatellite Typing

We selected eight loci: BH142, BH217, BH278, BH302, BH399, BH476, BH806 and BH808 for MT typing of *Blastocystis* sp. ST3 isolates. These loci were selected relying on the reliability of microsatellite length, clarity in representations, and amplification/reproducibility. Microsatellite based typing of isolates revealed that each isolate had a unique MT type (Table 2).

DISCUSSION

Blastocystis sp. is a common enteric stramenophile with a high genetic diversity between isolates and an unclear role in the development of intestinal diseases and pathogenicity. The molecular typing of *Blastocystis* sp. isolates is valuable to study its population structure of parasites on a global scale. Genetically diverse isolates may influence the frequency of *Blastocystis* sp., for example, host specificity and adaptation to novel hosts (24). In addition, several studies reported a decreased bacterial diversity and changed intestinal microbiome in certain *Blastocystis* sp. ST (6). The development of novel genotyping methods is important for an improved understanding of the genotype distribution of *Blastocystis* sp. isolates and phenotypic characteristics. In the

Table 1. Characterization of 12 microsatellite markers for the *Blastocystis* sp. ST3

Locus	Primer sequence (5′-3′)	Size	N_A	Motif	N_E	h	H_E	GenBank accession number
BHST3-142	F: TACAGCTGTTCCACCCACTC	216-234	4	$(GAT)^{13}$	1.841	0.457	0.399	JZRK01000142
	R: CTCCCCTCTCCCCTAGTCAC							
BHST3-217	F: GGAGGGAGGTTCTTGGTCTC	232-349	6	$(ATC)^{10}$	3.767	0.735	0.778	JZRK01000217
	R: AGAGGGATGTGGTGGAGTTG							
BHST3-278	F: CCTCCTTGCGCTTCTGAC	385-409	6	$(AGC)^{11}$	3.375	0.704	0.745	JZRK01000278
	R: AGGAGGCGGAAAGGAGAAAG							
BHST3-302	F: GAGATGCGACGATTCTCCTC	298-325	6	$(ATC)^{11}$	3.600	0.722	0.765	JZRK01000302
	R: GATTCGCGTTCAATGGTTCT							
BHST3-366	F: ATGGTCAATTGGCTGATGGTG	141-201	9	$(ATC)^{12}$	4.154	0.759	0.804	JZRK01000366
	R: AGTTTCTGAGCCACATGGAGA							
BHST3-399	F: ATTCTTCGCACGATTCTTCG	364-370	3	$(GAT)^{8}$	2.160	0.537	0.569	JZRK01000399
	R: TCATGGAGGTGGTCAACAAA							
BHST3-476	F: AGAAGAAGCTCTTCGCGTTG	321-357	7	$(AAG)^{8}$	4.050	0.753	0.811	JZRK01000476
	R: CAGATCCGCGTAGGTCATTT							
BHST3-500	F: GTGGTTGAGGAGGAGGATGA	-	-	$(GAT)^{8}$				JZRK01000500
	R: GAGAGGAGGCGTCGATGATA							
BHST3-654	F: ATTGGTGATCGTGTTGGTGA	297-471	11	$(ATC)^{11}$	6.480	0.846	0.895	JZRK01000654
	R: TGGTGACGAGTTCGATGAAG							
BHST3-806	F: GACGTGGGTGAGGAGGATTA	367-385	6	$(GAT)^{9}$	4.263	0.765	0.811	JZRK01000806
	R: GTTGGAGAGTTCGGGGGTAT							
BHST3-808	F: TGACAGGTTGCTCCTTACCC	304-325	4	$(ATC)^{9}$	2.492	0.599	0.634	JZRK01000808
	R: TTGGAGTCGTTGGACATTGA							
BHST3-838	F: TAAATGTCGGAGGGAAGGTG	158-295	10	$(GAT)8(GTT)^{8}$	8.526	0.883	0.935	JZRK01000838
	R: GGGAGATGAGTGCATTGACA							
Mean			6.55		4.064	0.705	0.747	

N_A: Observed number of alleles, I: Shannon's information index, N_E: Effective number of alleles; H_E: Expected heterozygosity

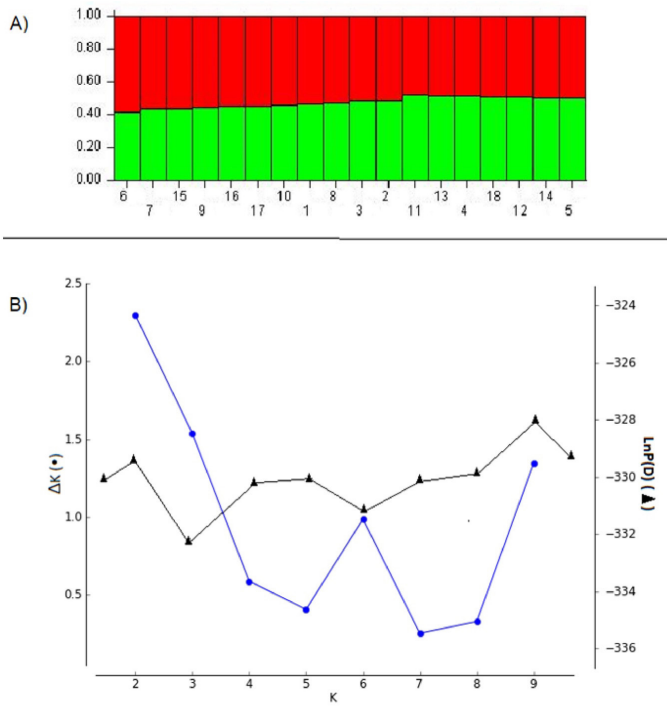

Figure 1. A) Bayesian clustering analysis (K=2) based on SSR data for the studied *Blastocystis* sp. ST3 (18 isolates), vertical black lines separate isolates, **B)** Scatter plot of the possible cluster numbers (K; horizontal axis) against the ad-hoc estimated likelihood of ΔK (vertical axis) by changing the likelihood rate (circle)

present study, we characterised the microsatellite markers for the most common *Blastocystis* sp. subtype in human faecal samples, namely ST3. The most significant finding from this study was that the microsatellite loci in *Blastocystis* sp. ST3 isolates were highly variable, with each of the 18 isolates exhibiting a distinct or unique microsatellite type. A great genetic difference between *Blastocystis* sp. ST was noted in the literature (25). The comparison of *Blastocystis* sp. ST1, ST4 and ST7 genomes found great divergence in terms of genome assembly size, number of protein-coding genes, guanine-cytosine content, average gene size (bp) and also number of introns (25,26). In addition to subtype level genetic difference in *Blastocystis* sp., the isolates were highly separated in terms of intra-subtype variation. A previous study investigated the intra-subtype genetic diversity and host specificity of *Blastocystis* sp. ST3 with multilocus sequence typing including SSU-rDNA and mitochondrion-like organelle sequences (27). The authors reported that human isolates were restricted to a single clade suggesting relatively high host specificity of ST3 human-to-human transmission. Another study reported that 11 human *Blastocystis* sp. ST3 isolates were distributed in nine sequence types with the same method. There were only three isolates that shared the same sequence type (28). However, the use of a single gene, most commonly SSU rRNA, detected a limited intra-subtype genetic diversity in *Blastocystis* sp. ST3 STs. For example, intra-subtype genetic polymorphisms were identified five in ST3 isolates in China and the similarity of SSU rRNA sequences was 99.8% in Iran (29,30).

In the present study, the population structure analysis of *Blastocystis* sp. ST3 isolates revealed two distinct groups. The genomic DNA samples in our study were limited to a specific location, the same hospital laboratory. Collecting samples

Table 2. The microsatellite types (MT) of *Blastocystis* sp. ST3 isolates

	Microsatellite loci								
Isolate	**142**	**217**	**278**	**302**	**399**	**476**	**806**	**808**	**MT**
1	3	5	2	3	2	5	6	3	MT1
2	3	2	4	5	1	1	4	3	MT2
3	3	1	6	1	1	5	4	2	MT3
4	3	2	5	2	1	5	6	2	MT4
5	5	6	4	2	1	1	6	3	MT5
6	3	3	3	6	2	1	5	4	MT6
7	4	6	3	1	2	6	3	3	MT7
8	3	3	3	3	2	4	1	2	MT8
9	3	4	5	3	2	3	2	2	MT9
10	1	2	3	3	1	5	6	1	MT10
11	3	2	5	3	1	2	2	2	MT11
12	3	5	3	3	2	3	2	2	MT12
13	3	2	3	3	2	1	6	2	MT13
14	3	2	5	4	2	5	4	3	MT14
15	1	2	3	2	3	2	5	3	MT15
16	2	4	1	3	2	5	6	2	MT16
17	3	5	3	2	2	2	3	3	MT17
18	3	2	5	5	2	5	6	3	MT18

from various localities, such as different cities or countries, will enable a detailed phylogenetic analysis of microsatellites in *Blastocystis* sp. ST3. The major contribution of the present study is the characterization of microsatellites in *Blastocystis* sp. ST3 and the presentation of the associated methodology. This characterization has important implications for future research and practices, particularly in areas such as zoonotic transmission, microbiota interactions, and pathogenesis. These are the widely discussed topics in the literature on *Blastocystis* (5). Microsatellite polymorphisms have previously been described as valuable genetic markers for investigating zoonotic transmission in both parasitic microorganisms. For instance, certain microsatellite alleles in *Cryptosporidium parvum* have been associated with human-adapted or zoonotic strains (31). Similarly, microsatellite markers have been used to compare *Plasmodium falciparum* isolates from patients with cerebral malaria and those with uncomplicated malaria, to determine if there is a possible link between genetic variation and pathogenicity (32).

CONCLUSION

In conclusion, the characterisation of microsatellite loci in *Blastocystis* sp. ST3 revealed different profiles or types showing high intra-subtype diversity in terms of microsatellite repeats. This novel genotyping approach may be used in molecular epidemiology and population structure screening studies.

*Ethics

Ethics Committee Approval: The ethical approval from a Local Ethical Committee in Aydın Adnan Menderes University Faculty of Medicine (no: 2015/10) was obtained.

Informed Consent: All participants were informed about the study, and their consents were obtained.

Acknowledgments

The study was presented at 3. International *Blastocystis* Conference, 2-4 June 2024, online.

Footnotes

*Authorship Contributions

Concept: S.E., H.E., B.B., Ö.G., Design: S.E., H.E., B.B., Ö.G., Data Collection or Processing: E.M., M.S., Analysis or Interpretation: S.E., E.M., M.S., Ö.G., Literature Search: S.E., E.M., H.E., Writing: S.E., E.M., H.E., Ö.G.

Conflict of Interest: No conflict of interest was declared by the authors.

Financial Disclosure: This study was supported by the Scientific and Technical Research Council of Türkiye (TUBITAK-215S655).

REFERENCES

1. Shams M, Shamsi L, Yousefi A, Sadrebazzaz A, Asghari A, Mohammadi-Ghalehbin B, et al. Current global status, subtype distribution and zoonotic significance of *Blastocystis* in dogs and cats: a systematic review and meta-analysis. Parasit Vectors. 2022; 15: 225.
2. Chen S, Meng W, Shi X, Chai Y, Zhou Z, Liu H, et al. Occurrence, genetic diversity and zoonotic potential of *Blastocystis* sp. in forest musk deer (*Moschus berezovskii*) in Southwest China. Parasite. 2022; 29: 34.
3. Malatyali E, Ertabaklar H, Ertug S. Subtype distribution of *Blastocystis* in Turkiye. Turkiye Parazitol Derg. 2023; 47: 184-9.
4. Santin M, Figueiredo A, Molokin A, George NS, Koster PC, Dashti A, et al. Division of *Blastocystis* ST10 into three new subtypes: ST42-ST44. J Eukaryot Microbiol. 2024; 71: e12998.
5. Wawrzyniak I, Poirier P, Viscogliosi E, Dionigia M, Texier C, Delbac F, et al. *Blastocystis*, an unrecognized parasite: an overview of pathogenesis and diagnosis. Ther Adv Infect Dis. 2013; 1: 167-78.
6. Deng L, Tan KSW. Interactions between *Blastocystis* subtype ST4 and gut microbiota in vitro. Parasit Vectors. 2022; 15: 80.
7. Martiny D, Bart A, Vandenberg O, Verhaar N, Wentink-Bonnema E, Moens C, et al. Subtype determination of *Blastocystis* isolates by matrix-assisted laser desorption/ionisation time-of-flight mass spectrometry (MALDI-TOF MS). Eur J Clin Mic Inf Dis. 2014; 33: 529-36.
8. Havryliuk T, Ferreira MU. A closer look at multiple-clone *Plasmodium vivax* infections: detection methods, prevalence and consequences. Mem Inst Oswaldo Cruz. 2009; 104: 67-73.
9. Ajzenberg D, Banuls AL, Tibayrenc M, Darde ML. Microsatellite analysis of *Toxoplasma gondii* shows considerable polymorphism structured into two main clonal groups. Int J Parasitol. 2002; 32: 27-38.
10. Schwenkenbecher JM, Wirth T, Schnur LF, Jaffe CL, Schallig H, Al-Jawabreh A, et al. Microsatellite analysis reveals genetic structure of *Leishmania tropica*. Int J Parasitol. 2006; 36: 237-46.
11. Simo G, Njiokou F, Tume C, Lueong S, De Meeus T, Cuny G, et al. Population genetic structure of Central African *Trypanosoma brucei gambiense* isolates using microsatellite DNA markers. Infect Genet Evol. 2010; 10: 68-76.
12. Imwong M, Nair S, Pukrittayakamee S, Sudimack D, Williams JT, Mayxay M, et al. Contrasting genetic structure in *Plasmodium vivax* populations from Asia and South America. Int J Parasitol. 2007; 37: 1013-22.
13. Faircloth BC. msatcommander: detection of microsatellite repeat arrays and automated, locus-specific primer design. Mol Ecol Resour. 2008; 8: 92-4.
14. Koressaar T, Remm M. Enhancements and modifications of primer design program Primer3. Bioinformatics. 2007; 23: 1289-91.
15. Untergasser A, Cutcutache I, Koressaar T, Ye J, Faircloth BC, Remm M, et al. Primer3-new capabilities and interfaces. Nucleic Acids Res. 2012; 40: e115.
16. Scicluna SM, Tawari B, Clark CG. DNA barcoding of *Blastocystis*. Protist. 2006; 157: 77-85.
17. Jolley KA, Maiden MC. BIGSdb: scalable analysis of bacterial genome variation at the population level. BMC Bioinformatics. 2010; 11: 595.
18. Peakall R, Smouse PE. GenAlEx 6.5: genetic analysis in Excel. Population genetic software for teaching and research--an update. Bioinformatics. 2012; 28: 2537-9.
19. Raymond M, Rousset F. An exact test for population differentiation. Evolution. 1995; 49: 1280-3.
20. Excoffier L, Estoup A, Cornuet JM. Bayesian analysis of an admixture model with mutations and arbitrarily linked markers. Genetics. 2005; 169: 1727-38.
21. Pritchard JK, Stephens M, Donnelly P. Inference of population structure using multilocus genotype data. Genetics. 2000; 155: 945-59.
22. Evanno G, Regnaut S, Goudet J. Detecting the number of clusters of individuals using the software STRUCTURE: a simulation study. Mol Ecol. 2005; 14: 2611-20.
23. Earl DA, vonHoldt BM. STRUCTURE HARVESTER: a website and program for visualizing STRUCTURE output and implementing the Evanno method. Cons Gen Res. 2012; 4: 359-61.
24. Noel C, Dufernez F, Gerbod D, Edgcomb VP, Delgado-Viscogliosi P, Ho LC, et al. Molecular phylogenies of *Blastocystis* isolates from different hosts: implications for genetic diversity, identification of species, and zoonosis. J Clin Microbiol. 2005; 43: 348-55. 3
25. Higuera A, Salas-Leiva DE, Curtis B, Patino LH, Zhao D, Jerlstrom-Hultqvist J, et al. Draft genomes of *Blastocystis* subtypes from human samples of Colombia. Parasit Vectors. 2023; 16: 52.

26. Gentekaki E, Curtis BA, Stairs CW, Klimes V, Elias M, Salas-Leiva DE, et al. Extreme genome diversity in the hyper-prevalent parasitic eukaryote *Blastocystis*. PLoS Biol. 2017; 15: e2003769.

27. Stensvold CR, Alfellani M, Clark CG. Levels of genetic diversity vary dramatically between *Blastocystis* subtypes. Infect Genet Evol. 2012; 12: 263-73.

28. Ertug S, Malatyali E, Ertabaklar H, Bozdogan B. Multilocus sequence typing of *Blastocystis* isolates in Aydin, Turkey. Parasitol Int. 2016; 65: 760-2.

29. Zhao W, Ren G, Wang L, Xie L, Wang J, Mao J, et al. Molecular prevalence and subtype distribution of *Blastocystis* spp. among children who have diarrheia or are asymptomatic in Wenzhou, Zhejiang Province, China. Parasite. 2024; 31: 12.

30. Alinaghizade A, Mirjalali H, Mohebali M, Stensvold CR, Rezaeian M. Inter- and intra-subtype variation of *Blastocystis* subtypes isolated from diarrheic and non-diarrheic patients in Iran. Infect Genet Evol. 2017; 50: 77-82.

31. Hunter PR, Hadfield SJ, Wilkinson D, Lake IR, Harrison FC, Chalmers RM. Subtypes of *Cryptosporidium parvum* in humans and disease risk. Emerg Infect Dis. 2007; 13: 82-8.

32. Ferreira MU, Nair S, Hyunh TV, Kawamoto F, Anderson TJ. Microsatellite characterization of *Plasmodium falciparum* from cerebral and uncomplicated malaria patients in southern Vietnam. J Clin Microbiol. 2002; 40: 1854-7.

Turkiye Parazitol Derg 2025;49(1):23-8
DOI: 10.4274/tpd.galenos.2025.66487

Evaluation of miR-146a Expression Levels in Archived Serum Samples for the Diagnosis/Follow-up of Patients with Cystic Echinococcosis

Kistik Ekinokokkozisli Hastaların Tanısı/Takibinde Kullanılan Arşiv Serum Örneklerinde miR-146a Ekspresyon Düzeylerinin Değerlendirilmesi

Eylem Akdur Öztürk[1], Mesude Angın[2], Çağıl Coşkun[3], Ayşegül Ünver[4]

[1]Çukurova University Faculty of Medicine, Department of Medical Parasitology, Adana, Türkiye
[2]Balıkesir University Faculty of Medicine, Department of Medical Biology, Balıkesir, Türkiye
[3]Çukurova University Faculty of Medicine, Department of Biophysics, Adana, Türkiye
[4]Ege University Faculty of Medicine, Department of Medical Parasitology, İzmir, Türkiye

Cite this article as: Akdur Öztürk E, Angın M, Coşkun Ç, Ünver A. Evaluation of miR-146a expression levels in archived serum samples for the diagnosis/follow-up of patients with cystic echinococcosis. Turkiye Parazitol Derg. 2025;49(1):23-8.

ABSTRACT

Objective: Cystic echinococcosis (CE) is a zoonotic disease that causes fluid-filled cysts in internal organs and is a major public health problem worldwide. The lack of standardized methods for the diagnosis/follow-up of CE disease necessitates the development of new non-invasive diagnostic tools, such as the determination of changes in the expression levels of circulating microRNAs (miRNA). In this study, we aimed to investigate the presence of miR-146a in archived serum samples of CE patients for the first time and to evaluate its potential role in the diagnosis and follow-up of CE over a three-year period.
Methods: This study included archived serum samples from 39 CE patients, 56 follow-up samples from 14 CE patients, and 3 healthy controls, and expression levels of miR-146a were evaluated in each group using quantitative real-time polymerase chain reaction. Due to the small and unbalanced control group, bootstrapped confidence intervals were used; time-dependent changes in follow-up patients were analyzed using a linear mixed-effects model and Welch's F test to address variance heterogeneity.
Results: The *miR146* gene was found to be significantly upregulated in archived serum samples of patients with CE compared to healthy control samples. Additionally, the expression level of the *miR146* gene in follow-up serum samples significantly decreased in the third year post-surgery compared to follow-up blood samples taken in previous years ($p<0.05$).
Conclusion: According to the obtained results, it was concluded that miR-146a can be recommended as a diagnostic biomarker in the diagnosis and follow-up of CE, and archived materials of CE patients can be utilized in new biomarker research.
Keywords: Cystic echinococcosis, MicroRNA, diagnosis, patient follow-up, archive serum

ÖZ

Amaç: Kistik ekinokokkozis (KE), iç organlarda sıvı dolu kistlere neden olan zoonotik bir hastalıktır ve dünya çapında önemli bir halk sağlığı sorunudur. KE hastalığının tanısı/takibi için standardize edilmiş yöntemlerin eksikliği, dolaşımdaki mikroRNA'ların (miRNA'lar) ifade seviyelerindeki değişikliklerin belirlenmesi gibi yeni invaziv olmayan tanı araçlarının geliştirilmesini gerekli kılmaktadır. Bu çalışmada, ilk kez KE hastalarının arşiv serum örneklerinde miR-146a'nın varlığını araştırmayı ve üç yıllık bir süre boyunca KE'nin tanısı ve takibindeki potansiyel rolünü değerlendirmeyi amaçladık.
Yöntemler: Bu çalışmaya 39 CE hastasının arşiv serum örneği, 14 CE hastasının 56 takip örneği ve sağlıklı kontrollerden 3 örnek dahil edildi ve miR-146a'nın ifade düzeyleri her grupta kantitatif gerçek-zamanlı polimeraz zincir reaksiyonu kullanılarak değerlendirildi. Grup karşılaştırmaları için küçük ve dengesiz kontrol grubuna bağlı olarak yeniden örneklemeli güven aralıkları kullanıldı; takip hastalarındaki zamana bağlı değişimler ise varyans heterojenliğini dikkate alan lineer karma etkili model ve Welch F testi ile analiz edildi.
Bulgular: *miR146* geninin, CE'li hastaların arşivlenmiş serum örneklerinde sağlıklı kontrol örneklerine kıyasla ifade düzeyinin önemli ölçüde arttığı bulunmuştur. Ayrıca, takip serum örneklerindeki *miR146* geninin ifade düzeyi, ameliyattan sonraki üçüncü yılda önceki yıllarda alınan takip kan örneklerine kıyasla önemli ölçüde azalmıştır ($p<0,05$).
Sonuç: Çalışmamızın sonuçlara göre miR-146a'nın KE'nin tanı ve takibinde tanısal biyobelirteç olarak önerilebileceği ve KE hastalarına ait arşiv materyallerinin yeni biyobelirteç araştırmalarında kullanılabileceği sonucuna varılmıştır.
Anahtar Kelimeler: Kistik ekinokokkozis, MikroRNA, tanı, hasta takibi, arşiv serum

Received/Geliş Tarihi: 13.02.2025 **Accepted/Kabul Tarihi:** 25.04.2025 **Publication Date/Yayınlanma Tarihi:** 09.05.2025

Address for Correspondence/Yazar Adresi: Eylem Akdur Öztürk, Çukurova University Faculty of Medicine, Department of Medical Parasitology, Adana, Türkiye
E-mail/E-Posta: akdureylem@gmail.com **ORCID ID:** orcid.org/0000-0002-4886-6175

Türkiye PARAZİTOLOJİ Dergisi

INTRODUCTION

Cystic echinococcosis (CE) is a zoonotic disease caused by the metacestode form of *Echinococcus granulosus*, characterized by the development of fluid-filled cysts in internal organs. CE is a public health issue affecting people from all age groups and is endemic in many countries, including Türkiye (1,2).

In the treatment of CE, the choice of method including surgery, PAIR (puncture, aspiration, injection, reaspiration), medical therapy, or "watch and wait" depends on the characteristics of the cyst, such as its location and stage. Following the treatment of CE, recurrence may reach up to 25%, making the management of the disease difficult (3).

The diagnosis of CE primarily relies on clinical findings and imaging techniques, but combining imaging and serological tests is recommended due to complicated early diagnosis (3). However, the accuracy of serological tests can be influenced by factors related to the patient, such as the stage, location, number, and size of the cyst, and seropositivity varies between 56% and 100% in different laboratories. Serologic tests have also limited performance in the follow-up of CE due to the long-term presence of disease-specific antibodies, the possibility of false results in seronegative patients, and the inability to distinguish between inactive and recurrent cysts (4).

The lack of standard methods for the diagnosis/follow-up of disease reveals the need for the development of new diagnostic tools such as liquid biopsy. Circulating free microRNAs (miRNAs) serve as biomarkers in various fields, including oncology, neurology, cardiology, spinal surgery, epilepsy, and neurodegenerative diseases, and play a critical role in modulating gene expression and many biological processes (5). miRNAs exhibit stability in body fluids such as serum and plasma due to their resistance to ribonuclease (RNase) activity, high temperatures, repeated freeze-thaw cycles, extreme pH levels, and long-term storage, allowing the analysis of their expression levels even in archived materials (6).

Parasitic infections affect both parasite and host miRNAs, leading to changes in host immune responses. This suggests that monitoring alterations in parasite-derived and/or parasite-specific miRNAs may help identify diagnostic biomarkers in parasitology (7-11).

In the present research, we have aimed to investigate the presence and changes in expression levels of miR-146a in serum samples collected during a three-year follow-up of CE patients; to our knowledge, this is the first study to assess its expression in archived serum samples.

METHODS

Ethics Statement

The present research received approval from Ethics Committee of Ege University Faculty of Medicine (approval no: 2023-0780/23-4.1T/67) and consent forms were obtained from the participants.

Clinical Samples

The study included archived serum samples of 39 patients (first blood samples with the letter "a" code taken during surgery) who were admitted to Ege University Hospitals between 2016 and 2019 and diagnosed with CE through radiological and serological examinations, and 3 healthy controls without underlying chronic diseases.

In addition, a total of 56 follow-up serum samples collected from 14 CE patients on the day of surgery (day 0), as well as one year, two years, and three years after surgery, were included [coded as the first (a), second (b), third (c) and fourth (d) blood samples for each follow-up CE patient, respectively]. During the three-year follow-up period, no recurrence of the disease was detected by serological and imaging methods. All materials were stored at -20 °C.

RNA Isolation

Total RNA was isolated using the mirVana™ miRNA Isolation Kit (Invitrogen) using 200 µL of archived serum samples from CE patients and control groups. Concentration and purity were assessed using a Nanodrop ND-1000 spectrophotometer (Thermo Fisher Scientific, Wilmington, DE, USA). Total RNAs were stored at -80 °C until cDNA synthesis.

TaqMan miRNA Assay

Complementary DNAs (cDNAs) were synthesized from total RNA, including miRNA, using the TaqMan® MicroRNA Reverse Transcription Kit (Applied Biosystems, Foster City, CA, USA). Quantitative real-time polymerase chain reaction was performed using the TaqMan® MicroRNA Analysis Kit to measure miRNA expression, and the primers used for miR-146a-5p and endogenous miR-16-5p are listed in Table 1. In this study, hsa-miR-16-5p was used as an endogenous miRNA for normalization in humans due to its suitability for miRNA studies reported in the literature (12,13). We calculated the relative expression levels of miRNAs using the $2^{-\Delta\Delta Ct}$ method.

Statistical Analysis

In the analysis of *miR-146* gene expression between control and archived first blood samples, the dataset was highly unbalanced, with only three observations in the healthy control group. Given the small sample size in the healthy control group, we determined that standard parametric and non-parametric tests were not appropriate. Instead, we used bootstrapped confidence intervals (CIs) to estimate the median response in each group, utilizing the boot package in R (14,15). We generated a total of 1,000 bootstrap resamples to construct 95% CIs for the group medians. Statistical significance was assessed by examining the overlap of CIs, where non-overlapping CIs suggest a potential difference between groups.

To analyze the effect of time on the individuals being followed up, a random intercept general linear model was created by optimizing the log-likelihood function, utilizing the lme4 and lmertest libraries (16,17). The model was formulated as follows: lmer(response ~ time + (1 | patient_id), data = data, REML = FALSE).

The intraclass correlation coefficient (ICC=0.064) indicated that only 6.4% of the total variance was due to differences between individuals, suggesting a weak dependency within subjects. The likelihood ratio test (LRT=0.19, p=0.66) confirmed that including a random intercept did not significantly improve the model. Given that the random intercept was not significant, we proceeded with a One-Way ANOVA framework to analyze time effects. Initially, we tested the data for normality and heterogeneity by using the Shapiro-Wilk test, Q_Q plots, and Levene's test. As there

Table 1. The TaqMan probes and miR sequences

miRBase ID	Assay ID	Mature miRNA sequence
hsa-miR-146a-5p	000468	UGAGAACUGAAUUCCAUGGGUU
hsa-miR-16	000391	UAGCAGCACGUAAAUAUUGGCG

Table 2. Demographic and clinical characteristics of 39 patients with CE

Patient	Gender	Age (yrs.)	Cyst number	Cyst location	Cyst size	Cyst stage
1	Male	64	1	Liver	M	CE3B
2	Male	42	Multiple	Liver	M	CE4
3*	Female	16	Multiple	Liver	M	CE1
4*	Female	44	1	Liver	L	CE2
5	Female	23	1	Liver	M	CE1
6	Male	26	Multiple	Liver	M	CE2
7	Female	63	Multiple	Liver	M	CE2
8*	Female	10	1	Lung	M	CE1
9*	Male	9	Multiple	Liver	M	CE1
10	Female	73	1	Liver	M	CE2
11	Female	18	1	Liver	L	CE1
12*	Male	25	Multiple	Liver	M	CE1
13*	Male	56	Multiple	Liver	L	CE3B
14*	Female	9	1	Liver	M	CE2
15	Male	62	Multiple	Liver	M	CE1
16	Male	42	Multiple	Liver	L	CE1
17	Female	50	Multiple	Liver	M	CE1
18*	Female	25	1	Liver	M	CE1
19*	Female	5	1	Liver	S	CE2
20*	Female	38	Multiple	Liver	L	CE1
21*	Male	13	Multiple	Liver	L	CE1
22*	Male	14	1	Lung	M	CE1
23	Male	62	Multiple	Liver	M	CE1
24*	Female	58	1	Liver	L	CE1
25	Female	30	Multiple	Liver	L	CE1
26*	Female	11	Multiple	Lung	L	CE3A
27	Male	5	Multiple	Lung	M	CE1
28	Female	85	1	Liver	L	CE2
29	Male	63	1	Liver	L	CE2
30	Female	13	Multiple	Liver	S	CE1
31	Male	7	Multiple	Liver	M	CE1
32	Female	9	1	Lung	L	CE2
33	Male	4	1	Liver	L	CE1
34	Female	59	1	Liver	L	CE1
35	Male	65	Multiple	Liver	L	CE4
36	Female	10	1	Lung	M	CE3A
37	Female	9	Multiple	Liver	S	CE3B
38	Female	26	1	Liver	L	CE2
39	Male	10	1	Liver	M	CE1

*: Follow-up patients, S: Small (≤5), M: Medium (5<-<10), L: Large (10≤), CE: Cystic echinococcosis

were issues with normality and heterogeneity, a square root transformation resolved the normality problem, but heterogeneity remained an issue. Therefore, we applied Welch's heteroscedastic F test which provides a robust alternative to standard ANOVA under variance heterogeneity. For post-hoc comparisons, we conducted pairwise Welch t-tests with Bonferroni correction using the R library onewaytest (18).

GraphPad Prism 8.0 (GraphPad software, CA) was used for other data analyses. Receiver operating characteristic (ROC) curve, Mann-Whitney U tests, unpaired t-tests, and One-Way ANOVA were also used for the relevant data analyses. Outliers were identified using the ROUT method with a Q value of 1%.

RESULTS

Characteristics of Patients

Among the 39 patients with CE, ages ranged from 4 to 85 years, with 41% under 18. The majority were female (56.4%), and all cysts showed liver localization except six cysts in the lungs. According to the World Health Organization, 95% of the cysts were in the active (CE1 and CE2) and transitional stages (CE3A and CE3B). Detailed demographic and clinical data are in Table 2.

miR146 Gene Expression Analyses

In this study, it was shown that the *miR146* gene was significantly up-regulated in the archived first blood samples of patients with CE compared to archived samples from a healthy control group. Figure 1 showed that miR-146a expression was elevated in archived serum samples from CE patients compared to healthy controls. In addition, the differences found between these two groups were detected to be statistically significant ($p<0.05$). The fold-change of *miR146* in CE patients was calculated to be 21.05. Furthermore, the area under the ROC for these groups

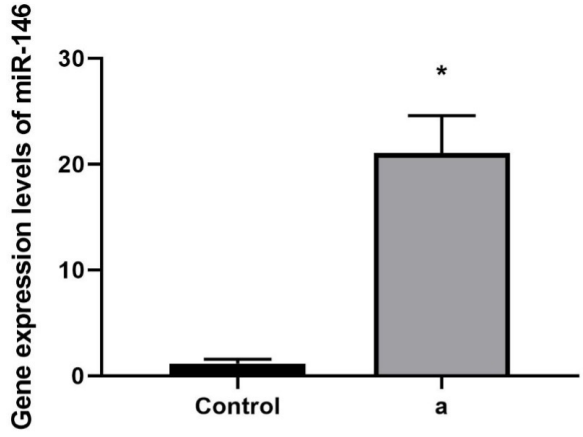

Figure 1. Gene expression levels of miR-146. The control group consists of archived samples from healthy individuals. Group "a" displays archived first blood samples from patients with CE. An asterisk ("*") denotes a significant difference between the CE patient group and the healthy control group ($p<0.05$). The data are expressed as the mean ± SEM

CE: Cystic echinococcosis, SEM: Standard error of the mean

was 0.9355, with a p-value of 0.0139. Figure 2 demonstrated the ROC analysis of *miR-146a*, showing its ability to distinguish CE patients from healthy control.

When examining the expression levels of the *miR146* gene in follow-up patients over the years, it was found that miR146 expression decreased in the third blood sample (c) compared to the first (a) and second (b) samples. However, these found differences were not statistically significant. In contrast, the fourth blood sample (d), collected in the third year, demonstrated a significant decrease in miR146 expression compared to the samples collected in the previous years. Figure 3 showed *miR-146a* gene expression levels in CE patients during three-year follow-up.

The expression level of miR-146 was analyzed in categorized CE patients, showing no significant differences with respect to gender, age, cyst number, cyst stage, or cyst localization.

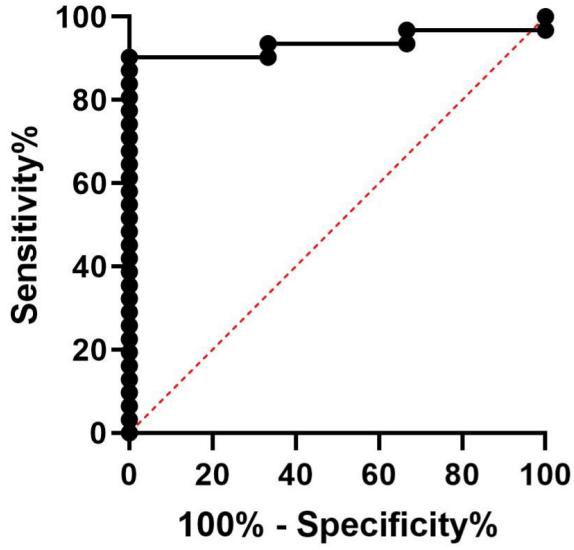

Figure 2. Receiving operating characteristic analysis of *miR146* gene expression level between healthy controls and the disease group

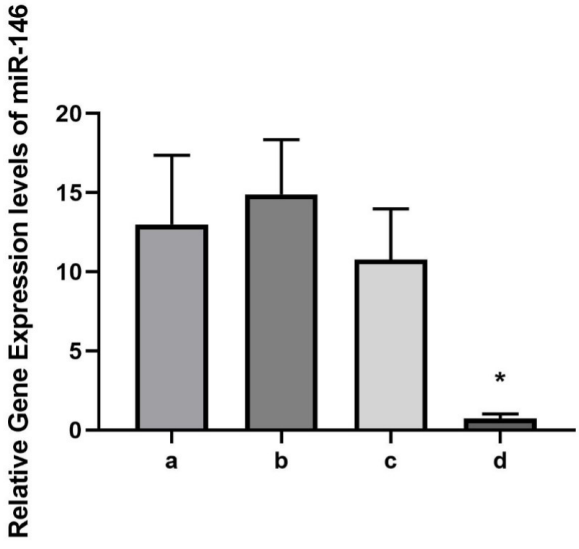

Figure 3. Gene expression levels of miR-146 in follow-up patients over the years. a (day 0), b (year 1), c (year 2), and d (year 3). The asterisk (*) indicates a significant difference found between the d group and all other follow-up groups ($p<0.05$). Data are shown as the mean ± SEM

SEM: Standard error of the mean

DISCUSSION

MicroRNAs (miRNAs), which consist of 17 to 25 nucleotides, are single-stranded, non-coding RNA that significantly contribute to host-pathogen interactions as well as the host's immune responses to microbial agents (19). During parasitic infection, microRNAs expressed in the host, either derived from parasites or specific to parasites, are passively or actively circulating in exosomes, and alterations in the expression levels of these miRNAs could provide a new approach in diagnostic and prognostic biomarker research (5).

In previous studies, miRNA pathway analysis was investigated at different life cycle stages of *Echinococcus* species. Notably, *E. granulosus* (egr)-miR-125-5p and egr-miR-2a-3p were shown to be abundant in protoscoleces (20). A mouse model study showed that pro-inflammatory factors like tumor necrosis factor (TNF) α, interleukin (IL)12, and IL6 inhibit key signaling pathways in CE (21). Additionally, Ren et al. (22) reported that miR-483-3p found in liver tissues and plasma could be suggested as a potential diagnostic biomarker for alveolar echinococcosis (AE).

This study investigated the expression levels of miRNA-146a in archived serum samples of patients with CE. This study is, to the best of our knowledge, the first investigation of the expression of particular miRNAs in archived sera from patients with CE. Recent research has explored how long-term storage conditions affect the stabilization of miRNAs in archived materials and their potential use in developing biomarkers. Rounge and colleagues investigated the quantity and quality of miRNA in serum samples from one of the world's oldest biobanks, stored at -20 °C for a duration of up to 40 years (6). Their findings confirm that the targeted miRNAs remained stable in archived serum materials after long-term storage, consistent with results from other studies with similar goals (23,24).

miR-146a plays an important role in regulating the Th1 response during helminth infections by reducing the release of IFN-γ and TNF-α. It also triggers and modulates the Th2 response in both allergic reactions and helminth infections (10,25). Mahami-Oskouei et al. (10) demonstrated in their study, which included 20 CE patients and 20 healthy controls, that miR-146a was significantly up-regulated in CE patient plasma samples. Similarly, Eroglu et al. (9) showed that miRNA 146a levels were higher in tissue samples from 30 CE patients and 20 AE patients compared to healthy individuals. In parallel with these studies, our research indicated that *miR-146* gene expression was notably elevated in archived blood samples from CE patients taken at the time of surgery compared to archived samples from healthy controls. Furthermore, ROC analysis indicates that the increase in miR-146 can be used as a biomarker for diagnosing CE.

Since the recurrence rate of CE can reach up to 25%, it is necessary to follow-up the patients after treatment. Current diagnostic methods, including imaging and serological tests, are inadequate for early diagnosis of CE and its recurrences. Zhang et al. (26) suggested that protoscoleces shed from cysts may lead to higher

expression levels in patients with active CE cysts. Monitoring changes in miRNA expression during recurrence could provide a new diagnostic and prognostic biomarker approach (26).

Alizadeh et al. (7) showed that egr- miR-71 and egr-let-7 expression levels in the plasma of patients with CE were significantly reduced three and six months after surgery and suggested that miRNAs derived from parasites (egr-miR-71) may be a promising diagnostic biomarker for early CE diagnosis and follow-up. Another study found that the levels of serum egr-miR-2a-3p in patients with CE were much higher than in the control groups, but these levels dropped significantly six months after surgery compared to the initial values (27).

In our study, it was observed that the expression level of the *miR146* gene in the blood samples of the patients followed up significantly decreased in the samples taken in the third year post-surgery, compared to the follow-up blood samples taken in previous years. Additionally, the fact that the same patient group showed no recurrence after three years of follow-up, as determined by serological and imaging methods, suggests that miR-146 could be an important biomarker candidate for follow-up CE patients by tracking changes in expression levels.

Another limitation in the diagnosis of CE is that serological tests cannot differentiate between active and inactive cysts, which complicates the monitoring of the disease. Th2 immune responses are crucial for protective immunity in active cysts, while Th1 responses are associated with immunity in inactive cysts (26,28). In a study aimed at defining the miRNA profile and potential cellular pathways in patients with CE, it was found that several miRNAs—specifically hsa-miR-4692, hsa-miR-181b-3p, hsa-miR-4491, hsa-miR-4518, hsa-miR-4659a-5p, and hsa-miR-3977— were downregulated, likely due to the presence of CE cysts. These miRNAs are associated with cellular processes such as cellular proliferation and apoptosis and they could potentially play a role in anti-cancer effects (11). Mariconti et al. (29) revealed that six immune-related miRNAs (miR- 223-3p, let-7g-5p, miR- 16-5p, let-7a-5p, miR- 26a-5p, miR- 30c-5p, miR- 195-5p and miR- 26b-5p) were up-regulated in CE patients with active cyst compared to CE patients with inactive cyst, indicating host-parasite interaction. Örsten et al. (13) focused on investigating the miRNAs derived from parasites in the serum samples of CE patients with active and inactive cysts and healthy controls; they reported that egr egr-miR71-5p, let-7-5p, and egr-miR-9-5p were more expressed in CE patients with active cysts than in those with inactive cysts. Since our study consisted of patients who underwent surgery and therefore mostly had active and transitional cysts, alteration in mir146a expression levels between active and inactive cyst stages may not have been thoroughly evaluated, but no statistically significant difference was observed in miR146a expression levels considering the cyst stages.

Considering the compatibility of the results of our study with similar CE-miRNA studies mentioned above, it is thought that miRNAs could be used as potential diagnostic biomarkers for the diagnosis/follow-up of CE.

Study Limitations

There are several limitations in our study due to the use of archived serum samples from CE patients with active cysts, which were used in a previous serological study. One of these is that the expression levels of target miRNAs could not be investigated in this patient group and could not be compared with CE patients with active cysts due to the small number of patients in the inactive cyst stage in our study. Additionally, the use of archived serum samples limited access to a healthy group. The potential of miR146a in CE patient diagnosis/follow- up needs to be validated with a larger sample group including all clinical variables.

Conclusions

Although there is an increase in studies on the use of circulating miRNAs in the diagnosis/follow-up of CE patients, the presence of microRNAs was demonstrated for the first time in archived serum samples of CE patients used in serological tests and stored at -20 degrees, providing a starting point for the search for new diagnostic biomarkers in CE archived materials. In addition, as a result of demonstrating the presence of miR-146a in archive serum samples and examining the alterations in expression levels during the three-year follow-up period, it was concluded that miR-146a could be used as a candidate diagnostic biomarker in the diagnosis and follow-up of CE.

*Ethics

Ethics Committee Approval: The present research received approval from Ethics Committee of Ege University Faculty of Medicine (approval no: 2023-0780 /23-4.1T/67).

Informed Consent: Consent forms were obtained from the participants.

Acknowledgments

We would like to thank Prof. Dr. Sinan Mavruk for his valuable contributions to the statistical analyses.

Footnotes

*Authorship Contributions

Concept: E.A.Ö., M.A., Ç.C., A.Ü., Design: E.A.Ö., M.A., A.Ü., Data Collection or Processing: E.A.Ö., M.A., Ç.C., A.Ü., Analysis or Interpretation: E.A.Ö., Ç.C., Literature Search: E.A.Ö., M.A., Ç.C., A.Ü., Writing: E.A.Ö., M.A., Ç.C.

Conflict of Interest: No conflict of interest was declared by the authors.

Financial Disclosure: This study was supported by the Ege University Scientific Research Project (project no: 29573).

REFERENCES

1. Altintas N. Past to present: Echinococcosis in Turkey. Acta Trop. 2003; 85: 105-12.
2. Manciulli T, Mariconti M, Vola A, Lissandrin R, Brunetti E. Cystic echinococcosis in the Mediterranean. Curr Trop Med Rep. 2017; 4: 235-44.
3. Brunetti E, Kern P, Vuitton DA. Expert consensus for the diagnosis and treatment of cystic and alveolar echinococcosis in humans. Acta Trop. 2010; 114: 1-16.
4. Manzano-Román R, Sánchez-Ovejero C, Hernández-González A, Casulli A, Siles-Lucas M. Serological diagnosis and follow-up of human cystic echinococcosis: a new hope for the future? Biomed Res Int. 2015; 2015.
5. Ozturk EA, Caner A. Liquid biopsy for promising non-invasive diagnostic biomarkers in parasitic infections. Acta Parasitol. 2022; 67: 1-17.
6. Rounge TB, Lauritzen M, Langseth H, Enerly E, Lyle R, Gislefoss RE.

MicroRNA biomarker discovery and high-throughput DNA sequencing are possible using long-term archived serum samples. Cancer Epidemiol Biomarkers Prev. 2015; 24: 1381-7.

7. Alizadeh Z, Mahami-Oskouei M, Spotin A, Kazemi T, Ahmadpour E, Cai P, et al. Parasite-derived microRNAs in plasma as novel promising biomarkers for the early detection of hydatid cyst infection and post-surgery follow-up. Acta Trop. 2020; 202: 105255.
8. Cucher M, Macchiaroli N, Kamenetzky L, Maldonado L, Brehm K, Rosenzvit M. High-throughput characterization of *Echinococcus* spp. metacestode miRNomes. Int J Parasitol. 2015; 45: 253-67.
9. Eroglu F, Dokur M, Ulu Y. MicroRNA profile in immune response of alveolar and cystic echinococcosis patients. Parasite Immunol. 2021; 43: e12817.
10. Mahami-Oskouei M, Norouzi B, Ahmadpour E, Kazemi T, Spotin A, Alizadeh Z, et al. Expression analysis of circulating miR-146a and miR-155 as novel biomarkers related to effective immune responses in human cystic echinococcosis. Microb Pathog. 2021; 157: 104962.
11. Orsten S, Baysal, Yabanoglu-Ciftci S, Ciftci T, Azizova A, Akinci D, et al. MicroRNA expression profile in patients with cystic echinococcosis and identification of possible cellular pathways. J Helminthol. 2021; 95: e1.
12. Donati S, Ciuffi S, Brandi ML. Human circulating miRNAs real-time qRT-PCR-based analysis: an overview of endogenous reference genes used for data normalization. Int J Mol Sci. 2019; 20: 4353.
13. Örsten S, Baysal İ, Yabanoglu-Ciftci S, Ciftci T, Ünal E, Akıncı D, et al. Can parasite-derived microRNAs differentiate active and inactive cystic echinococcosis patients? Parasitol Res. 2022; 121: 191-6.
14. Canty AJ, Ripley B. boot: Bootstrap R (S-Plus) functions. R Package Version. 2024.
15. Davison AC, Hinkley DV. Bootstrap methods and their applications. Cambridge University Press: Cambridge;1997.
16. Bates D, Maechler M, Bolker B, Walker S. Fitting linear mixed-effects models using lme4. Journal of Statistical Software. 2015; 67: 1-48.
17. Kuznetsova A, Brockhoff PB, Christensen RHB. lmerTest package: tests in linear mixed Effects models. Journal of Statistical Software. 2017; 82: 1-26.
18. Dag O, Dolgun A, Konar N. onewaytests: An R package for One-Way tests in independent groups designs.The R Journal. 2018; 10: 175-99.
19. Mariconti M, Vola A, Manciulli T, Genco F, Lissandrin R, Meroni V, et al. Correction to: role of microRNAs in host defense against *Echinococcus granulosus* infection: a preliminary assessment. Immunol Res. 2019; 67: 98. Erratum for: Immunol Res. 2019; 67: 93-7.
20. Cucher M, Prada L, Mourglia-Ettlin G, Dematteis S, Camicia F, Asurmendi S, et al. Identification of Echinococcus granulosus microRNAs and their expression in different life cycle stages and parasite genotypes. Int J Parasitol. 2011; 41: 439-48.
21. Lin K, Zhou D, Li M, Meng J, He F, Yang X, et al. Echinococcus granulosus cyst fluid suppresses inflammatory responses by inhibiting TRAF6 signalling in macrophages. Parasitology. 2021; 148: 887-94.
22. Ren B, Wang H, Ren L, Yangdan C, Zhou Y, Fan H, et al. Screening for microRNA-based diagnostic markers in hepatic alveolar echinococcosis. Medicine (Baltimore). 2019; 98: e17156.
23. Shaughnessy RG, Farrell D, Riepema K, Bakker D, Gordon S V. Analysis of biobanked serum from a mycobacterium avium subsp paratuberculosis bovine infection model confirms the remarkable stability of circulating mirna profiles and defines a bovine serum mirna repertoire. PLoS One. 2015; 10: e0145089.
24. Matias-Garcia PR, Wilson R, Mussack V, Reischl E, Waldenberger M, Gieger C, et al. Impact of long-term storage and freeze-thawing on eight circulating microRNAs in plasma samples. PLoS One. 2020; 15: e0227648.
25. Guo X, Zheng Y. Expression profiling of circulating miRNAs in mouse serum in response to Echinococcus multilocularis infection. Parasitology. 2017; 144: 1079-87.
26. Zhang X, Gong W, Cao S, Yin J, Zhang J, Cao J, et al. Comprehensive analysis of non-coding RNA profiles of exosome-like vesicles from the protoscoleces and hydatid cyst fluid of *Echinococcus granulosus*. Front Cell Infect Microbiol. 2020; 10: 316.
27. Karami MF, Beiromvand M, Rafiei A, Dayer D, Rahdar M, Bahreini A, et al. Serum level of egr-miR-2a-3p as a potential diagnostic biomarker for cystic echinococcosis. Acta Parasitol. 2023; 68: 114-21.
28. Siracusano A, Delunardo F, Teggi A, Ortona E. Host-parasite relationship in cystic echinococcosis : an evolving story. Clin Dev Immunol. 2012; 2012: 7-9.
29. Mariconti M, Vola A, Manciulli T, Genco F, Lissandrin R, Meroni V, et al. Role of microRNAs in host defense against *Echinococcus granulosus* infection: a preliminary assessment. Immunol Res. 2019; 67: 93-7.

Turkiye Parazitol Derg 2025;49(1):29-34
DOI: 10.4274/tpd.galenos.2025.70894

Clinical Features and Quality of Life in Patients with Scabies

Uyuzlu Hastalarda Klinik Bulgular ve Yaşam Kalitesi

Münevver Güven, Aybüke Parlakdağ Kılcıoğlu
Aydın Adnan Menderes University Faculty of Medicine, Department of Dermatology, Aydın, Türkiye

Cite this article as: Güven M, Parlakdağ Kılcıoğlu A. Clinical features and quality of life in patients with scabies. Turkiye Parazitol Derg. 2025;49(1):29-34.

ABSTRACT

Objective: Scabies is a contagious cutaneous infestation characterized by intense itching. In this study, we aimed to evaluate the clinical features of scabies and the effect of scabies on quality of life, and the change in quality of life with treatment.
Methods: This prospective and cross-sectional study included 40 adults patients with classical scabies. Detailed skin examinations of the patients were performed. Dermatological life quality index (DLQI) was used to evaluate quality of life in patients with scabies. Visual analog scale (VAS) was used to investigate the severity of nocturnal itching and itch-related sleep disturbance. VAS levels and DLQI scores of the patients were evaluated at baseline (week 0) and after treatment (weeks 2 and 4).
Results: The most common lesion in patients was tunnel (100%), followed by papule (97.5%), crusted papule (85%) and excoriation (77.5%). The abdomen (90%) was the most common area of lesions, followed by hands (87.5%) and forearm (85%). It was determined that the quality of life of 75% of the patients was moderate to extremely large affected. There was a significant improvement in average DLQI scores of patients after treatment compared to before treatment ($p<0.001$, week 0: 11.50±7.81, week 2: 5.50±4.68, week 4: 1.05±2.08). The baseline VAS values of the patients for nocturnal itching and itch-related sleep disturbance were 7.22±2.80 and 6.30±3.60, respectively. A statistically significant improvement was detected in these values in the week 2 and week 4 ($p<0.001$). Thirty-nine of the patients were given 10% sulfur ointment (3 consecutive days) and 35 of these patients (89.7%) recovered.
Conclusion: Scabies has significant impact on quality of life in the vast majority of patients. Itch-related sleep disturbance is common in patients with scabies. Sulfur is an effective treatment choice for scabies.
Keywords: Itching, quality of life, scabies, sulfur

ÖZ

Amaç: Uyuz, yoğun kaşıntı ile karakterize bulaşıcı bir deri enfestasyonudur. Bu çalışmada uyuzun klinik özelliklerini ve uyuzun yaşam kalitesine etkisini ve tedaviyle yaşam kalitesindeki değişimi değerlendirmeyi amaçladık.
Yöntemler: Bu prospektif, kesitsel çalışmaya klasik uyuzlu 40 erişkin hasta dahil edildi. Hastaların detaylı deri muayeneleri yapıldı. Uyuzlu hastalarda yaşam kalitesini değerlendirmek için dermatolojik yaşam kalite indeksi (DYKİ) kullanıldı. Gece kaşıntısı ve kaşıntı ilişkili uyku bozukluğunun şiddeti vizüel analog skala (VAS) kullanılarak incelendi. Hastaların VAS düzeyleri ve DYKİ skorları başlangıçta (0. hafta) ve tedaviden sonra (2. ve 4. hafta) değerlendirildi.
Bulgular: Hastalarda en sık görülen lezyon tünel (%100) idi, bunu papül (%97,5), krutlu papül (%85) ve ekskoriasyon (%77,5) izliyordu. Lezyonların en sık görüldüğü bölge karın (%90) olup, bunu eller (%87,5) ve ön kol (%85) takip ediyordu. Hastaların %75'inin yaşam kalitesinin orta ila çok fazla etkilendiği belirlendi. Tedavi sonrası hastaların ortalama DYKİ skorlarında tedavi öncesine göre anlamlı iyileşme saptandı ($p<0,001$, 0. hafta: 11,50±7,81, 2. hafta: 5,50±4,68, 4. hafta: 1,05±2,08). Hastaların gece kaşıntısı ve kaşıntı ilişkili uyku bozukluğu için başlangıç ortalama VAS değerleri sırasıyla 7,22±2,80 ve 6,30±3,60 idi. Bu değerlerde 2. ve 4. haftada istatistiksel olarak anlamlı iyileşme saptandı ($p<0.001$). Hastaların 39'una %10 sülfürlü merhem verildi (3 ardışık gün) ve bu hastaların 35'i (%89,7) iyileşti.
Sonuç: Uyuz, hastaların büyük çoğunluğunda yaşam kalitesi üzerinde önemli bir etkiye sahiptir. Sülfür, uyuz için etkili bir tedavi seçeneğidir.
Anahtar Kelimeler: Kaşıntı, yaşam kalitesi, uyuz, sülfür

Received/Geliş Tarihi: 10.03.2025 **Accepted/Kabul Tarihi:** 11.04.2025 **Epub:** 17.04.2025 **Publication Date/Yayınlanma Tarihi:** 09.05.2025

Address for Correspondence/Yazar Adresi: Münevver Güven, Aydın Adnan Menderes University Faculty of Medicine, Department of Dermatology, Aydın, Türkiye
E-mail/E-Posta: munevver.guven@adu.edu.tr **ORCID ID:** orcid.org/0000-0001-8643-435X
***The study was also presented as an oral presentation at the 16th Aegean Dermatology Days-ISD Regional Meeting held in İzmir in 2023.**

Türkiye PARAZİTOLOJİ Dergisi

INTRODUCTION

Scabies is a contagious cutaneous infestation caused by the mite *Sarcoptes scabiei var. hominis* and is a significant public health problem in all countries regardless of socio-economic status (1). The prevalence of scabies has increased in the worldwide and in our country (Türkiye) in recent years (2,3).

Scabies is usually transmitted through close skin-to-skin contact or sexual contact. Generalized itching that worsen at night and cutaneous lesions begin 3-6 weeks after primary infestation. Burrow which is pathognomonic lesion of scabies and non-specific lesions such as papules and nodules are seen in patients with scabies (4). Burrow often seen on the flexural side of the wrist, the finger webs, the palms and the sides of the fingers. After appropriate treatment, itching and cutaneous lesions may persist for several weeks however will disappear completely over time (5).

The diagnosis of scabies is based on history and clinical findings. However, the diagnosis of corfirmed scabies can be made by identifying of the scabies mite or mite products (eggs or faeces) using various devices such as light microscopy, dermoscopy (6).

Scabies causes social stigma because it is transmitted through skin-to-skin contact and the cutaneous lesions are located in exposed areas (7,8). In addition, most patients with scabies complain of sleep disturbance and disruption of their work and social activities due to itching. All these reasons may affect the quality of life of scabies patients. In this study, we aimed to evaluate the clinical features of corfirmed scabies, the effect of scabies on quality of life and sleep and the change in quality of life after treatment. Another aim of the study was to determine the effectiveness of the treatment applied to scabies patients.

METHODS

Study Design and Population

Ethical approval was received for this prospective and cross-sectional study from Aydın Adnan Menderes University, Medical Faculty, Non-Interventional Clinical Research Ethics Committee (approval number: 2021/179, date: 02.12.2021).

Forty people involved in this prospective study were selected among the patients with classical scabies who applied to the dermatology outpatient clinic of Aydın Adnan Menderes University Hospital in Türkiye. Patients whose diagnosis of scabies was confirmed by dermoscopy, being 16 years or older, patients with itching for at least 1 week, and being literate were included in the study. Patients younger than 16 years, being illiterate, patients with chronic cutaneous disease (e.g., psoriasis, atopic dermatitis), patients with crusted scabies, patients with uncontrolled systemic disease (e.g., diabetes mellitus), patients with severe neurological disease (e.g., dementia), patients using immunosuppressive drug, and pregnant or breastfeeding women were excluded in the study. Written informed consent was obtained from all the patients.

Detailed skin examinations of the patients included in the study were performed by a dermatologist. Socio-demographics data and clinical characteristics of the patients were collected.

Treatment

In week 0, 39 patients were given 10% sulfur ointment (10 gram precipitated sulfur in 90 gram vaseline, prepared in the pharmacies), while 1 patient was given the lotion (commercial preparation containing mainly benzyl benzoate, sulfur, peru balsam) as treatment. Patients using 10% sulfur ointment applied the ointment to their entire body except the head for 3 consecutive days and washed off on the fourth day. The effectiveness of the treatment was evaluated using dermoscopy at week 2. A patient was considered to have recovered if new lesions did not appear, old scabies lesions disappeared, and mites were not identified by dermoscopy. Patients who failed treatment were restarted 10% sulfur ointment (for 3 consecutive days) and re-evaluated at 4 week.

Questionnare and Measurements

The dermatology life quality index (DLQI) is the most extensively used questionnaire to measure the burden of cutaneous diseases and evaluate effectiveness of treatments based on patients' perspective (9). It was created by Finlay and Khan (10). The validity and reliability study of the Turkish version was made by Oztürkcan et al. (11). DLQI consists of 10 questions across 6 domains: Symptoms/feelings (questions 1 and 2), daily activities (questions 3 and 4), leisure (questions 5 and 6), work/school (questions 7), personal relationships (questions 8 and 9) and treatment (question 10). The questionnaire has four or five alternative responses for each question: not at all (0 score), a little (1 score), a lot (2 score), very much (3 score) and not relevant (0 score). The DLQI score is found by adding the scores of 10 questions. The DLQI score ranges from 0 to 30. The higher the DLQI score indicates the greater the deterioration in quality of life (10). The DLQI scores are categorized as follows: 0-1= no effect on patient's life; 2-5= small effect on patient's life; 6-10= moderate effect on patient's life; 11-20= very large effect on patient's life; and 21-30= extremely large effect on patient's life (12). The DLQI questionnaires were completed by patients at baseline (week 0), week 2, and week 4. The quality of life questionnaire team at Cardiff University Faculty of Medicine has granted us a free license to use the DLQI-Turkish version for the purposes of the study.

Patients' nocturnal itching and itch-related sleep disturbance were measured by visual analog scale (VAS), which has a numerical rating from 0 to 10 (0=no itch/no itch-related sleep disturbance, 10= worst imaginable itch/I couldn't sleep at all). VAS measurements were completed by patients at baseline (week 0), week 2, and week 4.

Statistical Analysis

Data analysis was conducted using IBM SPSS Statistics 25.0 (IBM Corp., Armonk, New York). Categorical variables were shown as numbers and percentages, while continuous variables were shown as mean and standard deviation. Wilcoxon signed-rank test was used on the data obtained at baseline and after treatment to evaluate the changes with treatment in the DLQI, nocturnal itching and itch-related sleep disturbance. A p-value less than 0.05 or 0.001 was considered statistically significant.

RESULTS

Of the 40 adults with scabies, 19 (47.5%) were males and 21 (52.5%) were females. The mean age of the patients was 33.2±14.2 years, and the ages ranged from 19 to 68 years. The mean duration of complaints was 11.8±14.6 weeks (range =1-52 weeks). All patients complained of itching. And 38 (95%)

patients had nocturnal itching. Thirteen (32.5%) patients also had a stinging sensation, and 16 (40%) patients had a burning sensation. Thirty-three patients (82.5%) reported itch-related sleep disturbance. Eighteen of the patients (45%) had at least one family member with similar complaints. Twenty-seven (67.5%) of the patients had previously applied to a health institution at least once due to their complaints, and only 6 (22.2%) of them were diagnosed with scabies and received topical scabies treatment.

Burrow, the pathognomonic lesion of scabies, was present in all patients. The most common non-spesific lesions seen in patients were the papules (97.5%), followed by crusted papules (85%), excoriations (77.5%) and macules (55%). Details of lesion types in scabies patients are shown in Table 1.

Lesions were most commonly observed on the abdomen (90%), followed by hands (87.5%) and forearm (85.0%). The face (2.5%) was the area with the least lesions. Localization details of lesions in scabies patients are shown in Table 2.

It was determined that scabies had a moderate or a very large effect on the quality of life in majority (57.5%) of the scabies patients. At week 2 after treatment, it was observed that scabies had small effect the quality of life of the majority (55%) of patients. At week 4 after treatment, it was observed that scabies had not effect the quality of life of the majority (80%) of patients. There was only 1 patient whose quality of life was very large affected at week 4, and this patient was one of two patients in whom sulfur treatment failed. Banding according to the DLQI scores at baseline and after treatment in scabies patients was shown in Table 3.

Symptoms/feelings domain was the most affected domain at baseline (week 0). After the treatment, it was determined that there was a decrease in the scores of other domains except the treatment domain (Table 4). Question 1 (related to symptoms, over the last week, how itchy, sore, painful or stinging has your skin been?) had the highest score (2.4±0.63) among the DLQI questions and all patients received at least 1 score. While the mean DLQI score of the patients was 11.50±7.81 before treatment (week 0), it was found as 5.50±4.68 (week 2) and 1.05±2.08 (week 4) after treatment. It was determined that the mean DLQI scores after treatment (week 2 and week 4) showed a statistically significant improvement compared to week 0. It was also determined that mean DLQI scores was decreased significantly the week 4 when compared to the week 2. The patients' baseline VAS values for nocturnal itching and itch-related sleep disturbance in week 0 were found be 7.22±2.80 and 6.30±3.60, respectively. A statistically significant improvement was detected in these values both in the week 2 and week 4 compared to the week 0 ($p<0.001$) (Table 5). While only 2 patients evaluated nocturnal itching as 0 points (no itching) in week 0, 7 patients evaluated it as 0 points in week 2, and 25 patients evaluated it as 0 points in the week 4. In addition, only 7 patients evaluated itch-related sleep disturbance as 0 points (no itch-related sleep disturbance) in week 0, 15 patients evaluated it as 0 points in week 2, and 30 patients evaluated it as 0 points in the week 4.

Thirty-six of 40 patients (90%) recovered at week 2. All 4 patients who failed treatment used 10% sulfur ointment. The success rate of 10% sulfur ointment was found to be 89.7% in patients who received 10% sulfur ointment. When 10% sulfur ointment was restarted in the four patients whose treatment failed, two of the four patients recovered at week 4. No major side effects were observed during sulfur treatment and the patients completed the treatment as recommended.

Table 1. Types of lesions in patients with scabies

Types of lesion	**Patients with scabies (n=40) n (%)**
Burrows	40 (100)
Papules	39 (97.5)
Crusted papules (papule covered with thin crust)	34 (85)
Excoriations	31 (77.5)
Macules	22 (55)
Eczematization	7 (17.5)
Vesicles	6 (15)
Pustules	5 (12.5)
Nodules	4 (10)
Superinfection/secondary infection (suppuration, abscess, secondary impetigo, *furuncle*)	0 (0)

Table 2. Localization details of lesions in patients with scabies (n=40)

Localization details of lesions	**n (%)**
Abdomen	36 (90)
Hand * Hand (except interdigital spaces) * Interdigital spaces	36 (87.5) 31(77.5) 33 (82.5)
Forearm * Forearm (except elbow and wrist) * Elbow * Wrist	34 (85) 28 (70) 13 (32.5) 23 (57.5)
Legs	26 (65)
Penis (n=21)	13 (61.9)
Buttock	24 (60)
Inguinal area + inner side of thigh	24 (60)
Thigh (except inner side of thigh)	20 (50)
Lower back	18 (45)
Upper back	15 (37.5)
Upper arm	12 (30)
Thorax (except breast)	12 (30)
Axilla	8 (20)
Genital (except penis in men)	6 (15)
Feet	6 (15)
Breast *Areola mammae *Breast (except areola mammae)	5 (12.5) 1 (2.5) 5 (12.5)
Ankle	3 (7.5)
Scalp	3 (7.5)
Neck	3 (7.5)
Face	1 (2.5)

Table 3. Banding according to the dermatology life quality index scores at baseline and after treatment in scabies patients

Week 0 n (%)	Week 2 n (%)	Week 4 n (%)	Range of DLQI scores	QoL effect
1 (2.5)	5 (12.5)	32 (80)	**0-1**	No effect
9 (22.5)	22 (55)	7 (17.5	**2-5**	Small effect
12 (30)	7 (17.5)	-	**6-10**	Moderate effect
11 (27.5)	5 (12.5)	1 (2.5)	**11-20**	Very large effect
7 (17.5)	1 (2.5)	-	**21-30**	Extremely large effect

DLQI: Dermatology life quality index, QoL: Quality of life

Table 4. Impairment* and scores of each DLQI domain at baseline (week 0) and after treatment (week 2 and week 4) in scabies patients

	Week 0		Week 2		Week 4	
	Score Mean ± SD	Impairment n (%)	Score Mean ± SD	Impairment n (%)	Score Mean ± SD	Impairment n (%)
Symptoms, feelings (questions 1 and 2)	4.26±1.53	40 (100)	1.75±1.14	34 (85)	0.30±0.79	7 (17.5)
Daily activities (questions 3 and 4)	1.90±1.86	27 (67.5)	0.85±1.05	21 (52.5)	0.05±0.31	1 (2.5)
Leisure (questions 5 and 6)	2.30±2.28	28 (70)	0.88±1.50	13 (32.5)	0.08±0.34	2 (5)
Work/school (question 7)	1.13±1.47	15 (37.5)	0.40±0.84	10 (25)	0.08±0.47	1 (2.5)
Personal relationships (questions 8 and 9)	1.18±1.51	19 (47.5)	0.40±0.74	11 (27.5)	0.05±0.22	2 (5)
Treatment (question 10)	0.65±1.02	13 (32.5)	1.35±0.86	32 (80)	0.50±0.59	18 (45)

DLQI: Dermatology life quality index, *: Impairment is equivalent to a score ≥1 in domain, SD: Standard deviation

Table 5. Nocturnal itching, itch-related sleep disturbance and DLQI scores of scabies patients at baseline (week 0) and after treatment (week 2 and week 4)

	Week 0 (Mean ± SD)	Week 2 (Mean ± SD)	Week 4 (Mean ± SD)	p
Total DLQI	11.50±7.81	5.50±4.68	1.05±2.08	<0.001[a,b,c]
Nocturnal itching-VAS	7.22±2.80	2.52±1.88	0.58±0.81	<0.001[a,b,c]
Itch-related sleep disturbance-VAS	6.30±3.60	2.12±2.15	0.30±0.65	<0.001[a,b,c]

DLQI: Dermatology life quality index, VAS: Visual analog scale, SD: Standard deviation. All values are expressed as mean ± SD, [a]: Week 0 vs. week 2, [b]: Week 0 vs. week 4, [c]: Week 2 vs. week 4

DISCUSSION

Patients with scabies present with non-specific lesions such as papules, nodules, eczematizations, excoriations, pustules, pyodermic lesions (impetigo and furuncles, etc.) and burrows, which are pathognomonic lesion of scabies (4,13). Various studies have reported that the most frequently observed lesions in patients with scabies are papules and excoriations (7,14,15). Consistent with these studies, the most common non-specific lesions in our study were papules and excoriations. Unlike these studies, our study was detected burrows in all patients. The reason for this is that scabies patients whose burrow was demostrated by dermoscopy were included in our study.

Various studies have shown that scabies lesions in older children and adults patients were mostly localized on the abdomen, inguinal area/medial parts of thights, axillas, hands, wrists, interdigital spaces, forearms, arms, legs, thorax, back, buttocks and genitals, rarely on the face, scalp, neck (7,14-16). It was observed that the lesion distribution of patients in our study was similar to other studies.

A study in China reported that scabies had a moderate to very large effect on quality of life in 71.9% of patients, with an mean DLQI score of 10.09 (8). A study in Nepal that scabies had a moderate to very large effect on quality of life in 80.6% of patients, and mean DLQI score of patients were 12.91 (17). In the study conducted in Iraq, it was reported that the scabies had a moderate to extremely large effect on quality of life in 100% of the scabies patients and the mean DLQI score was 14.95 (18). In two studies conducted in Türkiye, it was reported that the quality of life of the majority of scabies patients was moderately to extremely large affected, and mean DLQI scores of the patients were 10.54 and 13.16 (19,20). Similar to these studies, in our

study, it was determined that scabies had a moderate to extremely large effect on the quality of life in the majority (75%) of scabies patients. The mean DLQI score of our patients was 11.50±7.81 at baseline. Unlike our study and the studies mentioned above, in a study conducted in the Solomon Islands, it was reported that the quality of life of adults with scabies was small affected and mean DLQI score was 3.1 (21). Interestingly, another study conducted in Türkiye reported that the mean DLQI score in scabies patients was quite high at 27.75 (22). As shown in our study, although it is not life-threatening, scabies significantly affects the quality of life of patients. Therefore, it is important that patients are diagnosed early and their treatment begins as soon as possible. Although 27 (67.5%) of the our patients had previously applied a doctor at least once due to their complaints, unfortunately 21 of them were misdiagnosed. We think that reinforcing the training of physicians, about the scabies will be beneficial for early diagnosis and treatment of scabies.

In various studies, it has been reported that the most impaired domain in patients with scabies is symptoms/feelings (8,17,19,20). Similar to these studies, in our study, it was determined that the most frequently affected domain in scabies patients was symptoms/feelings. It was observed that the impairment of the symptoms/feelings domain gradually decreased after the treatment. Similarly, it was found that the impairment of other domain except the treatment domain decreased after the treatment. The increased impairment in the treatment domain at week 2 was probably related to the application of sulfur and fomite (clothing, towels, bedding, etc.) disinfection for the treatment of scabies.

Jackson et al. (7) demonstrated that 93.4% of scabies patients complained of itching, and 68.8% of them had itching classified as moderate to severe. Nair et al. (14) found that 99.9% of scabies patients had itching and 79.4% of scabies patients had night aggravation of itching. Worth et al. (15) showed that all scabies patients complained about itching, and the 75.1% of them had classified itching as moderate to severe. It was also reported that the severity and frequency of itching decreased significantly one week after ivermectin treatment (15). Similar to these studies, in our study, it was found that all patients complained of itching. In addition, the highest score among the DLQI questions was contained in question 1 (related to itching symptom). It was observed that the severity of nocturnal itching gradually decreased significantly both in the week 2 and week 4 after the treatment.

Studies have shown that the majority of patients with scabies have an itching-related sleep disturbance (7,14,15). Worth et al. (15) demostrated that 87.5% of patients with scabies had an itch-related sleep disturbance, and the majority of them had moderate to severe sleep disturbances. It was also reported that the severity of itch-related sleep disturbances decreased significantly one week after ivermectin treatment (15). In our study, consistent with the aforementioned study, 33 (82.5%) patients had itch-related sleep disturbance. It was observed that the severity of itch-related sleep disturbance gradually decreased after the treatment.

In a retrospective study from Türkiye, treatment success rate of 10% sulfur ointment was found to be superior to permethrin 5% treatment (83.5% vs. 50%, respectively) (23). In a retrospective study conducted by Altunel (24) from Türkiye, the success rate of the first course 5-10% sulfur treatment was reported as 71.9%. To the our knowledge, this is the first prospective study to evaluate the effectiveness of sulfur in the treatment of scabies in Turkish patients. We determined that the success rate of 10% sulfur ointment in scabies patients was 89.7%. Therefore, we think that sulfur, which is an effective and safe agent, be preferred as the first agent in the first-line treatment of scabies patients.

Study Limitations

The limitation of our study is the relatively small number of scabies patients. Another limitation is that it has not been investigated whether there is a relationship between quality of life and the clinical severity of scabies.

CONCLUSION

As a result, scabies significantly affects the quality of life in the vast majority of patients. After treatment, the quality of life in scabies patients returns to normal within a few weeks. Sulfur is an effective treatment choice for scabies.

*Ethics

Ethics Committee Approval: Ethical approval was obtained from Aydın Adnan Menderes University Faculty of Medicine, Non-Interventional Clinical Research Ethics Committee (date: 02.12.2021, approval number: 2021/179). The study was carried out according to the ethical standards stated in the Declaration of Helsinki and its amendments, and all patients were examined and included with respect to good clinical practice guidelines.

Informed Consent: Written informed consent form was obtained from the all participants.

Acknowledgments

We would like to thank all the patients who participated in the study. We are grateful to the quality of life questionnaire team in Cardiff University Faculty of Medicine for kindly granting us a free licence to use the DLQI. We would also like to thank Prof. Dr. Filiz Abacıgil from the department of public health for her valuable contributions to the statistical analysis of the study.

Footnotes

*Authorship Contributions

Surgical and Medical Practices: M.G., A.P.K., Concept: M.G., Design: M.G., A.P.K., Data Collection or Processing: M.G., A.P.K., Analysis or Interpretation: M.G., A.P.K., Literature Search: M.G., A.P.K., Writing: M.G.

Conflict of Interest: No conflict of interest was declared by the authors.

Financial Disclosure: The authors declared that this study received no financial support.

REFERENCES

1. Thomas C, Coates SJ, Engelman D, Chosidow O, Chang AY. Ectoparasites: Scabies. J Am Acad Dermatol. 2020; 82: 533-48.
2. Özden MG, Ertürk K, Kartal SP, Yayli S, Göktay F, Doğramacı CA, et al. An extraordinary outbreak of scabies in Turkey. J Eur Acad Dermatol Venereol. 2020; 34: e818-e20.
3. Schneider S, Wu J, Tizek L, Ziehfreund S, Zink A. Prevalence of scabies worldwide-an updated systematic literature review in 2022. J Eur Acad Dermatol Venereol. 2023; 37: 1749-57.
4. Arora P, Rudnicka L, Sar-Pomian M, Wollina U, Jafferany M, Lotti T, et al. Scabies: a comprehensive review and current perspectives. Dermatol Ther. 2020; 33: e13746.

5. Executive Committee of Guideline for the Diagnosis and Treatment of Scabies. Guideline for the diagnosis and treatment of scabies in Japan (third edition): Executive Committee of Guideline for the Diagnosis and Treatment of Scabies. The Journal Dermatolgy. 2017; 44: 991-1014.
6. Engelman D, Yoshizumi J, Hay RJ, Osti M, Micali G, Norton S, et al. The 2020 International Alliance for the Control of Scabies Consensus Criteria for the Diagnosis of Scabies. Br J Dermatol. 2020; 183: 808-20.
7. Jackson A, Heukelbach J, Filho AF, Júnior Ede B, Feldmeier H. Clinical features and associated morbidity of scabies in a rural community in Alagoas, Brazil. Trop Med Int Health. 2007; 12: 493-502.
8. Jin-gang A, Sheng-xiang X, Sheng-bin X, Jun-min W, Song-mei G, Ying-ying D, et al. Quality of life of patients with scabies. J Eur Acad Dermatol Venereol. 2010; 24: 1187-91.
9. Vyas J, Johns JR, Abdelrazik Y, Ali FM, Ingram JR, Salek S, et al. The dermatology life quality index (DLQI) used as the benchmark in validation of 101 quality-of-life instruments: A systematic review. J Eur Acad Dermatol Venereol. 2025; 39: 631-79.
10. Finlay AY, Khan GK. Dermatology life quality index (DLQI)--a simple practical measure for routine clinical use. Clin Exp Dermatol. 1994; 19: 210-6.
11. Oztürkcan S, Ermertcan AT, Eser E, Sahin MT. Cross validation of the Turkish version of dermatology life quality index. Int J Dermatol. 2006; 45: 1300-7.
12. Hongbo Y, Thomas CL, Harrison MA, Salek MS, Finlay AY. Translating the science of quality of life into practice: What do dermatology life quality index scores mean? J Invest Dermatol. 2005; 125: 659-64.
13. Uzun S, Durdu M, Yürekli A, Mülayim MK, Akyol M, Velipaşaoğlu S, et al. Clinical practice guidelines for the diagnosis and treatment of scabies. Int J Dermatol. 2024; 63: 1642-56.
14. Nair PA, Vora RV, Jivani NB, Gandhi SS. A study of clinical profile and quality of life in patients with scabies at a rural tertiary care centre. J Clin Diagn Res. 2016; 10: WC01-5.
15. Worth C, Heukelbach J, Fengler G, Walter B, Liesenfeld O, Hengge U, et al. Acute morbidity associated with scabies and other ectoparasitoses rapidly improves after treatment with ivermectin. Pediatr Dermatol. 2012; 29: 430-6.
16. Heukelbach J, Wilcke T, Winter B, Feldmeier H. Epidemiology and morbidity of scabies and pediculosis capitis in resource-poor communities in Brazil. Br J Dermatol. 2005; 153: 150-6.
17. Paudel S, Pudasaini P, Adhikari S, Pradhan MB, Shekhar Babu KC. Quality of life in patients with scabies: a cross- sectional study using dermatology life quality index (DLQI) questionnaire. JEADV Clin Pract. 2023; 2: 399-403.
18. Bilal K, Othman SM, Asaad YA. Quality of life in patients with scabies in Erbil, Iraq. Zanco J Med Sci. 2021; 25: 638-48.
19. Koç Yıldırım S, Demirel Öğüt N, Erbağcı E, Öğüt Ç. Scabies affects quality of life in correlation with depression and anxiety. Dermatol Pract Concept. 2023; 13: e2023144.
20. Karadoğan SK, Ulgen Altay B. Dermatology quality of life and depression, anxiety, and stress scale-42 in scabies patients. Dermatol Pract Concept. 2024; 14: e2024112.
21. Lake SJ, Engelman D, Sokana O, Nasi T, Boara D, Marks M, et al. Health-related quality of life impact of scabies in the Solomon Islands. Trans R Soc Trop Med Hyg. 2022; 116: 148-56.
22. Demirbas A, Demirbas GU, Durmaz K, Metin Z. Investigation of the effect of oral ivermectin on systemic inflammatory response and quality of life in scabies patients. Arch Dermatol Res. 2024; 316: 601.
23. Ertugrul G, Aktas H. Comparison of sulfur ointment and permethrin treatments in scabies. Dermatol Ther. 2022; 35: e15897.
24. Altunel CT. The efficacy, safety and tolerability of sulfur in the treatment of scabies: A cross-sectional study. Turkiye Klinikleri J Dermatol. 2022; 32: 175-83.

Turkiye Parazitol Derg 2025;49(1):35-44
DOI: 10.4274/tpd.galenos.2025.32154

Molecular Characterization of *Culicoides* Species and Their Vector Potentials for Haemosporidia Infections in the İzmir Region of Türkiye

Türkiye'nin İzmir Yöresinde Yayılış Gösteren Culicoides Türlerinin Moleküler Karakterizasyonu ve Haemosporidia Enfeksiyonları Yönünden Vektörlük Potansiyelleri

Hakan Yeşilöz[1], Zuhal Önder[2], Alparslan Yıldırım[2]
[1]Republic of Türkiye, Ministry of Agriculture and Forestry, Veterinary Control Institute, İzmir, Türkiye
[2]Erciyes University Faculty of Veterinary Medicine, Department of Parasitology, Kayseri, Türkiye

Cite this article as: Yeşilöz H, Önder Z, Yıldırım A. Molecular characterization of *Culicoides* species and their vector potentials for haemosporidia infections in the İzmir region of Türkiye. Turkiye Parazitol Derg. 2025;49(1):35-44.

ABSTRACT

Objective: This study aimed to determine the *Culicoides* species distributed across different districts of İzmir province, reveal their molecular characterization, and assess their vector potential for the transmission of avian haemosporidian parasites.
Methods: The study material comprised 800 female *Culicoides* specimens collected from Bergama, Ödemiş, Kemalpaşa, and Foça districts between May and August 2016. Following morphological identification, specimens from each identified species underwent molecular analyses. The *mt-COI* gene region of genomic DNA isolates from the specimens was amplified by polymerase chain reaction (PCR) and subjected to sequence analyses to reveal their molecular characterization and phylogenetic relationships. Haemosporidian DNA was investigated by nested PCR in the gDNA isolates of head/thorax (HTP) and abdomen pools, constituted from specimens separated by species and location. Molecular characterization of identified parasites was performed using sequence analyses.
Results: Morphological identification revealed that *C. circumscriptus* (39.4%) and *C. imicola* (33.8%) were the most common species in the research areas, followed by *Culicoides* sp. (ERU-Izm-Culi1) (9.1%), *C. nubeculosus* complex (7.6%), *C. obsoletus* (4.3%), *C. gejgelensis* (2.3%), *C. punctatus* (1.9%), and *C. newsteadi* (1.8%). A total of 175 polymorphic sites were distributed among the COI sequences of the obtained isolates, leading to the detection of 18 different haplotypes. The highest haplotype diversity was observed in *C. circumscriptus*, *C. punctatus*, and *C. newsteadi*. Phylogenetic analyses clustered the characterized haplotypes of *Culicoides* species into three major groups. *Haemoproteus* sp. GAGLA05 and *H. minutus* TURDUS2 lineages were detected in *C. circumscriptus* HTP genomic DNA isolates, providing evidence of this species' vector potential for *Haemoproteus* lineages in the research area.
Conclusion: This study determined the *Culicoides* species distributed in the İzmir Region using an integrated morphological and molecular diagnostic approach, providing original data for the molecular epidemiology of these important flies. Furthermore, the results suggest the potential importance of *C. circumscriptus* in the transmission dynamics of *Haemoproteus* lineages.
Keywords: *Culicoides*, molecular characterization, avian Haemosporidians, vector potential, İzmir

ÖZ

Amaç: Bu çalışmada İzmir'in farklı ilçelerinde yayılış gösteren *Culicoides* türlerinin belirlenmesi, moleküler karakterizasyonlarının yapılması ve kanatlı haemosporidian parazitleri yönünden vektörlük potansiyellerinin araştırılması amaçlanmıştır.
Yöntemler: Çalışma materyalini, 2016 yılının Mayıs-Ağustos ayları arasında Bergama, Ödemiş, Kemalpaşa ve Foça ilçelerinden toplanan toplam 800 adet dişi *Culicoides* örneği oluşturmuştur. *Culicoides* örneklerinin morfolojik teşhislerini takiben belirlenen her türe ait örnekler moleküler analizlere dahil edilmiştir. Örneklere ait genomik DNA izolatlarının *mt-COI* gen bölgesi polimeraz zincir reaksiyonunda (PZR) amplifiye edilmiş ve sonraki basamakta amplifikasyon ürünlerinin sekans analizleri gerçekleştirilerek moleküler karakterizasyonları ve filogenetik analizleri yapılmıştır. Tür ve lokasyonuna göre ayrılan örneklerin baş/toraks (BTH) ve abdomenlerinden ayrı havuzlar oluşturularak elde edilen gDNA izolatlarında haemosporidian DNA'sının varlığı nested PZR ile araştırılmış ve tespit edilen parazit nesillerinin sekans analizleri ile moleküler karakterizasyonları yapılmıştır.

Received/Geliş Tarihi: 07.04.2023 **Accepted/Kabul Tarihi:** 22.04.2025 **Publication Date/Yayınlanma Tarihi:** 09.05.2025

Address for Correspondence/Yazar Adresi: Alparslan Yıldırım, Erciyes University Faculty of Veterinary Medicine, Department of Parasitology, Kayseri, Türkiye
E-mail/E-Posta: yildirima@erciyes.edu.tr **ORCID ID:** orcid.org/0000-0001-9868-0363

Türkiye PARAZİTOLOJİ Dergisi

Bulgular: Morfolojik teşhis sonuçlarına göre araştırma bölgelerinde *C. circumscriptus* (%39,4) ve *C. imicola*'nın (%33,8) en yaygın türler olduğu bunu sırasıyla *Culicoides* sp. (ERU-Izm-Culi1) (%9,1), *C. nubeculosus* kompleks (%7,6), *C. obsoletus* (%4,3), *C. gejgelensis* (%2,3), *C. punctatus* (%1,9) ve *C. newsteadi*'nin (%1,8) izlediği saptanmıştır. Belirlenen türlere ait mt-COI sekansları arasında 18 farklı haplotipi ortaya koyan 175 polimorfik bölge saptanmış olup haplotip çeşitliliği en yüksek *C. circumscriptus, C. punctatus* ve *C. newsteadi*'de belirlenmiştir. Filogenetik analizlerde belirlenen *Culicoides* türlerine ait haplotipler üç major küme içerisinde monofiletik olarak gruplanmıştır. *Culicoides circumscriptus* BTH'ye ait genomik DNA izolatlarında *Haemoproteus* sp. GAGLA05 ve *H. minutus* TURDUS2 nesillerinin varlığı saptanmış ve bu türün araştırma yöresinde ilgili *Haemoproteus* nesillerinin muhtemel potansiyel vektörü olabileceği ortaya çıkarılmıştır.
Sonuç: Bu çalışma ile İzmir yöresinde yaygınlık gösteren *Culicoides* türleri entegre morfolojik ve moleküler teşhis yaklaşımlarıyla belirlenerek bu önemli sineklerin moleküler epidemiyolojisi açısından özgün veriler sağlanmıştır. Ayrıca çalışma sonuçları İzmir yöresinde *C. circumscriptus*'un *Haemoproteus* nesillerinin nakli açısından potansiyel bir öneme sahip olduğuna dair kanıtlar sağlamıştır.
Anahtar Kelimeler: *Culicoides*, moleküler karakterizasyon, kanatlı Haemosporidian parazitler, vektör potansiyeli, İzmir

INTRODUCTION

Culicoides Latreille, 1809 (Diptera: Ceratopogonidae), also known as biting midges, are the smallest blood-feeding insects with a body length of 1 to 3 mm among other biting insects (1). The genus *Culicoides* is important due to their ability to act as biological vectors for pathogens of medical and veterinary significance (2). Several nematode and protozoan species, as well as more than 50 arboviruses, have been isolated from various *Culicoides* species, and their roles in the transmission of veterinary (1,3,4) and human pathogens (5) have been reviewed. Currently, the most important economic impact of *Culicoides* flies is their association with the transmission of diseases such as Blue Tongue virus (BTV), Epizootic Hemorrhagic Disease virus, Schmallenberg virus, and African Horse Sickness virus. These arboviruses are highly significant for ruminants, deer, and ungulates, and have been reported by the World Organization for Animal Health to cause outbreaks (6,7).

Culicoides flies are the main vectors of *Haemoproteus* (Haemosporida) species, which are important parasites of birds and can cause lethal pathology in non-adapted birds (8-11). Despite more than 1360 *Culicoides* species have been known (12), completeness of sporogonic phase of avian *Haemoproteus* parasites have been shown only in 13 species which indicates those serve as active vectors (13,14). In addition to about 150 *Haemoproteus* species identified from birds (15). In a study conducted in Türkiye to investigate haemosporidian parasites in *Culicoides* species (16), various *Haemoproteus* lineages were molecularly characterized in specimens of *C. nubeculosus* comp., *C. riethi*, *C. circumscriptus*, *C. submaritimus*, *C. gejgelensis*, *C. longipennis*, *C. festivipennis*, and *C. newsteadi* collected from the Sultan Marshes Region. The data obtained from this study (16) provided information on the vectorial potentials of the relevant *Culicoides* species.

The first records on *Culicoides* species in Türkiye were provided by Kieffer (17), and data on species diversity have mainly increased after the 1970s. In a review by Dik (18), the number of *Culicoides* species in Türkiye was reported as 61. Later, Korkmaz et al. (19) identified new species through a comprehensive four-year research conducted in 51 provinces at 104 sampling stations, increasing the total number of species to 72 (20). Limited research has been conducted on the genetic diversity of *Culicoides* species in Türkiye. Dik et al. (21) characterized the *Culicoides* species collected from the Southern and Southeastern Anatolian Regions based on the ribosomal *ITS-1* gene region. The characterization of *Culicoides* species collected from Sultan Marshes (16), the Western Black Sea Region, and Konya (22,23) was conducted based on the *mitochondrial cytochrome oxidase subunit I* (*mt-COI*) gene region, and their phylogenetic relationships were determined. Korkmaz et al. (19) characterized the *mt-COI* gene region of the *C. grisescens* and *C. chiopterus* species, that were reported for the first time in Türkiye.

In the current study, we aimed to determine the *Culicoides* species prevalent in different districts of İzmir province using conventional morphological and molecular methods, to perform molecular characterization of the isolates, and to reveal their vector potentials for the transmission of avian haemosporidian parasites.

METHODS

Study Area and Collection of *Culicoides* Specimens

The *Culicoides* specimens comprising the study material were collected from areas in the districts of Bergama, Ödemiş, Kemalpaşa, and Foça, located within the boundaries of İzmir province, between May and August 2016. "EVS Black CO2 Light Trap, 4W Black Light Tube (Bioquip Inc., 2801BL)" and Onderstepoort light traps were set up approximately 1.5-2 meters high, one hour before sunset, and operated until one hour after sunrise in livestock facilities in the corresponding districts. After sampling, the nets of the light traps were stored in a deep freezer to immobilize the caught flies. Non-target flies were separated macroscopically, and the remaining flies were placed in 70% alcohol and transported to the laboratory on ice packs. From each region, 200 samples were randomly selected and included in the study.

Morphological Identification

Identification of the *Culicoides* specimens was made based on wing morphology using a combination of established and more recent diagnostic keys (24-26). Examinations were conducted under a digital camera attachment stereomicroscope (Olympus SZX-16). The imaging of the wing morphologies of *Culicoides* species was performed using CellSens Standard 1.13 software (Olympus) under the camera attachment stereomicroscope.

Genomic DNA Extraction

Morphologically identified *Culicoides* specimens were separated individually from the collection material preserved in 70% ethyl alcohol for genotyping and phylogenetic analyses. The remaining specimens were pooled in groups of ten (10 samples/pool) to investigate the presence of Haemosporidian parasites, including females, according to species and collection area. To demonstrate the vector potential of *Culicoides* specimens, the heads/thoraxes (HTP) (sporozoite development) and abdomens (AP) (haemosporidian generations acquired through blood feeding) of each specimen were dissected separately and placed in separate sterile microcentrifuge tubes and pooled accordingly,

resulting in 88 pools each for HTP and AP. Genomic DNA isolation was performed using the GeneJET Genomic DNA Purification Kit (Thermo Scientific) following the manufacturer's instructions.

Amplification of *Culicoides* Mt-COI and Avian Haemosporidian *Mt-CYTB* Gene Regions

Genomic DNA extracts isolated from individual female *Culicoides* specimens were subjected to polymerase chain reaction (PCR) analysis using primers C1-J-1718M (F) (5'-GGAGGATTTGGAAATTGATTAGT-3') and C1-N-2191M (R) (5'-CAGGTAAAATTAAAATATAAACTTCDGG-3'), which amplify a 523 bp partial fragment of the *mt-COI* gene of the *Culicoides* genus (27). The reaction mixture was prepared to a final volume of 25 µL. It contained 10X PCR buffer, 2.5 mM $MgCl_2$, 100 nM of each primer, 200 µM of each dNTP, 2.5 U Taq DNA polymerase, and 10-20 ng template DNA. The thermal cycling protocol was as follows: Initial denaturation at 94 °C for 3 min, followed by 35 cycles of denaturation at 94 °C for 30 s, annealing at 50 °C for 30 s, and extension at 72 °C for 30 s, with a final extension step at 72 °C for 7 min.

The genomic DNA isolates obtained from Culicoides HTP and AP were analyzed by Nested PCR targeting a 524 bp portion of the *mt-CYTB* gene region of haemosporidian parasites. In the first step of the Nested PCR analysis, universal primers HaemNFI (5'-CATATATTAAGAGAATATGGAG-3') and HaemNR3 (5'-ATAGAAAGATAAGAAATACCATTC-3') were used for haemosporidians. In the second step, *Leucocytozoon*-specific primers HaemFL (5'-ATGGTGTTTTAGATACTTACATT-3') and HaemR2L (5'-CATTATCTGGATGAGATAATGGIGC-3'), and *Plasmodium/Haemoproteus*-specific primers HaemF (5'-ATGGTGCTTTCGATATATGCATG-3') and HaemR2 (5'-GCATTATCTGGATGTGATAATGGT-3') were used (28,29). The reaction mixture for both primer sets was prepared to a final volume of 20 µL, containing 10X PCR buffer, 2.5 mM $MgCl_2$, 100 nM of each primer, 200 µM of each dNTP, and 2.5U Taq DNA polymerase. The PCR products were subjected to electrophoresis on a 1.5% agarose gel (10 µL), visualized and analyzed using the CLP Gel Documentation System and Gene Snap from Syngene analysis program (UVP INC Uplant, CA).

Sequence and Phylogenetic Analyses

The amplicons of mt-COI from individual *Culicoides* specimens and haemosporidian mt-cytb from pools were subjected to gel purification (using the High Pure PCR Product Purification Kit, Roche) for sequence analyses. Sequencing was utilized (Macrogen Europe) bi-directionally with the primers used in the PCR (the second primer pair for haemosporidian mt-CYTB). Chromatograms for forward and reverse reads were processed with DeNovo Assembly in Geneious R10 (30) software to obtain consensus sequences. The molecular characterizations of the identified isolates were achieved by aligning the sequences with the published sequences of the isolates using BLASTn algorithm (http://blast.ncbi.nlm.nih.gov/Blast.cgi) and the MalAvi Haemosporidian lineage sequence database (http://mbio-serv2.mbioekol.lu.se/Malavi/), and data sets were created for phylogenetic analyses. The *mt-COI* gene sequences of the identified *Culicoides* isolates in the study were recorded in the GenBank database with accession numbers MF594384-MF594401; and the mt-CYTB sequences of haemosporidian isolates were recorded with accession numbers MF594402-MF594403. DnaSP 5.10.01 (31) software was used to determine DNA polymorphism and haplotype diversity in the characterized *Culicoides* isolates. Intra- and inter-specific genetic differences were performed using the Kimura (32) two-parameter (K2P) distance model in MEGA 7 software (33). Bayesian inference (BI) analyses were applied to determine the phylogenetic relationships of *Culicoides* species and haemosporidian lineages. jModelTest v.0.1.1 (34) was used to determine the best-fit substitution model for sequence evolution, and the models with the lowest Akaike Information Criterion values were used to construct the phylogenetic trees. BI analyses were performed using the MrBayes (35) plugin in Geneious R10 (30) software. Markov Chain Monte Carlo scans were run for 1,100,000 generations with four chains, and tree sampling was performed every 200 generations with the first 100,000 trees discarded as "burn-in".

Statistical Analysis

Statistical analysis is not required for the data available in this study.

RESULTS

Culicoides Species and Distribution

The distribution of the morphologically identified *Culicoides* specimens by species, collection area, and month are shown in Table 1. A total of eight *Culicoides* species were identified in the research areas, and their distribution rates are shown in Figure 1. Generally, the most common species were *C. circumscriptus* (39.4%) and *C. imicola* (33.8%), while the species with the lowest distribution rates were *C. punctatus* (1.9%) and *C. newsteadi* (1.8%).

A unique *Culicoides* lineage was identified that exhibited a similar wing morphology to the species in the Silvaticulicoides subgenus (36,37), and was genetically closer to the species in this group. This lineage was characterized as *Culicoides* sp. ERU-Izm-Culi1. The specimens of *Culicoides* sp. ERU-Izm-Culi1 were detected in Bergama and Ödemiş districts in July and August samples (Table 1), and the overall distribution rate was determined to be 9.1% (Figure 2).

Sequence and Phylogenetic Analyses of *Culicoides* Specimens

Genomic DNA isolates of the specimens identified by morphological identification were amplified with the relevant primers for the *mt-COI* gene region, and target amplicons of 553 bp were obtained. The morphological diagnosis results were confirmed by aligning the sequences of the relevant isolates with reference isolates in GenBank using the BLASTn algorithm (http://blast.ncbi.nlm.nih.gov/Blast.cgi), and the molecular characterization of the isolates was provided. The isolates belonging to the species whose *mt-COI* gene region sequences and haplotype characterization were determined were given in Table 2 with GenBank accession numbers. One hundred seventy five polymorphic regions were found among the mt-COI sequences of the identified species, revealing 18 different haplotypes, and the average genetic diversity among haplotypes was found to be 25.3%±2.4. The haplotype diversity was determined to be highest in *C. circumscriptus, C. punctatus,* and *C. newsteadi* (Table 2). ERU-Izm-Culi1 was found to be genetically closer to species under the

Table 1. Distribution of *Culicoides* species collected from various districts of İzmir province by collection sites and months

***Culicoides* species**	**Collection area**				**2016**				**Total**
	Bergama	**Ödemiş**	**Kemalpaşa**	**Foça**	**May**	**June**	**July**	**August**	
C. circumscriptus	46	82	112	75	68	128	38	81	315
C. nubeculosus komp.	40	18	0	3	22	6	9	24	61
C. newsteadi	14	0	0	0	14	0	0	0	14
C. imicola	27	53	70	120	80	56	65	69	270
Culicoides sp. (*ERU-Izm-Culi1*)	58	15	0	0	0	0	65	8	73
C. gejgelensis	8	0	8	2	0	0	4	14	18
C. obsoletus	7	17	10	0	16	0	16	2	34
C. punctatus	0	15	0	0	0	10	3	2	15
Total	200	200	200	200	200	200	200	200	800

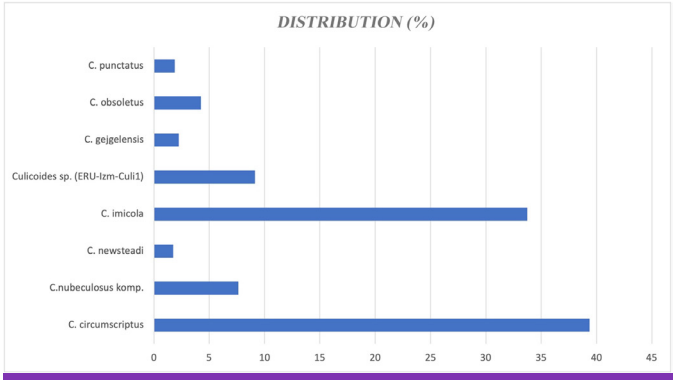

Figure 1. Distribution of *Culicoides* species identified in the study area

Figure 2. *Culicoides* sp. ERU-Izm-Culi1 wing morphology. There are no white spots in the middle of cells m1 (1) and m2 (2), the m cell is combined with the r-m cross-vein white spots (3), and the white spots on the distal parts of cells r3 and m1 are not clear (4). Scale bar: 200 µm

Silvaticulicoides subgenus, showing the highest genetic similarity of 92.9% with *C. subfasciipennis*.

The phylogenetic relationships of the identified isolates in this study along with reported isolates from various regions of Türkiye and the world, were shown in Figure 3. The mt-COI sequences formed three major clusters on the phylogenetic tree, containing monophyletic species, and this resolution was highly supported by posterior probabilities (0.9-1.0). The first major cluster was divided into two subclusters. The first subcluster included *C. nubeculosus, C. gejgelensis, C. riethi, Culicoides* sp. ERU-Izm-Culi1, and *C. subfasciipennis* species, and the phylogenetic relationship between the species was moderately supported by posterior probability (0.58). The second subcluster was formed by *C. circumscriptus*, and the phylogenetic relationship of the isolates belonging to this species was highly supported by posterior probability (1.0). The second major cluster consisted of haplotypes of *C. punctatus, C. newsteadi-1*, and *C. newsteadi-2* species, which were highly supported by posterior probability (0.92). The third major cluster included *C. obsoletus* and *C. imicola* species, and the phylogenetic relationship of the isolates belonging to these species was highly supported by posterior probability (1.0).

Identification, Distribution, and Molecular Characterization of Haemosporidian Parasites in *Culicoides* Specimens

The molecular analysis results of haemosporidian parasites in *Culicoides* specimens, which were collected during the study and diagnosed by morphological and molecular identifications, are provided in Table 3 for HTP and AP samples. An agarose gel image including the amplicons from some positive samples is given in Figure 4. Of the 88 AP samples examined, 9 (10.22%) were found to be infected with *Plasmodium/Haemoproteus* species or lineages, and 7 (7.95%) of the 88 HTP samples were also found to be infected with these parasites. No positivity for *Leucocytozoon* sp. was found in any of the samples.

The haemosporidian parasite species or lineages identified by sequence analysis along with their GenBank accession numbers, are given in Table 4. The GenBank accessions were provided only for isolates identified in the head/thorax pools as an indicator of their vector potential. Of the seven positive isolates from *C. circumscriptus* HTP, four belonged to the *Haemoproteus* sp. GAGLA05 lineage, and three belonged to the *H. minutus* TURDUS2 lineage. All of the positive AP isolates were characterized by *Plasmodium* lineages, and this result could be related to infected avian blood in their abdomens. The latest finding provided evidence of the widespread occurrence of various *Plasmodium* lineages, especially the *P. relictum* SGS1, in avian populations in the study area.

Table 2. Haplotypes identified in *Culicoides* species molecularly characterized by *Mt-COI* gene region sequence analyses

***Culicoides* species**	**No. of sequenced isolates**	**Determined haplotype**		
		Name	**Number**	**GenBank accession**
C. circumscriptus	6	ERU-Izm-C.circ1	3	MF594384
		ERU-Izm-C.circ2	2	MF594385
		ERU-Izm-C.circ3	1	MF594386
C. gejgelensis	7	ERU-Izm-C.gejg1	7	MF594387
C. imicola	6	ERU-Izm-C.imic1	4	MF594388
		ERU-Izm-C.imic2	2	MF594389
C. newsteadi	7	ERU-Izm-C.news1	4	MF594390
		ERU-Izm-C.news2	2	MF594391
		ERU-Izm-C.news3	1	MF594392
C. nubeculosus	6	ERU-Izm-C.nube1	5	MF594393
		ERU-Izm-C.nube2	1	MF594394
C. riethi	1	ERU-Izm-C.rie1	1	MF594400
C. obsoletus	13	ERU-Izm-C.obs1	6	MF594395
		ERU-Izm-C.obs2	7	MF594396
C. punctatus	6	ERU-Izm-C.punc1	4	MF594397
		ERU-Izm-C.punc2	1	MF594398
		ERU-Izm-C.punc3	1	MF594399
Culicoides sp.	7	ERU-Izm-Culi1	7	MF594401

Table 3. Molecular analysis results of Haemosporidian parasites in examined *Culicoides* specimens

Insect species	**No. of examined pools**										***Plasmodium/Haemoproteus* positivity**									
	Bergama		**Ödemiş**		**Kemalpaşa**		**Foça**		**Total**		**Bergama**		**Ödemiş**		**Kemalpaşa**		**Foça**		**Total**	
	AP	**HTP**	**AP**	**HTP**	**AP**	**HTP**	**AP**	**HTP**	**AP**	**HTPT**	**AP**	**HTP**	**AP**	**HTP**	**AP**	**HTP**	**AP**	**HTP**	**AP**	**HTP**
C. circumscriptus	5	5	7	7	10	10	7	7	29	29	1	1	0	1	0	3	0	2	1	7
C. imicola	3	3	6	6	7	7	11	11	27	27	0	0	0	0	1	0	2	0	3	0
Culicoides sp. (close to *C. truncorum*)	6	6	2	2	0	0	0	0	8	8	0	0	0	0	0	0	0	0	0	0
C. nubeculosus comp.	4	4	3	3	0	0	1	1	8	8	0	0	0	0	0	0	0	0	0	0
C. obsoletus	1	1	3	3	3	3	0	0	7	7	1	0	2	0	0	0	0	0	3	0
C. gejgelensis	1	1	0	0	2	2	1	1	4	4	0	0	0	0	2	0	0	0	2	0
C. punctatus	0	0	3	3	0	0	0	0	3	3	0	0	0	0	0	0	0	0	0	0
C. newsteadi	2	2	0	0	0	0	0	0	2	2	0	0	0	0	0	0	0	0	0	0
Total	22	22	24	24	22	22	20	20	88	88	2	1	2	1	3	3	2	2	9	7

DISCUSSION

The molecular genotyping and DNA barcoding studies of blood-sucking insects with medical and veterinary importance such as mosquitoes, biting midges, and black flies continue to gain importance in many regions of the world (38-41), while genetic studies in Türkiye have been limited (21,22,42,43). The *Culicoides* genus is important because it contains many species that are biological vectors for numerous pathogens of medical and veterinary importance (1,4,5,36). In the province of İzmir, due to its climatic characteristics (high temperature and humidity), the circulation of BTV is continuous in the field because *Culicoides* activity continues for a long period of the year. Therefore, it has been reported that BTV disease causes significant losses in the livestock sector in the province of İzmir every year (44). In this study, field surveys conducted in the regions of Bergama, Ödemiş, Kemalpaşa, and Foça districts of İzmir between May and August revealed that those regions were suitable ecosystems for the development of *Culicoides* species. As a result of the morphological and molecular diagnoses of *Culicoides* generations collected from the sampling areas, it was determined that *C. circumscriptus* and *C. imicola* were the most frequently encountered species during the

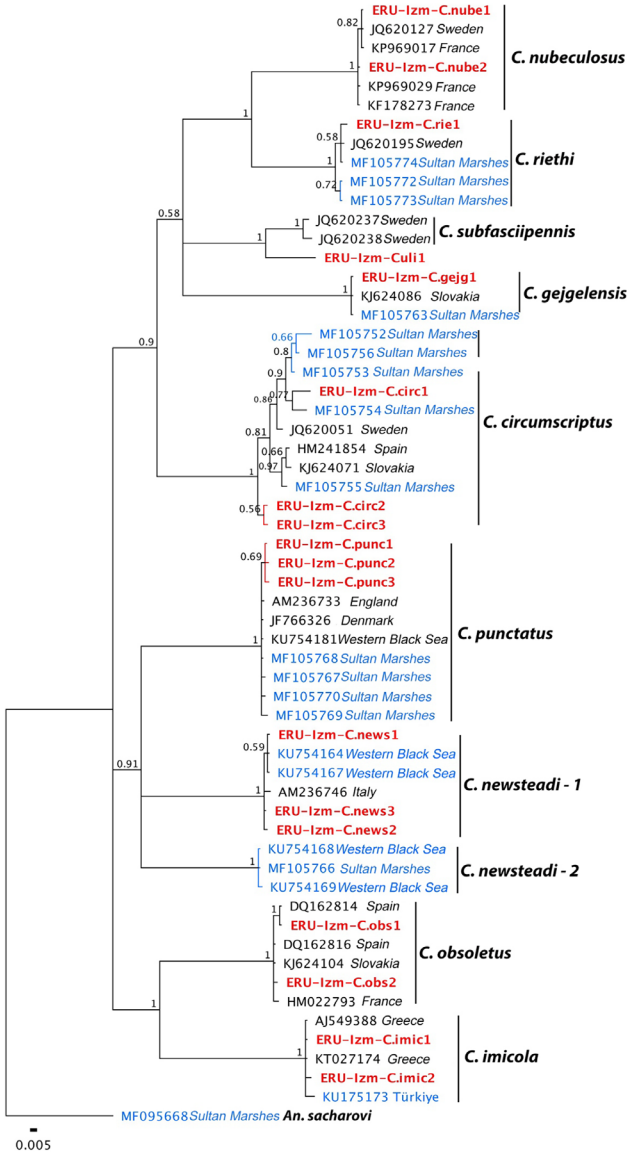

Figure 3. Phylogenetic relationships of *Culicoides* isolates based on *mt-COI* gene region Bayesian inference (BI) analysis. The isolates identified in the study are shown in bold red characters, while those reported from Türkiye are shown in blue. The numbers in front of the nodes represent BI posterior probabilities. *A. sacharovi* was used as an outgroup. The scale bar indicates the number of nucleotide substitutions per site

study period, representing 39.4% and 33.8% of the total collected specimens, respectively. In particular, it is known that *C. imicola* is one of the most effective vectors of BTV in many geographies, especially in Southern Europe (45,46), and it may play a role in the transmission dynamics of BTV observed in the research areas in the current study. Studies on populations sampled from Türkiye (47) and Italy (48) have suggested that *C. circumscriptus*, which was identified as the most frequently encountered species in our study, could also potentially contribute to the transmission dynamics of BTV. In research conducted in the last 10 years (21,22,47,49-54), both species have been reported as widespread

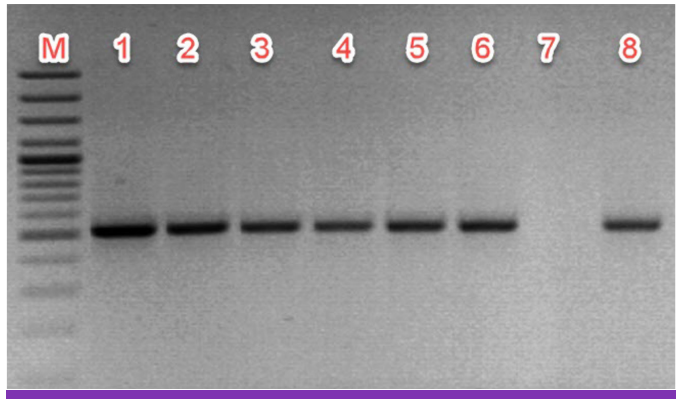

Figure 4. Agarose gel electrophoresis of *Haemoproteus/Plasmodium* amplicons obtained from Nested polymerase chain reaction analysis of gDNA isolates from selected *Culicoides* pools. M: 100 bp marker; 1-6: positive samples; 7: Negative control; 8: Positive control (Plasmodium DNA)

in Southern and Southeastern Anatolia, Central and Western Black Sea, Central Anatolia, Western Inner Anatolia, and the Marmara Region in Türkiye. The other species *C. nubeculosus* complex (7.6%), *C. obsoletus* (4.3%), *C. gejgelensis* (2.3%), *C. punctatus* (1.9%), and *C. newsteadi* (1.8%), which have a more limited distribution in our study, were found in various regions of Türkiye such as Southern and Southeastern Anatolia, Central and Western Black Sea, Central Anatolia, Western Inner Anatolia, and the Marmara Region (21,22,47,49-54). A unique *Culicoides* lineage was identified in Bergama and Ödemiş districts. This lineage showed similarities to members of the Silvaticulicoides subgenus based on wing morphology and was genetically closer to the species in this group based on mt-COI sequence characterization. The wing morphologies of these specimens were consistent and symmetrical across all samples. Furthermore, sequence analysis of a representative number of specimens confirmed the genetic similarity within this group. There was no genetic heterogeneity among the mt-COI sequences of samples belonging to this Culicoides lineage, and this group was designated as Culicoides sp. ERU-Izm-Culi1.

Based on the phylogenetic analysis of the mt-COI gene sequences of the isolates identified in our study, the characterized haplotypes were monophyletically placed in three major clusters. Low genetic diversity (0.2±0.2%) was identified between *C. nubeculosus* ERU-Izm-C.nube1-2 haplotypes within the first sub-cluster of the first major cluster, with ERU-Izm-C.nube1 haplotype being 100% identical to isolates from Sweden (JQ620127) and France (KP969017, 55), and ERU-Izm-C.nube2 haplotype being 100% identical to isolates from France (KP969029, KF178273, 55, 56). The ERU-Izm-C.rie1 haplotype, identified within the *C. nubeculosus* complex and molecularly characterized as belonging to *C. riethi*, formed a cluster showing high identity (99.6% and 99.4% respectively) with isolates reported from Sultan Marshes, Türkiye (MF105774, 16) and Sweden (JQ620237). This isolate also showed 99.1% identity with other *C. riethi* isolates reported from Sultan Marshes, Türkiye (MF105772, MF105773, 16). The *C. gejgelensis* ERU-Izm-C.gejg1 haplotype showed 100% identity with isolates reported from Sultan Marshes, Türkiye (MF105763, 16) and Slovakia (KJ624086, 37), and formed a cluster together. The mt-COI sequences of the specimens characterized as *Culicoides* sp. ERU-Izm-C.culi1 showed 100% identity to each

Table 4. Molecular characterization of Haemosporidian parasites according to the sequence analysis results

Species	No. of sequenced isolates		Sequence characterization of Haemosporidia			
	AP	HTP	*Plasmodium* species/ lineage	Number (AP)	*Haemoproteus* species/ lineage	Number (HTP) GenBank accession
Culicoides						
C. circumscriptus	1	7	*Plasmodium* sp./CXPIP10	1	*H. minutus*/TURDUS2	3 (MF594402)
					Haemoproteus sp./GAGLA05	4 (MF594403)
C.imicola	3	0	*P. relictum*/SGS1	2	-	-
			Plasmodium sp./YWT4	1		
C. obsoletus	3	0	*P. relictum*/SGS1	1	-	-
			Plasmodium sp./CXPIP23	1		
			Plasmodium sp./SYCON02	1		
C. gejgelensis	2	0	*P. relictum*/SGS1	1	-	-
			Plasmodium sp./YWT4	1	-	-

*: Sequence data obtained only from the BT pools were deposited in GenBank and accession numbers were provided for Haemosporidian species and lineages based on their vector potential, AP: Abdomen, HTP: Head/thorax

other, thus representing the same haplotype. The ERU-Izm-C. culi1 haplotype showed the highest genetic similarity (92.9%) with *C. subfasciipennis* isolates reported from Sweden (JQ620237, JQ620238), and formed a cluster together. This *Culicoides* lineage was closer to the species in the Silvaticulicoides subgenus with more than 7% genetic differences than to other *Culicoides* species. Therefore, the related *Culicoides* lineage may be an unidentified new species, and further studies are needed for species identification. The isolates of *C. circumscriptus* in the second sub-cluster of the first major cluster were found to form three separate groups. The ERU-Izm-C.circ1 haplotype showed high identity (average 97.3%) and formed a cluster with isolates from Sweden and Sultan Marshes, Türkiye (JQ620051, MF105754, 16). One isolate each from Spain (HM241854), Slovakia (KJ624071, 37), and Sultan Marshes, Türkiye (MF105755, 16) were included in the second group. A genetic difference of 0.4±0.3% was identified between the ERU-Izm-C.circ2 and ERU-Izm-C.circ3 haplotypes, and these two haplotypes formed the third cluster within the relevant group.

The second major group was formed by haplotypes belonging to *C. punctatus, C. newsteadi-1*, and *C. newsteadi-2* species. The clustering of the *C. newsteadi-1* and *2* species were made according to the classification of Pages et al. (25). A genetic difference of 0.3±0.2 was detected between the ERU-Izm-C.punc1-3 haplotypes *of C. punctatus*, and these haplotypes exhibited mean similarities of 99.5%, 99.7%, 99.4% and 99.6% to *C. punctatus* isolates from Sultan Marshes, Türkiye (MF105768-70, 16), Western Black Sea (KU754181, 22), England (AM236733, 24), and Denmark (JF766326, 57), respectively. Phylogenetic analysis of *C. newsteadi* revealed two separate groups, one of which was close to *C. punctatus*. ERU-Izm-C.news1-3 haplotypes were found in the first phylogenetic group, with the ERU-Izm-C. news1 haplotype grouping with the Western Black Sea isolates (KU754164, KU754167, 22) with 100% identity. The ERU-Izm-C. news2,3 haplotypes showed the highest identity with ERU-Izm-C. news1 and again with the Western Black Sea isolates (KU754164, KU754167, 22) (avg. 99.7%). The characterized isolates were also found to be on average 99.5% identical to the *C. newsteadi* isolate reported from Italy (AM236746, 24) in the same phylogenetic group. Isolates from the Western Black Sea (KU754168, KU754169, 22) and Sultan Marshes, Türkiye (MF105766, 16) comprised the second phylogenetic group of *C. newsteadi*, and this group showed an average genetic difference of 19.5±2.7% with the first phylogenetic group of *C. newsteadi*.

In the third major cluster, *C. obsoletus* and *C. imicola* are present. There is a genetic difference of 0.6±0.4% between the ERU-Izm-C. obs1 and ERU-Izm-C.obs2 haplotypes of *C. obsoletus*. The ERU-Izm-C.obs1 haplotype is identical to the isolate reported from Spain (DQ162814, 57) and is grouped accordingly. The ERU-Izm-C.obs2 haplotype has the highest similarity of 99.8% with the isolates from Spain (DQ162814, 57) and Slovakia (KJ624104, 36). *C. imicola* has a genetic difference of 0.4±0.3% between the haplotypes ERU-Izm-C.imic1 and ERU-Izm-C.imic2. The ERU-Izm-C.imic1 haplotype is 100% identical to the isolates from Greece (KT027174, 58), while the ERU-Izm-C.imic2 haplotype has a 99.6% similarity with the same isolates. Furthermore, the characterized haplotypes have shown similarities of 99.4% and 98.9% with the isolate reported from the Konya Region of Türkiye (KU175173).

In this study, as various researchers have indicated (59,60), to determine the infective and infected *Culicoides* specimens with haemosporidian parasites in the research area, pools were formed by dissecting the head-thorax (potentially infective) and abdomen (potentially infected) of each fly diagnosed at the species level. As is known, infective stage sporozoites are transmitted through the salivary glands of the female fly during feeding. The salivary glands extend towards the esophagus on the lateral sides of the thorax (61). Fertilization and oocyst development (non-infective

stage) take place in the mid-gut part (abdomen) of the fly. It has been expressed in various studies (59,60,62) that head-thorax pool (HTP) positivity can be considered an indicator of potential vector competence. Indeed, in our study, sequence analyses of the positive isolates obtained from HTP confirmed the presence of *Haemoproteus* parasites that *Culicoides* species are known to vector. In contrast, the sequences obtained from abdomen pools (AP) showed sequences of *Plasmodium* parasites, which are likely not vectored by *Culicoides*, possibly due to infected blood intake.

The *Haemoproteus* sp. GAGLA05 lineage identified in *C. circumscriptus* has been recorded in the blood of the Eurasian jay (*Garrulus glandarius*) belonging to the Passeriformes order (63), and parallel to our study, it was also isolated from *C. circumscriptus* in the Sultan Marshes Region of Türkiye (16). The *H. minutus* TURDUS2 lineage has been found to be common in avian communities, reported from 17 bird species belonging to eight families in the Passeriformes order and one bird species in the Psittaciformes order (MalAvi: http://mbio-serv2.mbioekol.lu.se/Malavi/). Additionally, the TURDUS2 lineage has been reported in mosquito species such as *Cx. pipiens* (64) and in *Culicoides* species including *C. festivipennis*, *C. kibunensis* (65), and *C. pictipennis* (66). Our study has revealed the first record of the potential vector status of *C. circumscriptus* for the possible transmission of the *H. minutus* TURDUS2 lineage. The *Plasmodium* sp. CXPIP10 lineage isolated and characterized from the abdominal pools of *C. circumscriptus* in our study has been reported in MalAvi records as a potential vector by various *Culex* species (67,68). The *Plasmodium* sp. CXPIP23 lineage isolated from *C. obsoletus* has been reported in the Little Bittern (*Ixobrychus minutus*) belonging to the Ciconiiformes order in the Sultan Marshes Region, Türkiye (16) and potential mosquito vectors *Cx. pipiens* (16) and *O. caspius* (62). The *P. relictum* SGS1 lineage identified in AP from *C. gejgelensis, C. imicola*, and *C. obsoletus* is a common lineage in birds and has been isolated from numerous bird species in 11 orders. *Plasmodium* sp. YWT4 isolated from *C. imicola* and *C. gejgelensis* AP and *Plasmodium* sp. SYCON02 from *C. obsoletus* AP have been reported in a limited number of bird species in the Passeriformes order up to the present day (MalAvi: http://mbio-serv2.mbioekol.lu.se/Malavi/). The results obtained in this study have revealed the prevalence of the relevant *Plasmodium* lineages in avian communities in the İzmir Region and that *Culicoides* species feed on infected hosts.

CONCLUSION

Culicoides species that are prevalent in the İzmir Region have been morphologically and molecularly characterized, and unique epidemiological data have been provided based on molecular ecology regarding the vector potential of these species for avian haemosporidian parasites. The identification of species, such as *C. imicola*, known as the active vector for the BTV, highlights the need for control and management strategies for this disease in the context of host-pathogen-vector. Furthermore, the results of this study have shown that molecular-based techniques, in conjunction with morphometric analyses, can reliably determine species diversity of *Culicoides* in different geographies in Türkiye, and can also reveal cryptic or sibling species in epidemiological context. Considering the different biogeographical characteristics in Türkiye, there is a need for detailed studies on *Culicoides* species and the diseases they transmit based on molecular epidemiology.

*Ethics

Ethics Committee Approval: No need to get ethics approval due to the material used in the study were insect specimens.

Informed Consent: Not required.

Peer-review:

Acknowledgments

The authors would like to thank the Erciyes University Scientific Research Projects Unit, which supported this study.

Footnotes

*Authorship Contributions

Concept: H.Y., Z.Ö., Design: H.Y., Z.Ö., Data Collection or Processing: H.Y., Z.Ö., A.Y., Analysis or Interpretation: H.Y., Z.Ö., Literature Search: H.Y., Z.Ö., A.Y., Writing: H.Y., Z.Ö., A.Y.

Conflict of Interest: No conflict of interest was declared by the authors.

Financial Disclosure: This research was financially supported by Scientific Research Projects Coordination Unit of Erciyes University with the PhD thesis project coded TDK-2016-6397.

REFERENCES

1. Mellor PS, Boorman J, Baylis M. *Culicoides* biting midges: their role as arbovirus vectors. Annu Rev Entomol. 2000; 45: 307-40.
2. Harrup LE, Bellis GA, Balenghien T, Garros C. *Culicoides* Latreille (Diptera: Ceratopogonidae) taxonomy: current challenges and future directions. Infect Genet Evol. 2015; 30: 249-66.
3. Borkent A. The biting midges, the Ceratopogonidae (Diptera), biology of disease vectors, 2nd ed. Elsevier, Burlington, MA: USA; 2004: 113-126.
4. Meiswinkel R, Venter GJ, Nevill EM. Vectors: *Culicoides* spp. In: Coetzer JAW, Tustin RC, editors. Infectious Diseases of Livestock. Cape Town: Oxford University Press; 2004: 93-136.
5. Carpenter S, Groschup MH, Garros C, Felippe-Bauer MF, Purse B. *Culicoides* biting midges, arboviruses and public health in Europe. Antiviral Res. 2013; 13: 102-13.
6. OIE. OIE-Listed diseases, infections and infestations in force in 2014, updated: 1st January 2014, accessed: 17th January 2014. Available at: http://www.oie.int/animal-health-in-the-world/oie-listed-diseases-2014/.
7. Elbers AR, Meiswinkel R, van Weezep E, van Oldruitenborgh-Oosterbaan MM, Kooi EA. Schmallenberg virus in *Culicoides* spp. biting midges, the Netherlands, 2011. Emerg Infect Dis. 2013; 19: 106-9.
8. Valkiūnas G. Avian malaria parasites and other haemosporidia. Boca Raton: CRC Press; 2005.
9. Atkinson CT. *Haemoproteus*. In: Atkinson CT, Thomas NJ, Hunter BC, editors. Parasitic diseases of wild birds. Ames: Wiley-Blackwell; 2008. p.13-35.
10. Donovan TA, Schrenzel M, Tucker TA, Pessier AP, Stalis IH. Hepatic hemorrhage, hemocoelom, and sudden death due to *Haemoproteus* infection in passerine birds: eleven cases. J Vet Diagn Invest. 2008; 20: 304-13.
11. Ortiz-Catedral L, Brunton D, Stidworth MF, Elsheikha HM, Pennycott T, Schulze C, et al. *Haemoproteus minutus* is highly virulent for Australasian and South American parrots. Parasit Vector. 2019; 12: 40.
12. Borkent A. World species of biting midges (Diptera: Ceratopogonidae). New York: American Museum of Natural History; 2019.
13. Bukauskaitė D, Iezhova TA, Ilgūnas M, Valkiūnas G. High susceptibility of the laboratory-reared biting midges *Culicoides nubeculosus* to *Haemoproteus* infections, with review on *Culicoides* species that transmit avian haemoproteids. Parasitology. 2019; 146: 1-9.

14. Bernotienė R, Žiegytė R, Vaitkutė G, Valkiūnas G. Identification of a new vector species of avian haemoproteids, with a description of methodology for the determination of natural vectors of haemosporidian parasites. Parasites & Vectors. 2019; 12: 307.
15. Iezhova TA, Dodge M, Sehgal RN, Smith TB, Valkiunas G. New avian *Haemoproteus* species (Haemosporida: Haemoproteidae) from African birds, with a critique of the use of host taxonomic information in hemoproteid classification. J Parasites. 2011; 97: 682-94.
16. Yıldırım A, Dik B, Düzlü Ö, Gürsoy Ergen A. Sultan sazlığı ekosisteminde kanatlı Haemosporidialarının moleküler ekolojisi. TÜBİTAK 1001 Projesi, Proje no: 114 O 646, 2017.
17. Kieffer JJ. Chironomides d'Afrique et d'Asie conservés au Museum National Hongrois de Budapest. Ann Hist Nat Mus Nat Hung. 1918; 16: 31-136.
18. Dik B. *Culicoides* (Diptera: Ceratopogonidae) vektörlükleri ve mücadelesi. İçinde: Özbel Y (editör), Vektör artropodlar ve mücadelesi. Türkiye Parazitoloji Derneği: İzmir; 2017. s.46-122.
19. Korkmaz C, Alten B, Erol U, Deniz A. Updated checklist of *Culicoides* Latreille (Diptera: Ceratopogonidae) of Türkiye with ten new records. J Vector Ecol. 2021; 46: 124-36.
20. Turgut F. Morphological characteristics of two *Culicoides* Latreille biting midges (Diptera, Ceratopogonidae) with a new record for Turkish fauna. Trakya Univ J Nat Sci. 2023; 23: 3-8.
21. Dik B, Muz D, Muz MN, Uslu U. The geographical distribution and first molecular analysis of *Culicoides* Latreille (Diptera: Ceratopogonidae) species in the Southern and Southeastern Türkiye during the 2012 outbreak of bovine ephemeral fever. Parasitol Res. 2014; 113: 4225-32.
22. Yildirim A, Dik B, Duzlu O, Onder Z, Ciloglu A, Yetismis G, et al. Genetic diversity of *Culicoides* species within the Pulicaris complex (Diptera: Ceratopogonidae) in Türkiye inferred from mitochondrial COI gene sequences. Acta Trop. 2019; 190: 380-8.
23. Şevik M, Oz ME. Detection of Peste des petits ruminants virus RNA in *Culicoides imicola* (Diptera: Ceratopogonidae) in Türkiye. Vet Ital. 2019; 55: 173-9.
24. Nolan DV, Carpenter S, Barber J, Mellor PS, Dallas JF, Mordue Luntz AJ, et al. Rapid diagnostic PCR assays for members of the *Culicoides obsoletus* and *Culicoides pulicaris* species complexes, implicated vectors of bluetongue virus in Europe. Vet Microbiol. 2007; 124: 82-94.
25. Pages N, Munoz-Munoz F, Talavera S, Sarto V, Lorca C, Núñez JI. Identification of cryptic species of *Culicoides* (Diptera: Ceratopogonidae) in the subgenus *Culicoides* and development of species-specific PCR assays based on barcode regions. Vet Parasitol. 2009; 165: 298-310.
26. Mathieu B, Cêtre-Sossah C, Garros C, Chavernac D, Balenghien T, Carpenter S, et al. Development and validation of IIKC: an interactive identification key for *Culicoides* (Diptera: Ceratopogonidae) females from the Western Palaearctic region. Parasites & Vectors. 2012; 5: 137.
27. Dallas JF, Cruickshank RH, Linton YM, Nolan DV, Patakakis M, Braverman Y, et al. Phylogenetic status and matrilineal structure of the biting midge, *Culicoides imicola*, in Portugal, Rhodes and Israel. Med Vet Entomol. 2003; 17: 379-87.
28. Hellgren O, Waldenström J, Bensch S. A new PCR assay for simultaneous studies of *Leucocytozoon*, *Plasmodium*, and *Haemoproteus* from avian blood. J Parasitol. 2004; 90: 797-802.
29. Bensch S, Hellgren O, Pérez-Tris J. MalAvi: A public database of malaria parasites and related haemosporidians in avian hosts based on mitochondrial cytochrome b lineages. Mol Ecol Resour. 2009; 9: 1353.
30. Kearse M, Moir R, Wilson A, Stones-Havas S, Cheung M, Sturrock S, et al. Geneious basic: an integrated and extendable desktop software platform for the organization and analysis of sequence data. Bioinformatics. 2012; 28: 1647-9.
31. Librado P, Rozas J. DnaSP v5: a software for comprehensive analysis of DNA polymorphism data. Bioinformatics. 2009; 25: 1451-2.
32. Kimura M. A simple method for estimating evolutionary rates of base substitutions through comparative studies of nucleotide sequences. J Mol Evol. 1980; 16: 111-20.
33. Tamura K, Stecher G, Peterson D, Filipski A, Kumar S. MEGA6: molecular evolutionary genetics analysis version 6.0. Mol Biol Evol. 2013; 30: 2725-9.
34. Posada D. jModelTest: phylogenetic model averaging. Mol Biol Evol. 2008; 25: 1253-6.
35. Huelsenbeck JP, Ronquist F. MRBAYES: bayesian inference of phylogenetic trees. Bioinformatics. 2001; 17: 754-5.
36. Ramilo DW, Nunes T, Madeira S, Boinas F, da Fonseca IP. Geographical distribution of *Culicoides* (Diptera: Ceratopogonidae) in mainland Portugal: presence/absence modelling of vector and potential vector species. PLoS One. 2017; 12: e0180606.
37. Sarvašová A, Kočišová A, Halán M, Delécolle JC, Mathieu B. Morphological and molecular analysis of the genus *Culicoides* (Diptera: Ceratopogonidae) in Slovakia with five new records. Zootaxa. 2014; 3872: 541-60.
38. Carvalho LPC, Costa GDS, Pereira Júnior AM, de Paulo PFM, Silva GS, Carioca ALPM, et al. DNA Barcoding of genus *Culicoides* biting midges (Diptera: Ceratopogonidae) in the Brazilian Amazon. Acta Trop. 2022; 235: 106619.
39. Gopurenko D, Bellis G, Pengsakul T, Siriyasatien P, Thepparat A. DNA barcoding of *Culicoides* Latreille (Diptera: Ceratopogonidae) from Thailand reveals taxonomic inconsistencies and novel diversity among reported sequences. J Med Entomol. 2022; 59: 1960-70.
40. Ortega-Morales AI, Hernández-Triana LM, Chan-Chable RJ, Garza-Hernández JA, González-Álvarez VH, Ruiz-Arrondo I, et al. DNA barcoding of mosquitoes from the Pantanos de Centla biosphere reserve, Southeastern Mexico. J Am Mosq Control Assoc. 2021; 37: 198-207.
41. Dähn O, Werner D, Mathieu B, Kampen H. Large-scale cytochrome C Oxidase Subunit I gene data analysis for the development of a multiplex polymerase chain reaction test capable of identifying biting midge vector species and haplotypes (Diptera: ceratopogonidae) of the *Culicoides* Subgenus *Avaritia* Fox, 1955. Genes (Basel). 2024; 15: 323.
42. Onder Z, Yildirim A, Duzlu O, Arslan MO, Sari B, Tasci GT, et al. Molecular characterization of black flies (Diptera: Simuliidae) in areas with pest outbreaks and simuliotoxicosis in Northeast Anatolia Region, Türkiye. Acta Trop. 2019; 199: 105149.
43. Inci A, Yildirim A, Duzlu O, Onder Z, Ciloglu A, Seitz G, et al. Genetic diversity and identification of Palearctic black flies in the subgenus Wilhelmia (Diptera: Simuliidae). J Med Entomol. 2017; 54: 888-94.
44. Anon. İzmir Bornova Veteriner Kontrol Enstitüsü Kayıtları; 2016.
45. Goredo M, Catalani M, Federici V, Portanti O, Marini V, Mancini G, et al. Vector species of *Culicoides* midges implicated in the 2012-2014 Bluetongue epidemics in Italy. Vet Ital. 2015; 51: 131-8.
46. Goredo M, Meiswinkel R, Federici V, Di Nicola F, Mancini G, Ippoliti C, et al. The "*Culicoides obsoletus* group" in Italy: Relative abundance, geographic range, and role as vector for Bluetongue virus. Vet Ital. 2016; 52: 235-24.
47. Yavru S, Dik B, Bulut O, Yavru N, Kale M, Bulut A. New *Culicoides* vector species for BTV transmission in Central and Central west of Anatolia. Annu Res Rev Biol. 2018; 27: 1-9.
48. Foxi C, Meloni G, Puggioni G, Manunta D, Rocchigiani A, Vento L, et al. Bluetongue virus detection in new *Culicoides* species in Sardinia, Italy. Vet Re. 2019; 184: 621.
49. Dik B, Kuçlu Ö, Öztürk R. *Culicoides* Latreille, 1809 (Diptera: Ceratopogonidae) species in the Western Black Sea region of Türkiye, new records for the Turkish fauna. Turk J Vet Anim Sci. 2017; 41: 228-37.
50. Reyhan E. Güney Doğu Anadolu Bölgesinin Gaziantep, Kahramanmaraş ve Kilis illerinde *Culicoides* (Diptera: Ceratopogonidae) türlerinin yayılışı, Yüksek Lisans Tezi, Gaziantep Üniversitesi Fen Bilimleri Enstitüsü: Gaziantep; 2018.
51. Turgut F, Kilic AY. The Ceratopogonidae (Insecta: Diptera) fauna of the Central Black Sea region in Türkiye. Turk Zool Derg. 2015; 39: 1071-89.
52. Muz D, Dik B, Muz MN, Öztürk R. Tekirdağ ili *Culicoides* (Diptera: Ceratopogonidae) faunasının mavi dil virus ve Schmallenberg virus varlığı yönünden araştırılması. Namık Kemal Üniversitesi Araştırma Projesi: 2016, Proje no: NKUBAP.00.23.AR.14.08.

53. Turgut F. Samsun ili *Culicoides* Latreille, 1809 (Diptera: Ceratopogonidae) faunasına katkılar. GBAD. 2018; 7: 14-20.

54. Turgut F. Contributions to *Culicoides* Latreille, 1809 (Diptera: Ceratopogonidae) fauna of Sinop province. SAUJS. 2018; 22: 1683-93.

55. Hadj-Henni L, De Meulemeester T, Mathieu B, Depaquit J, Augot D. Taxonomic assessment of *Culicoides brunnicans*, *C. santonicus* and *C. vexans* (Diptera: Ceratopogonidae) in France: Implications in systematics. Infect Genet Evol. 2015; 33: 324-31.

56. Augot D, Ninio C, Akhoundi M, Lehrter V, Couloux A, Jouet D, et al. Characterization of two cryptic species, *Culicoides stigma* and *C. parroti* (Diptera: Ceratopogonidae), based on barcode regions and morphology. J Vector Ecol. 2013; 38: 260-5.

57. Lassen SB, Nielsen SA, Skovgård H, Kristensen M. Molecular differentiation of *Culicoides* biting midges (Diptera: Ceratopogonidae) from the subgenus *Culicoides* Latreille in Denmark. Parasitol Res. 2012; 110: 1765-71.

58. Pagès N, Sarto I Monteys V. Differentiation of *Culicoides obsoletus* and *Culicoides scoticus* (Diptera: Ceratopogonidae) based on mitochondrial cytochrome oxidase subunit I. J Med Entomol. 2005; 42: 1026-34.

59. Ishtiaq F, Guillaumot L, Clegg SM, Phillimore AB, Black RA, Owens IP, et al. Avian haematozoan parasites and their associations with mosquitoes across Southwest Pacific Islands. Mol Ecol. 2008; 17: 4545-55.

60. Njabo KY, Cornel AJ, Bonneaud C, Toffelmier E, Sehgal RN, Valkiūnas G, et al. Nonspecific patterns of vector, host and avian malaria parasite associations in a central African rainforest. Mol Ecol. 2011; 20: 1049-61.

61. James AA, Rossignol PA. Mosquito salivary glands: parasitological and molecular aspects. Parasitol Today. 1991; 7: 267-71.

62. Inci A, Yıldırım A, Njabo KY, Duzlu O, Biskin Z, Ciloglu A. Detection and molecular characterization of avian *Plasmodium* from mosquitoes in central Türkiye. Vet Parasitol. 2012; 188: 179-84.

63. Mata VA, da Silva LP, Lopes RJ, Drovetski SV. The strait of gibraltar poses an effective barrier to host-specialised but not to host-generalised lineages of avian Haemosporidia. Int J Parasitol. 2015; 45: 711-9.

64. Martinez-de la Puente J, Munoz J, Capelli G, Montarsi F, Soriguer R, Arnoldi D, et al. Avian malaria parasites in the last supper: identifying encounters between parasites and the invasive Asian mosquito tiger and native mosquito species in Italy. Malaria J. 2015; 14: 32.

65. Synek P, Munclinger P, Albrecht T, Votypka J. Avian haemosporidians in haematophagous insects in the Czech Republic. Parasitol Res. 2013; 112: 839-45.

66. Bobeva A, Zehtindjiev P, Bensch S, Radrova J. A survey of biting midges of the genus *Culicoides* Latreille, 1809 (Diptera: Ceratopogonidae) in NE Bulgaria, with respect to transmission of avian haemosporidians. Acta Parasitol. 2013; 58: 585-91.

67. Ferraguti M, Martinez-de la Puente J, Munoz J, Roiz D, Ruiz S, Soriguer R, et al. Avian *Plasmodium* in *Culex* and *Ochlerotatus* mosquitoes from Southern Spain: effects of season and host-feeding source on parasite dynamics. PLoS One. 2013; 8: e66237.

68. Kim KS, Tsuda Y. Avian *Plasmodium* lineages found in spot surveys of mosquitoes from 2007 to 2010 at Sakata wetland, Japan: do dominant lineages persist for multiple years? Mol Ecol. 2012; 21: 5374-85.

Video Article
Video Makale

Turkiye Parazitol Derg 2025;49(1):45-6
DOI: 10.4274/tpd.galenos.2025.24855

A New Imaging Method in Dermatology: Smartphone-based Microscope

Dermatolojide Yeni Bir Görüntüleme Yöntemi: Akıllı Telefon Tabanlı Mikroskop

Aslan Yürekli[1], İlkay Can[2], Melis Bal Akdoğan[3]

[1]University of Health Sciences Türkiye, Gülhane Training and Research Hospital, Department of Dermatology, Ankara, Türkiye
[2]Balıkesir University Faculty of Medicine, Department of Dermatology, Balıkesir, Türkiye
[3]Private Clinic, Clinic of Dermatology, Ankara, Türkiye

Cite this article as: Yürekli A, Can İ, Bal Akdoğan M. A new imaging method in dermatology: smartphone-based microscope. Turkiye Parazitol Derg. 2025;49(1):45-6.

Keywords: *Demodex*, scabies, imaging, smartphone, microscope
Anahtar Kelimeler: *Demodeks*, skabiyez, görüntüleme, akıllı telefon, mikroskop

Microscopic examination is routinely utilized in the diagnosis of various dermatological conditions, particularly parasitic and fungal diseases. However, this diagnostic tool is often time-consuming, as it requires patient sampling and specialized equipment. With advancements in technology, imaging methods are rapidly evolving. Recently, there has been an increase in studies focused on smartphone-integrated imaging techniques. For instance, a smartphone-based intraocular lens microscope has been employed in the field of ophthalmology (1). Similarly, in dermatology, skin cancers have been assessed using a lens integrated into a smartphone (2). We believe that more practical and accessible technologies should be adopted in the field of medicine.

In our study, we utilized a microscopic lens capable of 400x magnification. By integrating this lens into an apparatus designed to function as a phone case and using the smartphone's camera, we successfully captured images akin to those obtained with a traditional 40x microscope lens. The lens featured not only significant magnification but also an illumination source to enhance the examined area. This innovative approach eliminates the need for patient sample collection and circumvents the expense of using a conventional microscope for microscopic examinations. Additionally, it allows for the capture of photos and videos during the examination of lesions. In our research, we observed the tunnels in scabies patients and examined superficial skin biopsy samples for *Demodex* evaluation using this smartphone-based microscope. This enabled us to visualize the tunnels, mites, and eggs at a microscopic level (Figure 1). Through this diagnostic method, we were able to observe the movement of the mites within the tunnels (Video 1). When directly examining the superficial skin biopsy sample for *Demodex* detection with the smartphone, we clearly identified *Demodex* mites (Figure 2). We assessed *Demodex* density by scanning the entire area during preparation (Video 2).

While smartphone manufacturers are continuously enhancing camera features with each new model, the market has yet to offer a lens catering specifically to the medical community. By equipping smartphones with a simple lens capable of 400x magnification, we can effectively meet the significant needs of doctors, biology educators, and microscopy enthusiasts-particularly in dermatology. We believe that our study will greatly facilitate the work of dermatologists and physicians using microscopes in their daily practice while showcasing the potential of advancing technology.

Received/Geliş Tarihi: 24.09.2024 **Accepted/Kabul Tarihi:** 14.04.2025 **Publication Date/Yayınlanma Tarihi:** 09.05.2025

Address for Correspondence/Yazar Adresi: Aslan Yürekli, University of Health Sciences Türkiye, Gülhane Training and Research Hospital, Department of Dermatology, Ankara, Türkiye
E-mail/E-Posta: aslanyurekli03@hotmail.com **ORCID ID:** orcid.org/0000-0003-2812-2133

Türkiye PARAZİTOLOJİ Dergisi

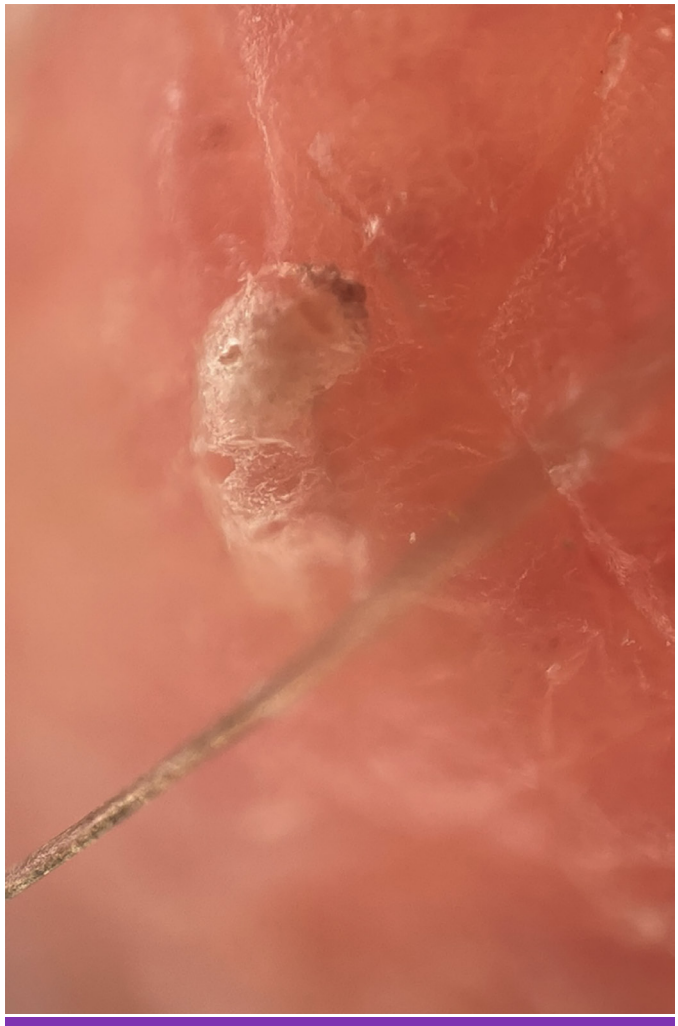

Figure 1. View of tunnel and mite under smartphone-based microscope

Figure 2. View of *Demodex* mites under a smartphone-based microscope

Video 1: https://youtube.com/shorts/fwT1a_rfSNg
Video 2: https://youtube.com/shorts/YtEoaFyLWSw

*Ethics

Footnotes

*Authorship Contributions

Data Collection or Processing: M.B.A., Literature Search: İ.C., Writing: A.Y.

Conflict of Interest: No conflict of interest was declared by the authors.

Financial Disclosure: The authors declared that this study received no financial support.

REFERENCES

1. Chandrakanth P, Chandrakanth KS. Smartphone-based intraocular lens microscope. Indian J Ophthalmol. 2020; 68: 2213-5.
2. Jahan-Tigh RR, Chinn GM, Rapini RP. A Comparative study between smartphone-based microscopy and conventional light microscopy in 1021 dermatopathology specimens. Arch Pathol Lab Med. 2016; 140: 86-90.